Water-use of commercial bamboo species in KwaZulu-Natal, South Africa

by

MP Gumede

Submitted in partial fulfillment of the academic requirements of

Master of Science in Hydrology

School of Agricultural, Earth and Environmental Sciences

College of Agriculture, Engineering and Science

University of KwaZulu-Natal

Pietermaritzburg

South Africa

December 2020

ABSTRACT

With the increasing impacts of global change, depletion of natural resources and increased degradation of the world's environment, there is a need for more sustainable development. One such innovation is to convert degraded land into viable bamboo plantations, which will provide timber and fuel to achieve sustainable development. Also, with their very fast growth rate, high productivity and tensile strength, bamboo has the potential to reduce the deforestation of South Africa's natural forests. However, the bamboo species that have the most potential to solve South Africa's fuelwood crisis are not indigenous and the water-use is not well understood under South African climatic conditions. Therefore, this study was conducted to quantify water-use of two commercial bamboo species namely *Bambusa balcooa* var. balcooa and *Bambusa balcooa* var. beema in KwaZulu-Natal with the water-use of nearby Eucalyptus grandis and Acacia mearnsii plantations also quantified for comparison. Two different sap flow measuring sensors were used to quantify the water-use of bamboo to determine their impact on water resources: (i) the heat ratio method (HRM), which quantifies sap flow with respect to its depth into the sap wood and (ii) the stem steady state (SSS) sensor that involves the application of continuous heat energy all around a section of the stem through dynamax collars, which are used to quantify the total sap passing through a fixed area on a stem. The daily water-use in the beema, balcooa, eucalyptus and wattle plantation was 2.0 - 3.2 mm day^{-1}, 3.8 - 6.0 mm day^{-1}, ~ 8.0 mm and ~ 5.0 mm day^{-1} in summer (the wet season) where as 1.0 - 1.6 mm day^{-1}, 2.0 - 2.8 mm day^{-1}, ~ 4.0 mm day^{-1} and > 3.0 mm day^{-1} was recorded in winter (the dry season). These data demonstrated low water-use of bamboo species when compared to eucalyptus and wattle plantations. While the hydrological modelling of bamboo as a stream flow reduction activity (SFRA) was beyond the scope of the current study, the determination of the transpiration coefficient (K_{cb}) values was a critical component of this process. Therefore, the estimated K_{cb} in the Beema plantation was ~ 0.35 in dry winter and ~ 0.53 in the wet summer. Estimated K_{cb} in the balcooa culms were 0.51 in winter and ~ 0.9 in summer when transpiration was not limited by moisture and energy. Unlike bamboo, higher winter K_{cb} values ~ 0.75 were measured in winter in the Eucalyptus plantation when ~ 1.0 was measured in summer. The K_{cb} in wattle trees was > 0.7 in winter but < 1.2 in the wet summer months. These data indicated that wattle and eucalyptus trees were higher water-users than bamboo species at Shooter's Hill.

PREFACE

The research contained in this dissertation was completed by the candidate while based in the Discipline of Hydrology, School of Agricultural, Earth and Environmental Sciences of the College of Agriculture, Engineering and Science, University of KwaZulu-Natal, Pietermaritzburg campus, South Africa. The research was financially supported by the Water Research Commission (WRC) & Department of Agriculture, Forestry and Fisheries (DAFF).

The contents of this work have not been submitted in any form to another university and, except where the work of others is acknowledged in the text, the results reported are due to investigations by the candidate.

[redacted]

Supervisor: Dr Alistair Clulow

Date: 03 December 2020

[redacted]

Co-supervisor: Prof Colin Everson

Date: 04 December 2020

[redacted]

Co-supervisor: Dr Terry Everson

Date: 04 December 2020

DECLARATION: PLAGIARISM

I, Mxolisi Percyval Gumede, declare that:

i. the research reported in this dissertation, except where otherwise indicated or acknowledged, is my original work;

ii. this dissertation has not been submitted in full or in part for any degree or examination to any other university;

iii. this dissertation does not contain other persons' data, pictures, graphs or other information unless specifically acknowledged as being sourced from other persons;

iv. this dissertation does not contain other persons' writing unless specifically acknowledged as being sourced from other researchers. Where other written sources have been quoted, then:

a. their words have been re-written, but the general information attributed to them has been referenced;

b. the exact words used in writing have been placed inside quotation marks, and referenced;

v. where I have used a material for which publications followed, I have indicated in detail my role in the work;

vi. this dissertation is primarily a collection of material, prepared by myself, published as journal articles or presented as a poster and oral presentations at conferences. In some cases, additional material has been included;

vii. this dissertation does not contain text, graphics or tables copied and pasted from the internet, unless specifically acknowledged, and the source being detailed in the dissertation and in the References sections.

[redacted]

Mr Mxolisi Percyval Gumede Date: 04 December 2020

ACKNOWLEDGEMENTS

A special thanks and appreciations for support and encouragement to the following:
Firstly, and above all, to God Almighty through His Son Jesus Christ for carrying me through the journey of research until the study was completed. His unfailing, unconditional and sustaining love motivated me to work devotedly. To Professor Colin Everson of the University of KwaZulu-Natal, a project leader for giving me a chance in the field of research and for the amazing support throughout the study both in field work and compiling the outcomes. Also, to Dr Terry Everson of the University of KwaZulu-Natal, a special appreciation for her dedication in ensuring success in this study. For the patience and support she has given me in writing, preparing for seminar presentations, field work and for all the commitment in making this work an accomplishment. To Dr Alistair Clulow of the University of KwaZulu-Natal, thank you so much firstly for believing in me from the first moment you assigned me for this project. Your devotion and support throughout the study cannot be explained by any words only the heart can be able to express. Thank you for introducing Prof Colin and Terry Everson in my life. To my brother Emmanuel for the support in installing equipment up at Shooter's Hill. To Mr Guy Solomon, a farmer at Shooter's Hill thank you so much for allowing us to use your property, for the support and interest you have shown to this project from the first meeting until it was completed may the good Lord richly bless you.

Finally, to my family thank you for the patience, support and encouragements. I would not have completed the study if it weren't because of the support from my mother Mrs Nokulunga Nxumalo my father Mr Mandla Nxumalo and my lovely and wonderful mother of my beautiful daughter (Nontsikelelo Gumede) Sinenhlanhla Ntshangase, you are amazing and thank you for the unfailing love and support.

TABLE OF CONTENTS

ABSTRACT 1

PREFACE 2

DECLARATION: PLAGIARISM 3

ACKNOWLEDGEMENTS 4

LIST OF FIGURES 9

LIST OF TABLES 14

LIST OF PLATES 15

LIST ABBREVIATIONS AND SYMBOLS 17

1. INTRODUCTION 18

1.1 Justification 19

1.2 Aim and objectives 20

1.2.1 Aim 20

Objectives 20

1.2.2 Research hypothesis 20

2. LITERATURE REVIEW: THE WATER-USE OF BAMBOO AND SPECIES DISTRIBUTION IN SOUTH AFRICA 21

2.1 Historical background of bamboo species 21

2.2 Commercial monopodial bamboo species 28

2.2.1 Subtropical and tropical bamboo species 28

2.2.2 Temperate bamboo species 29

2.3 Commercial sympodial bamboo species 31

2.3.1 Subtropical and tropical bamboo species 31

2.3.2 Temperate bamboo species 34

2.4 Commercially grown bamboo species in South Africa 35

2.4.1 Balcooa (Bambusa balcooa) 35

2.4.2 Sweet bamboo (Dendrocalamus asper) 36

2.4.3 Small scale cultivated bamboo species in South Africa 38

2.5 Bamboo market in South Africa 40

2.6 SFRA status and exotic bamboo distribution in South Africa 40

2.7 Water-use and sap flow quantifying techniques 43

2.7.1 Understanding evapotranspiration and environmental effects 43

2.7.2 Effect of bamboo structure on water-use 44

2.7.3 Measuring bamboo water-use 46

2.8 Bamboo sap flow measuring challenges and limitations 52

2.9 Conclusion 53

3. Materials and methods 54

3.1 Meteorological station 54

3.1.1 Automatic weather station (AWS) 54

3.2 Volumetric water content (VWC) 55

3.3 Bamboo selection 57

3.4 *Eucalyptus grandis* (eucalyptus) selection 58

3.5 *Acacia mearnsii* (wattle) selection 58

3.6 Experimental design of the Beema and Balcooa sites at Shooter's Hill farm 59

3.6.1 Bamboo culms, eucalyptus, and wattle tree growth monitoring 60

3.6.2 Leaf area index (LAI) 61

3.7 Bamboo anatomy 62

3.7.1 Sample and blocks preparation 62

3.7.2 Sample blocks trimming and viewing 63

3.8 HRM water-use measurements at Shooter's Hill farm 63

3.8.1 Assessing the culm area of beema and balcooa culms 64

3.8.2 HRM setup of beema and balcooa 68

3.8.3 Water-use of Eucalyptus grandis (eucalyptus) 70

3.8.4 Water-use of Acacia mearnsii (black wattle) 71

3.9 Stem steady state (SSS) 72

3.9.1 Preparation of bamboo culms for Dynagauge installation 76

3.9.2 Automatic zero set 77

3.9.3 Data output 78

3.10 Transpiration coefficient (K_{cb}) 78

3.11 Root mean square error (RMSE) 79

4. Results 80

4.1 Meteorological data 80

4.2 Soil profile water content 85

4.3 Growth of *Bambusa balcooa* 91

4.4 Bamboo anatomy 96

4.5 Water-use estimates using the HRM sensors 100

4.6 Water-use estimated using SSS 114

4.7 Total water-use of the beema, balcooa, eucalyptus and wattle at Shooter's Hill 121

4.8 Comparison of SSS and HRM 126

5. Discussion 128

6. Conclusion and Recommendation 134

7. References 136

8. Appendix 142

LIST OF FIGURES

Figure 2.1 Bamboo species within genera and species status (Canavan et al., 2017). 22

Figure 2.2 Countries and islands with the highest bamboo richness (Canavan et al., 2017). 24

Figure 2.3 A rhizome anatomical structure of sympodial bamboo species (Botanicals, 2019). 25

Figure 2.4 A rhizome anatomical structure of monopodial bamboo species (Botanicals, 2019). 26

Figure 2.5 Giant thorny bamboo (*Bambusa bambos*) plant structures (CABI, 2019). 32

Figure 2.6 Geographic distribution of *Bambusa bambos* in India and Asia (Schröder, 2007) 33

Figure 2.7 Pachymorph rhizome of sweet bamboo (Lahr et al., 2015) 37

Figure 2.8 Bamboo activities in South Africa (Scheba et al., 2018). 41

Figure 2.9 Distribution of different types of alien bamboo species in South Africa from 1896 to 2017 (Canavan et al., 2021). 42

Figure 2.10 Schematic diagram for evapotranspiration (Muhammad, 2018) 43

Figure 2.11 a) Cross-section of Phyllostachys pubescens bamboo species b) cross-section of culm wall showing vascular bundle arrangement and c) vascular bundle with metaxylem (Mx), phloem (P) and fibre caps (Wang et al., 2012)… 45

Figure 2.12 Schematic diagram of former stem flow sensor (Lascano et al., 2016). 49

Figure 2.13 Schematic diagram of EXO-SkinTM Sap flow Model SGEX-13 (Dynamax Inc., Houston, TX) (Lascano et al., 2016). 50

Figure 2.14 Schematic diagram of Heat ratio method (Bayona-Rodríguez and Romero, 2016). 52

Figure 3.1 Site layout of bamboo clumps and equipment at the beema site, Shooter's Hill. 59

Figure 3.2 Regression of culm diameter vs hollow diameter for Beema.......... 65

Figure 4.1 Daily total incoming solar radiation and mean vapour pressure deficit from September 2018 to February 2020 at Shooter's Hill, KwaZulu-Natal. 80

Figure 4.2 Daily average ambient air temperature and vapour pressure deficit from September 2018 to February 2020 at shooter's Hill, KwaZulu-Natal. 81

Figure 4.3 Daily relative humidity (%) and vapou pressure deficit measured at Shooter's Hill grassland site from September 2018 to February 2020. 82

Figure 4.4 Daily rainfall measured at Shooter's Hill grassland site from September 2018 to February 2020. 83

Figure 4.5 Average daily windspeed measured at Shooter's Hill grassland site from September 2018 to February 2020. 84

Figure 4.6 Rainfall and soil water content with respect to soil depth at Beema site, KwaZulu-Natal. 86

Figure 4.7 Total soil water content and rainfall at the Beema site, KwaZulu-Natal. 87

Figure 4.8 Rainfall and soil water content with respect to soil depth at the Balcooa site, KwaZulu-Natal. 88

Figure 4.9 Total soil water content and rainfall at the Balcooa site, KwaZulu-Natal. 89

Figure 4.10 Rainfall and soil water content with respect to soil depth at the Eucalyptus site, KwaZulu-Natal. 90

Figure 4.11 Total soil water content and rainfall at the Eucalyptus site, Shooter's Hill, KwaZulu-Natal. 91

Figure 4.12 Frequency size classes of beema and balcooa. 92

Figure 4.13 Leaf area index of beema, balcooa, eucalyptus and wattle at Shooter's Hill. 95

Figure 4.14 Average stem diameters of beema, balcooa, eucalyptus and wattle trees at Shooter's Hill. 96

Figure 4.15 Total daily sap-flow (L day^{-1}) of the beema stand for different seasons at Shooter's Hill from 2018 to 2020. 101

Figure 4.16 Total daily sap-flow (mm day^{-1}) of the beema stand for different seasons at Shooter's Hill from 2018 to 2020. 102

Figure 4.17 Daily sap-flow (mm day^{-1}) of the beema stand in the summer period in relation to A) solar radiation (MJ m^{-2}) and B) VPD using HRM. 103

Figure 4.18 Daily sap-flow (mm day^{-1}) of beema stand in winter period in relation to A) solar radiation (MJ m^{-2}) and B) VPD using HRM. 104

Figure 4.19 Total daily sap-flow (L day^{-1}) of the balcooa stand for different seasons at Shooter's Hill from 2018 to 2020. 105

Figure 4.20 Total daily sap-flow (mm day^{-1}) of the balcooa stand for different seasons at Shooter's Hill from 2018 to 2020. 105

Figure 4.21 Daily sap-flow (mm day^{-1}) of the balcooa stand in the summer period in relation to A) solar radiation (MJ m^{-2}) and B) VPD using HRM. 106

Figure 4.22 Daily sap-flow (mm day^{-1}) of the balcooa stand in the winter period in relation to A) solar radiation (MJ m^{-2}) and B) VPD using HRM. 107

Figure 4.23 Seasonal daily sap-flow (L day^{-1}) at the eucalyptus plantation in Shooter's Hill from 2018 to 2020. 108

Figure 4.24 Seasonal daily transpiration (mm day^{-1}) of the eucalyptus plantation at Shooter's Hill from 2018 to 2020. 109

Figure 4.25 Daily sap-flow (mm day^{-1}) of the eucalyptus trees in the summer period in relation to A) solar radiation (MJ m^{-2}) and B) VPD using HRM. 110

Figure 4.26 Daily sap-flow (mm day^{-1}) of the eucalyptus trees in the winter period in relation to A) solar radiation (MJ m^{-2}) and B) VPD using HRM. 110

Figure 4.27 Seasonal sap-flow (L day^{-1}) of the black wattle trees at Shooter's Hill from 2018 to 2020. 111

Figure 4.28 Daily transpiration (mm day^{-1}) of black wattle trees for different seasons at Shooter's Hill from 2018 to 2020. 112

Figure 4.29 Daily sap-flow (mm day^{-1}) of the wattle trees in summer in relation to A) solar radiation (MJ m^{-2}) and B) VPD using HRM. 113

Figure 4.30 Daily sap-flow (mm day^{-1}) of the wattle trees in winter in relation to A) solar radiation (MJ m^{-2}) and B) VPD using HRM. 114

Figure 4.31 Seasonal daily sap-flow (L day^{-1}) of the beema stand at Shooter's Hill. 115

Figure 4.32 Daily transpiration (mm day^{-1}) of the beema stand for different seasons at Shooter's Hill. 115

Figure 4.33 Daily sap-flow (mm day^{-1}) of the beema stand in the summer period in relation to A) solar radiation (MJ m^{-2}) and B) VPD using SSS. 117

Figure 4.34 Daily sap-flow (mm day^{-1}) of the beema stand in winter in relation to A) solar radiation (MJ m^{-2}) and B) VPD using SSS. 118

Figure 4.35 Seasonal daily sap-flow (L day^{-1}) of the balcooa stand at Shooter's Hill. 118

Figure 4.36 Total daily sap-flow (mm day^{-1}) of the balcooa stand for different seasons at Shooter's Hill. 119

Figure 4.37 Daily sap-flow (mm day^{-1}) of the balcooa stand in the summer period in relation to A) solar radiation (MJ m^{-2}) and B) VPD using SSS. 120

Figure 4.38 Daily sap-flow (mm day^{-1}) of the balcooa stand in the winter period in relation to climatic variables using SSS. 121

Figure 4.39 Monthly transpiration (mm day^{-1}) in relation to K_t values for the A) beema B) balcooa C) eucalyptus and D) wattle trees at Shooter's Hill. 126

Figure 4.40 Regression analysis of daily transpiration of A) beema and B) balcooa culms using HRM and SSS. 127

LIST OF TABLES

Table 2.1 Comparison of culm area (mm^2) and tensile strength ($N\ mm^{-2}$) of bamboo species (Awalluddin et al., 2017)... 27

Table 2.2 Indigenous bamboo species in South Africa and growing conditions in relation to adapted environments... 39

Table 2.3 Estimated transpiration of mature bamboo species (Kleinhenz and Midmore, 2000). 46

Table 3.1 Stem diameters and areas of Beema and Balcooa bamboo at Shooters Hill, KZN. 66

Table 3.2 List of gauges used at the Beema site and the inital program constants and parameters used to measure sap flow.. 74

Table 3.3 Mechanical specifications of the Dynamax gauges used at the Beema site......... 75

Table 4.1 Total monthly measurements of realtive humidity, air temperature and rainfall at Shooter's Hill.. 84

Table 4.2 Culm diameter measurements (mm) of beema.. 93

Table 4.3 Summary of culm diameter (mm) measurements of balcooa............................. 93

Table 4.4 Total water-use of beema, balcooa, eucalyptus and wattle trees from 2019/01/01 to 2019/12/31 using HRM and SSS. 122

Table 4.5 Comparison of the water-use for different land-uses and ET_0 at Shooter's Hill. 123

Table 8.1 Land-use data for HRM water-use analysis A) beema, B) balcooa, C) eucalyptus and D) wattle trees.. 142

LIST OF PLATES

Plate 2.1 Hardy clumping bamboo (*Fragesia rufa*) root structure (Botanicals, 2019). 34

Plate 3.1 Automatic weather station A) anenometer, B) temperature and RH probe shield, C) thermocouple wire, D) NR lite net radiometer, E) solar panel, F) datalogger box and G) rain gauge at Shooters Hill, KwaZulu-Natal.................. 55

Plate 3.2 Installed soil water probes (CS 616) for measuring soil water content. 56

Plate 3.3 KwaZulu-Natal study site at Shooter's Hill farm... 57

Plate 3.4 Measuring the culm diameters in the 10 X 10 m study plot with Vernier callipers. 60

Plate 3.5 Anatomical structure of bamboo stem (Li et al., 2015). 63

Plate 3.6 Measuring different stem diameters and wall thickness of A) balcooa and B) beema bamboo sp.. 68

Plate 3.7 Heater probes connected to a data logger and multiplexer. 68

Plate 3.8 HRM installation in the balcooa clump at Shooter's Hill. 69

Plate 3.9 Safe boxes for batteries (grey boxes) and the logger enclosure (white box) in the Beema site.. 70

Plate 3.10 Eucalyptus plantation at Shooter's Hill, KwaZulu-Natal. 71

Plate 3.11 Black wattle trees at Shooter's Hill, KwaZulu-Natal. 71

Plate 3.12 The wiring of the Dynamax system with a CR1000 data logger and AM16/32B multiplexer with two adjustment potentiometers of the AVRD in the centre. 73

Plate 3.13 Preparation and installation of the dynamax collars... 76

Plate 3.14 A) Securing the sensor and B) Completed Dynamax collar installation. 77

Plate 4.1 Cross-sectional layout of beema cellular structures... 97

Plate 4.2 Anatomical structure of a vascular bundle of beema... 97

Plate 4.3 Cross-section of beema culm and vascular bundles distribution........................ 98

Plate 4.4 Balcooa bamboo culm cross-section... 99

Plate 4.5 Balcooa bamboo vascular bundle structure... 99

Plate 4.6 Cross-section of balcooa culm and vascular bundle distribution. 100

LIST ABBREVIATIONS AND SYMBOLS

Abrreviations	Meaning	Additional abrreviations	Meaning
AVRD	Adjustable voltage regulator	cm	Centimetre
AWS	Automatic weather station	cm hr^{-1}	Centimetre per hour
DBH	Diameter at breast height	cm^2	Square centimetre
DEFF	Department of Environment, Forestry and Fisheries	J	Joules
DTI	Department of Trade and Industry	kg s^{-1}	kilogram per second
ET	Evaporation	L	Litres
ET0	FAO 56 Reference evaporation	L day^{-1}	Litres per day
FC	Field capacity	m^2	Square metre
HPV	Heat pulse velocity	mm	Millimetres
HRM	Heat ratio method	mm day^{-1}	millimetres per day
Kc	Crop coefficient	^oC	degree Celsius
LAI	Leaf area index	W	Watts
Mx	Metaxylem		
P	Phloem		
PAW	Plant available water		
PWP	Permanent wilting point		
SEM	Scanning electron microscope		
SFRA	Stream flow reduction activity		
SSS	Stem steady state		
TDP	Thermal dissipation probe		
TSPWC	Total soil profile water content		
VPD	Vapour pressure deficit		
VWC	Volumetric water content		

Greek symbols	Meaning
~	Approximately
<	Less than
>	More than
≤	Less or equals to
≥	More or equals to
ƛ	Ambda
ɵ	Theta

1. INTRODUCTION

With the increasing impacts of global climate change, depletion of natural resources and increased degradation of the world's environment there is a need for more sustainable development. Sustainable development and growth can be achieved by improved management of ecosystems (McCartney et al., 2014) and more strategic use of water, land and other natural resources such as trees. In South Africa, the traditional use of energy sources in the form of fuelwood has resulted in substantial negative environmental impacts. Removal of trees for timber and energy has caused degradation of large parts of South Africa, resulting in poor water infiltration, severe soil erosion and loss of biodiversity. Biomass, particularly firewood, is the most widely used fuel in many rural areas of South Africa. However, timber is not readily available anymore due to heavy harvesting. This has resulted in the degradation of large areas causing environmental problems as well as social concerns, with poor households being unable to afford the purchase of timber from outside sources. If sustainable development is to be achieved, it will be necessary to seek alternative options and technological innovations to improve the efficiency of timber harvesting as well as finding solutions to economic and environmental problems associated with timber shortage.

One such innovation is to convert degraded land into viable bamboo plantations, which will provide timber and fuel to achieve sustainable development. The sustainability of bamboo is related to its fast growth rate and vegetative growth pattern, which produce shoots (tillers) that mature into stems (culms). The function of these culms is to conduct water and nutrients from the soil to the leaves.

The culms are characterized by extended woody internodes with intermittent, thickened nodes which gives the bamboo its high tensile strength. If managed correctly, multiple culms are produced annually, which grow into clumps that reach maturity within six to seven years of planting. When harvesting takes place, not all the culms are removed. Generally, a selection of 5-6 culms from each plant is harvested each year. This ensures that the harvesting is sustainable as the remaining culms will continue to produce new shoots in subsequent years, a process that continues for many years.

With this very fast growth rate, high productivity and tensile strength, bamboo has the potential to reduce the deforestation of South Africa's natural forests. However, the bamboo species that have the most potential to solve South Africa's fuelwood crisis are not indigenous. Nevertheless, it must be acknowledged that some alien plants are potentially important contributors to the economy with a place for them in agricultural systems. Bamboo plantations in South Africa have the potential to create employment, provide viable economic and resource outputs and contribute to poverty alleviation and carbon sequestration. However, in spite of growing public and private investment, little is known about the opportunities, challenges and impacts of commercial bamboo growing in Africa (Scheba et al., 2018).

1.1 Justification

The Government, through the Departments of Trade and Industry (DTI) and Agriculture Forestry and Fisheries (DAFF), is promoting the planting of bamboo species as part of rural agricultural development. According to the Bamboo Association of South Africa, about 40 000 ha are earmarked for bamboo plantations in both KwaZulu-Natal (KZN) and the Eastern Cape (EC). However, the water-use of this crop is not well understood under the South African climatic conditions. Therefore, the amount of transpiration by the relevant species of bamboo need to be quantified in South Africa to provide a scientific basis to decide on the status of this crop as a streamflow reduction activity (SFRA).

Knowledge of the water-use of bamboo species is also important for its water management to obtain optimum yields. Knowledge must be obtained of the total and seasonal water-use to enable the judicious expansion of the bamboo industry. This is an important requirement to justify or substantiate applications for water-use licences, for production to be undertaken within official water-use authorisations.

Knowledge of the water-use is also required to motivate a periodic review of water-use licences for the long-term production of bamboo. Understanding the effect of changing land-use on water requires knowledge of the natural 'baseline' vegetation. In order to compare the water-use of bamboo with other species, this study also monitored the water-use of Eucalyptus grandis trees (eucalyptus), Acacia mearnsii (wattle), and natural grassland.

1.2 Aim and objectives

The aims, objectives and the hypothesis of this research study are as follows:

1.2.1 Aim

To quantify the water-use of two commercial bamboo species namely *Bambusa balcooa* var. balcooa and *Bambusa balcooa* var. beema in KwaZulu-Natal to determine their impact on water resources.

Objectives

i. To determine the water-use of selected bamboo species using heat ratio method (HRM) and stem steady state (SSS) techniques.
ii. To determine the structure and distribution of vascular tissues within the stems of two selected bamboo species to quantify the sap wood area within the culm.
iii. To carry out a comparative study of the water-use of wattle, eucalyptus and bamboo.

1.2.2 Research hypothesis

Bamboo species in KwaZulu-Natal have a high water-use due to their high growth rates.

2. LITERATURE REVIEW: THE WATER-USE OF BAMBOO AND SPECIES DISTRIBUTION IN SOUTH AFRICA

2.1 Historical background of bamboo species

Bamboo, a perennial monocotyledonous woody grass species (Awalluddin et al., 2017) was historically known as a poor man's timber and a traditional plant species. However, in recent times it has been regarded as a wonder "green gold" plant due to its numerous uses and is of growing interest to the scientific community (Laplace et al., 2017). Bamboo is a *Poaceae* (Bambusoideae) family grass species and constitutes about 88 genera and 1500 identified species in the world (Awalluddin et al., 2017). Awalluddin et al. (2017) also indicated that more than 70 genera grow naturally in the temperate, tropical and subtropical regions (Figure 2.1). This was also supported by Tsuruta et al. (2016), although other scientific works have indicated that the identified species have reached 1662 in 121 genera (Canavan et al., 2017).

Bamboo is native to Asia growing predominant in south and south east Asia and comprising about 80% of different bamboo species in the world with Brazil and Australia (Figure 2.2). Ying et al. (2016) showed an expansion of 161 % of bamboo plantation between 1984 to 2014 in Tianmushan, Zhejiang Province and China. However, the study has also indicated a 20% decline in recent years due to human activities such as deforestation (Ying et al., 2016). The value of bamboo is in its multiple uses. Bamboo's main use is as a construction material. Awalluddin et al. (2017) indicated that hardened culms of *Bambusa vulgaris, Gigantochloa scortechinii* and *Dendrocalamus asper* have higher tensile and compressive strength than most timber.

The tensile strength of different bamboo species in relation to their usefulness as a construction material is shown in Table 2.1. They are a good substitute for steel and timber, as the plants are more economical and environmentally friendly, and unlike the manufacture of steel, do not contribute significantly to the increase of dangerous gases to the atmosphere.

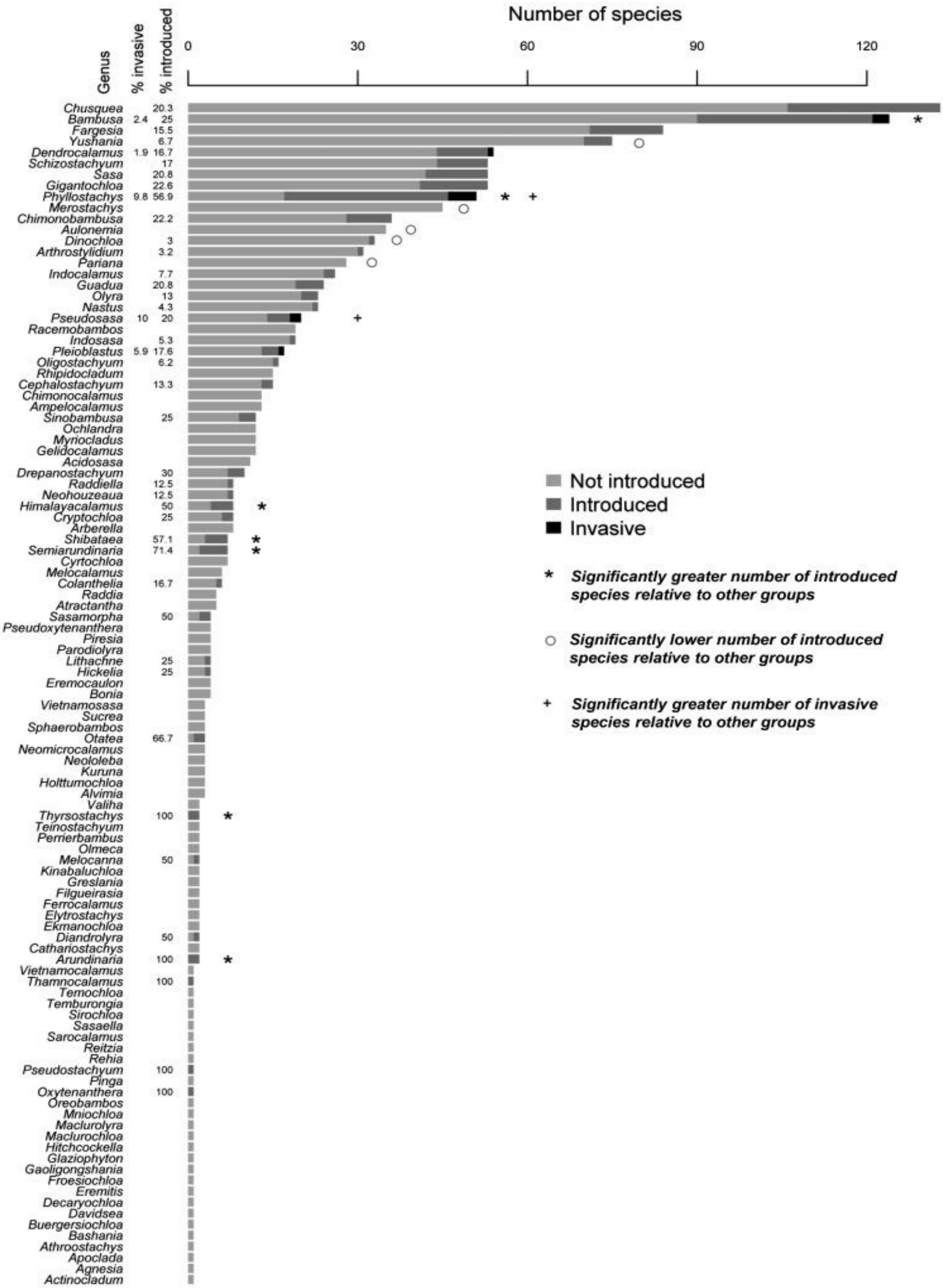

Figure 2.1 Bamboo species within genera and species status (Canavan et al., 2017).

The fresh shoots of bamboo are also a good source of nutritious food and are consumed fresh, canned, pickled, cooked or fermented with potential growth in the food processing industry where it is produced on a commercial scale (Amlani et al., 2017). Bamboo culms have been used for paper manufacturing (Amlani et al., 2017). The bamboo industry that produces paper has been in existence for over 2000 years showing that the species is reliable for paper production (Shroti et al., 2012). Bamboo can also serve as an energy source in Africa substituting for use of fossil fuels that cause air pollution, deforestation, and depletion of ozone because it provides clean energy, and viable and sustainable wood fuel (Sette Jr et al., 2016). Bamboo species are extremely high in lignin content > 29% and therefore desirable for solid biofuel production globally (Chin et al., 2013). The switch from fossil fuel to bamboo fuel was caused by a drastic reduction in the availability of fossil fuels and the environmental protection act that required an alternative to fossil fuel due to extensive land degradation that affected biodiversity (Fatriasari et al., 2014). Also, the study by Bebbington et al. (2018) showed that there is indeed an extreme reduction in total forest areas in the world with regards to human intervention through deforestation and land degradation. However, because of bamboo's sustainable characteristics and its fast growth, bamboo plantations had less effect on destroying land and that bamboo forests have been increasing compared with the decrease in coniferous forests (Xu et al., 2020). Currently, bamboo production is expanding tremendously and new food products such as bamboo juice, bamboo vinegar and also clothing items made through fibre extracted from the culms as well as bamboo coal are being derived from various bamboo species (Amlani et al., 2017).

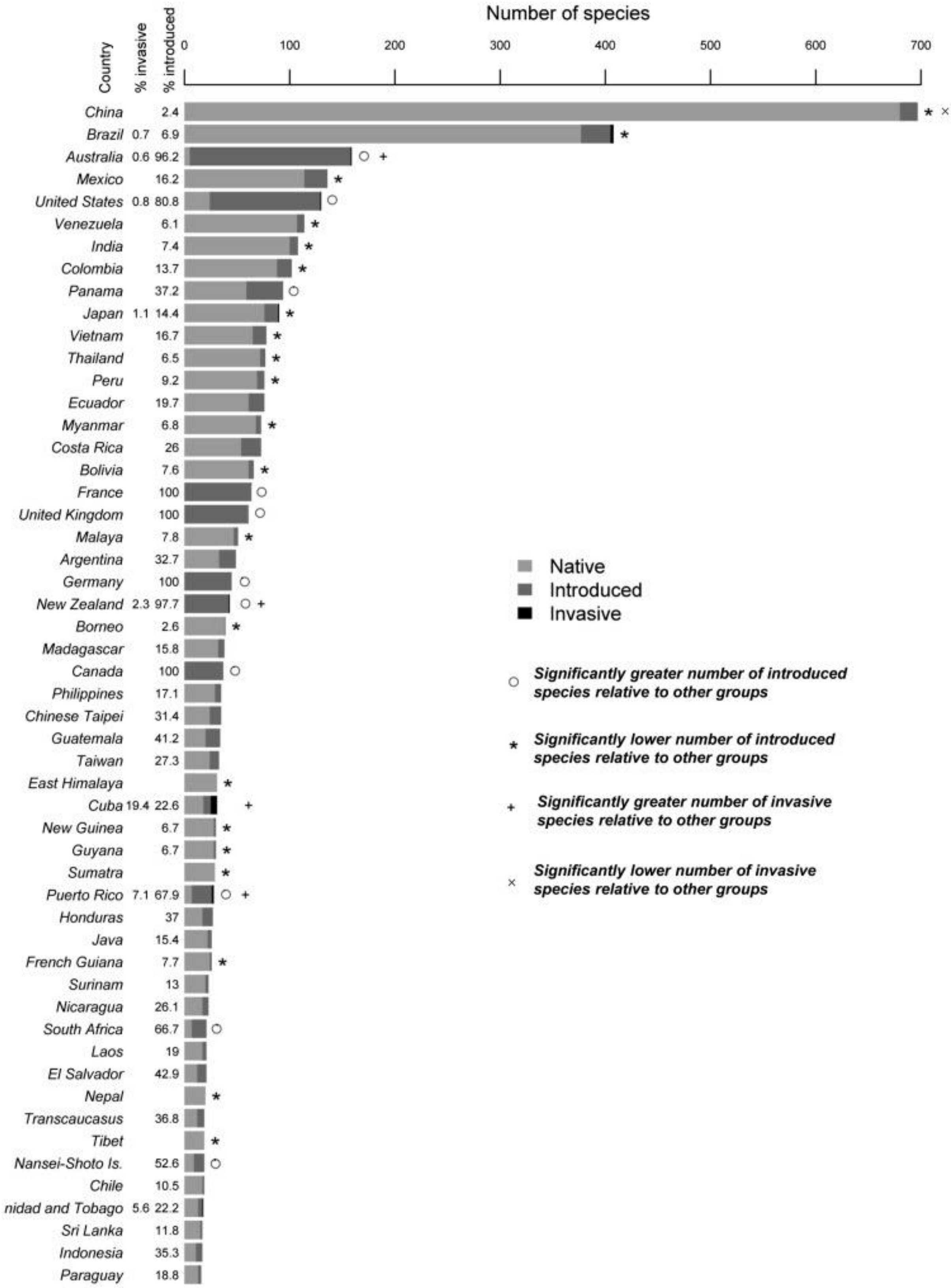

Figure 2.2 **Countries and islands with the highest bamboo richness (Canavan et al., 2017).**

Bamboo species comprise various different growth forms including giant woody species and understory herbaceous species (Canavan et al., 2017; Mulkey, 1986). Bamboo species grow and spread in their habitat through two different growth forms, either sympodial growth popularly known as clumping (Figure 2.3) or monopodial growth also known as runner bamboo rhizome structures (Figure 2.4).

Floral structures are only visible once in a 30-50-year period because bamboo only flowers once in its lifetime at which time seeds may or may not develop. This then encourages vegetative propagation. The flowers are subdivided into two categories namely Dendrocalamus-type known as the closed structure and Bambusa-type known as open floral structure, although these characteristics may also be species dependent (Das et al., 2017). Herbaceous bamboo species are generally temperate species and thrive in regions where there is less sunlight or cool air temperatures (Canavan et al., 2017). By contrast, the giant woody species (e.g. *Pharus latifolius*) that prefers exposure to sunlight are predominant in tropical and subtropical regions where they can optimize their photosynthetic ability due to high radiation levels in low altitude regions (Mulkey, 1986).

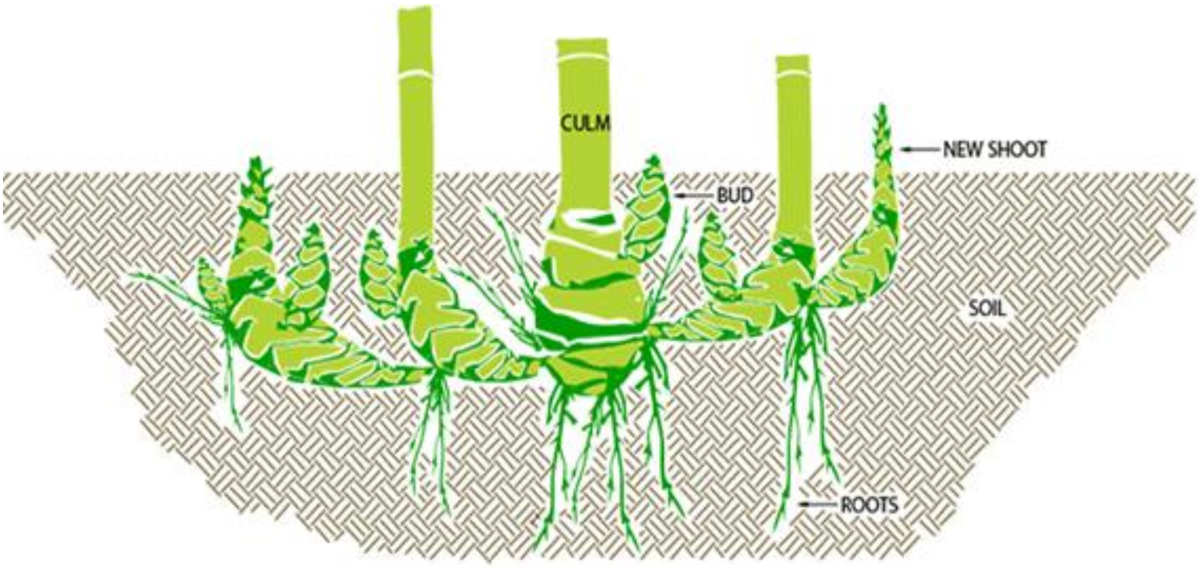

Figure 2.3 A rhizome anatomical structure of sympodial bamboo species (Botanicals, 2019).

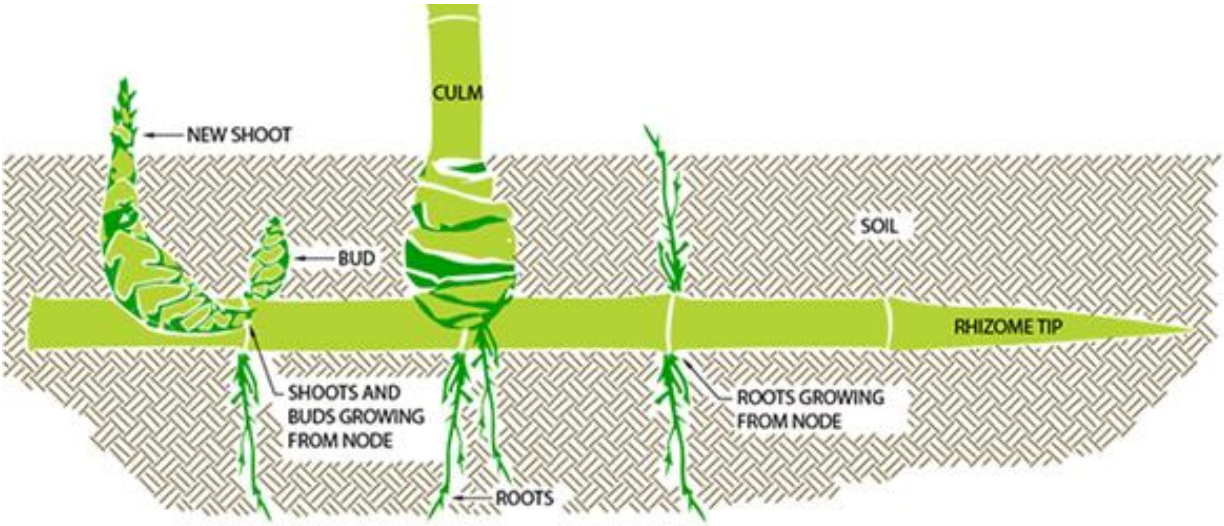

Figure 2.4 A rhizome anatomical structure of monopodial bamboo species (Botanicals, 2019).

Species that grow through monopodial rhizomes are very invasive and tend to be a great threat to the hydrological cycle in a forest (Viana and Filgueiras, 2014). Depending on sufficient resources like sunlight, nutrients, and adequate water, some bamboo plants have a fast growth rate and can reach a height of 30 m within four months (Awalluddin et al., 2017).

This fast growth rate and the highly developed rhizomes beneath the soil surface can result in the development of numerous culms and shoots that forms dense stands and tends to overcrowd (Xu et al., 2020) and compete with other species within the forest habit for water, sunlight and nutrients. Depending on the type of species and rhizome structure, running bamboo (leptomorph) are invasive, aggressive and they form long thread rhizomes that extend to water sources unlike the non-invasive clumping bamboo (pachymorph) which forms thick and dense rhizomes fixed within the cultivated area (Guanglu, 1988).

According to reports, poor management of bamboo plantations has resulted in large impacts on the water resources in many countries. Some reports indicated that bamboo plantations were even abandoned in the early centuries because there was little knowledge concerning management practices and industrial use of the plant (Tsuruta et al., 2016).

However, subsequent research studies and the increase in bamboo production have shown that the previously abandoned plantations are now properly managed and rural communities are benefiting from the productive bamboo plantations. However, more information is needed on the water-use of bamboo. Bamboo fresh shoots are largely constituted of water which indicates the importance of understanding the relationship between bamboo growth and development with water uptake, especially in the early growth stages.

This relationship is important in understanding its impact on stream flow reduction and the effect of species on the hydrological cycle. This review aims to describe the characteristics of the different bamboo species in the world, especially those that are cultivated in South Africa on a commercial scale and highlight how these species may affect the local hydrological cycle in comparison to other commercially grown forest species. Understanding this relationship will assist in decision making, on whether expanding bamboo plantations on a commercial basis will be ideal with regards to the limited water in the country.

Table 2.1 Comparison of culm area (mm^2) and tensile strength ($N\ mm^{-2}$) of bamboo species (Awalluddin et al., 2017).

Bamboo species	**Average culm area (mm^2)**			**Tensile strength (Nmm^{-2})**		
	Top	**Middle**	**Bottom**	**Top**	**Middle**	**Bottom**
Dendrocalamus asper	89.47	98.09	112.96	232.80	200.75	232.31
Bambusa vulgaris	57.31	61.29	67.20	231.67	233.98	230.63
Gigangochloa scortechinii	49.30	48.50	53.04	187.67	144.92	176.22
Schizostachyum grande	48.21	49.18	49.50	149.20	114.93	113.01

2.2 Commercial monopodial bamboo species

Monopodial plants are typically bamboo species characterised by thin rhizomes. These species spread by means of rhizomes under the soil surface to long distances particularly towards moist environments and streams to access large quantities of fresh water and therefore causing a negative impact on water resources. Also, these are known for competing with neighbouring species for sunlight and soil nutrients.

2.2.1 Subtropical and tropical bamboo species

The following selected bamboo species are typical grown in South Africa and thrive in the warmer temperature average around 18 ^{o}C annually.

2.2.1.1 Canebrake (Arundinaria gigantea)

River cane or canebrake, scientifically known as *Arundinaria gigantae* (Walter) Muhl., is among the most accredited eastern North American bamboo species. It is one of the three native temperate bamboo species of North America that grows along the stream banks in moist clayey soils types and in forest edges where soils are water saturated (Krayesky and Chmielewski, 2014; Neal et al., 2012).

Canebrake serves as a habitat for various wildlife species especially threatened species (e.g. arthropods, birds and mammals). The populations of these species are drastically declining because of river channelization, agricultural practices and land degradation (Brantley and Platt, 2001; Dattilo and Rhoades, 2005). Cirtain (2004) reported that many of the canebrake species are already extinct because of human impact on the environment. This is supported by various studies which have shown that this species extinction has subsequently affected the biodiversity in these areas Neal et al. (2012). Other studies have indicated that since the 18th century about a 98% reduction has been observed in canebrake species in North America and this has to be fixed according to Brantley and Platt (2001). Therefore, many studies have been initiated to investigate how the remaining species can be preserved and produced in large quantities to counteract the decline of threatened species because of habitat loss (Cirtain, 2004).

Canebrake species, like other bamboo species, are semelparous (i.e. characterized by a single reproductive episode before death), only flowering once in a lifetime. Longevities of 20 to 100 years before the development of floral structures makes it difficult to propagate the species through seeds.

Therefore, studies have been initiated to investigate alternative methods of propagation. Scientific research has shown that an alternative to seed propagation is to cultivate canebrake species by means of rhizome cuttings and culm cuttings (Krayesky and Chmielewski, 2014).

Nevertheless, this has proven to have limitations due to the poor establishment of vegetative shoots especially after transplanting from the nursery (Cirtain, 2004). Canebrake establishment has the potential to improve the water quality in catchment areas and to control soil erosion caused by excess runoff which erodes topsoil containing organic matter, chemicals and foreign substances (Cirtain et al., 2009).

Through soil stability and stream bank stabilization, the species is said to be of high importance for improving water quality (Neal et al., 2012). Therefore, the reduction in canebrake distribution not only affects biodiversity but also compromises water quality and quantity.

2.2.2 Temperate bamboo species

The following species are typical bamboo species that thrive in cold temperature conditions especially areas with annual temperature ranges from -3 ^{o}C to 18 ^{o}C:

2.2.2.1 Moso bamboo (Phyllostachys edulis)

The rate of burning of fossil fuels in the production of various industrial products has increased significantly over the past two decades, primarily influenced by market demand and creating millions of jobs in the world. Nevertheless, depositing and burning fossil fuels contributes to various toxic gases in the atmosphere such as carbon dioxide, methane, and nitrous oxide. These gases trap heat from escaping the earth surface resulting in global warming and rises in atmospheric temperatures (Seethalakshmi et al., 2009). Extreme temperatures have many consequence including coral bleaching in the sea due to a rising of sea level, and may also cause a reduction in freshwater and subsequently health complications (Lowe et al., 2016), loss in biodiversity (Hughes et al., 2003), and a breakdown of the trophic pyramid (McMichael et al., 2006).

Associated with burning fossil fuels is the high rate of deforestation and land degradation that also contributes to the extreme gas concentrations in the atmosphere. Therefore, these effects have led to research studies on reducing the levels of these toxic gases to the atmosphere by substituting fossil fuels for renewable and sustainable plant species that are environmentally friendly and capture high amounts of carbon dioxide. Bamboo is a good and reliable source of energy (e.g. Moso bamboo) that can be processed either thermally or biochemically to produce various products such as biofuel, charcoal and syngas (Truong and Le, 2014). Due to low moisture content (< 23%), alkali index, ash content and its higher heat value (HHV) than any other agricultural residue, fuel and energy characteristics of bamboo were relatively desirable than other sources currently used (Truong and Le, 2014).

Moso bamboo, which is scientifically known as *Phyllostachys edulis* is a useful bamboo species utilized for energy which is characterized by its ability to fix high carbon dioxide concentrations from the atmosphere (Chen et al., 2018). The species grows very fast and serves as a good source of nutritious food.

Moso bamboo is a temperate woody bamboo species native to East Asia but has been domesticated in the subtropical and tropical regions of China as early as 1700 to be cultivated commercially (Shinohara et al., 2013). Currently, it has occupied over 73.8% of China's forest area (Chen et al., 2018), and about 10% of India's forest area (Shinohara et al., 2013). Moso bamboo has been intensively used for construction purposes and for food production. Nevertheless, many industries have used the plant to manufacture paper and pulp.

In addition, the species is a good source of charcoal replacing coal whose mining causes severe land degradation and water pollution through acid mine drainage (Onozawa et al., 2009). Therefore, these characteristics make Moso bamboo a high economic value plant. However, its extensive use has led to concern over its impact on water resources. Research studies have therefore been conducted to investigate the water use of Moso bamboo species at different growth stages in order to evaluate its hydrological effect. A research study by Komatsu et al. (2010), indicated that these bamboo plants consume large amounts of water for growth and development when they were being compared to neighbouring coniferous plantations. In the latter study, it was found that the species exceeds coniferous water use by 12%.

By contrast, Shinohara et al. (2013), and Onozawa et al. (2009) reported a lower water consumption (10%) than the coniferous plantation and concluded their study by promoting the commercial production of Moso bamboo.

2.3 Commercial sympodial bamboo species

2.3.1 Subtropical and tropical bamboo species

2.3.1.1 Giant thorny (*Bambusa bambos*)

Giant thorny bamboo (Figure 2.5), also referred to as *Bambusa bambos* (L.) Voss, is a south east Asian bamboo, with a clumping growth habit, which grows in the tropical regions of Asia. The species is widely cultivated throughout the Western Ghats Mountains of India because of its good mechanical properties and environmental impact on increasing carbon dioxide fixation and bee collection (Koshy et al., 2001). Figure 2.6 illustrates the distribution of giant thorny bamboo throughout India and Asia showing a high population of the species in Asia, especially around Myanmar, Cambodia, and Thailand.

Giant thorny bamboo has high levels of silica which can be extracted and used to manufacture medicinal products that cure osteoarthritis. The species is also highly recommended for construction, making it an economically valued plant in the rural areas of Kerala in India (Kumar et al., 2006), especially because of its intensive potential for high biomass accumulation (Gupta and Kumar, 2008). Also, studies have indicated that giant thorny bamboo has a high ability to withstand salt concentrated environments and salty water (Pulavarty and Sarangi, 2018), making it a useful plant in salt concentrated environments where other plant species can’t grow. Studies on the impact of commercial cultivation of this species are few. Research concerning the ecological importance and industrial use of the species for various products is therefore recommended.

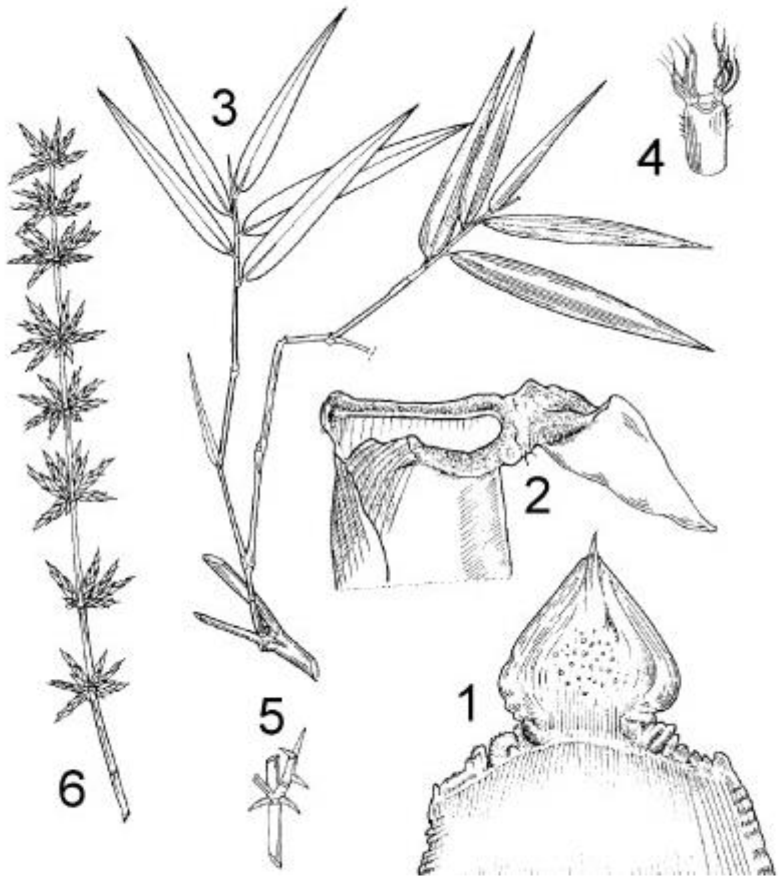

1. Culm leaf (abaxial side) 2. Culm leaf (side view) 3. Leafy branch 4. Top of leaf sheath with ligule and auricles 5: Part of the branch with spines 6: Flowering branch

Figure 2.5 Giant thorny bamboo (*Bambusa bambos*) plant structures (CABI, 2019).

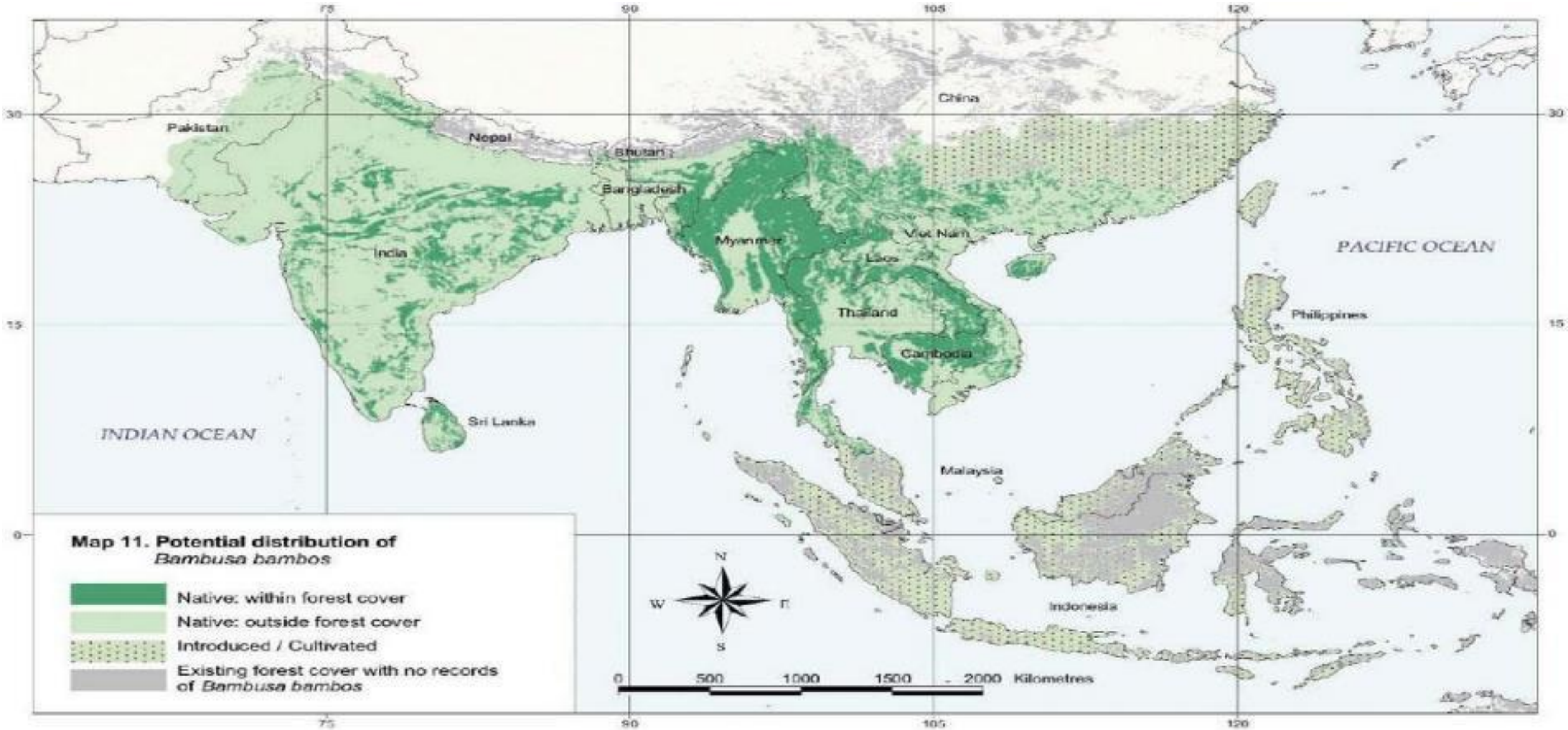

Figure 2.6 Geographic distribution of *Bambusa bambos* in India and Asia (Schröder, 2007)

2.3.2 Temperate bamboo species

2.3.2.1 Hardy bamboo (Fragesia rufa)

The evergreen sympodial bamboo species known as hardy bamboo (*Fragesia rufa* Yi.) is a temperate bamboo that is native to China. The species grows as an understory in the coniferous forests of China and is shade tolerant and also withstands low temperatures (Liu et al., 2017). Hardy bamboo is a dwarf structured bamboo species that has a shallow root system (Plate 2.1) making the species mostly dependent on saturated soil conditions (Liu et al., 2015). The species normally grows along the streams under coniferous plantations to access water easily. A study by Liu et al. (2017) indicated that hardy bamboo cannot withstand dry environments with low rainfall and where their roots cannot access water easily. This has negative consequences in unfavourable growing conditions which cause early flowering, leaf abscission and premature death.

Fragesia rufa serves as the main source of nutritious food for forest pandas. Therefore, temperature increases, river channelization, and urbanization which adversely affect water availability are having a negative effect on forest panda populations because of food scarcity. Therefore, transplanting has been implemented as a means to prevent the extinction of hardy bamboo and also to conserve panda species (Liu et al., 2015).

Plate 2.1 Hardy clumping bamboo (*Fragesia rufa*) root structure (Botanicals, 2019).

2.4 Commercially grown bamboo species in South Africa

The following species are commercially grown in South Africa for industrial purposes and in large areas both in KwaZulu-Natal and the Eastern Cape:

2.4.1 Balcooa (Bambusa balcooa)

Bambusa balcooa Roxb. (Bambusoideae) is a tropical clumping species that is indigenous to India (Ray and Ali, 2016). It is an economic investment plant due to multiple uses in industry, for paper and pulp production (Sharma and Sarma), and can be processed to produce biofuel, syngas and charcoal (Le, 2014). Recently, in South Africa balcooa has gained popularity. Globally, the species serves as a good source of nutritious food consumed in most regions of Asia and China, especially in rural areas (Ray and Ali, 2016). Due to its nutritional value, there has been a growth in bamboo food production industries and the bamboo pickle industry (Sharma and Sarma). In ancient times, this species was only popular with rural communities as a source of food and as a poor man's timber, but recently industries are encouraging cultivation of balcooa bamboo species for various food products for wider consumption.

Studies have indicated that the species has the potential to grow up to 25 meters in most favourable environments under tropical humid climatic conditions (Upreti and Sundriyal, 2001), and in moist alluvial flat environments with altitudes of 1500 m above the sea level (Sharma and Sarma). Cultivation of this species has the potential to improve climatic conditions because of its high potential for carbon sequestration which can be used to ameliorate anthropogenic negative effects on the environment. It can be cultivated worldwide to improve climatic conditions by reducing carbon dioxide concentrations of up to 17 tons per year by a hectare bamboo plantation (Seethalakshmi et al., 2009). This can also improve air quality, oxygen concentrations and reduces air pollution (Seethalakshmi et al., 2009). Moreover, agricultural industries have adopted cultivating the species as a means of reducing high wind velocities that affect cultivated crops by causing lodging and fruit drops before fruit maturity. It also has the potential for improving soil stability and soil properties (Amlani et al., 2017).

There have been studies aimed at developing effective propagating techniques for *Bambusa balcooa* that allow optimum growth, plant tolerance to various conditions and diseases that also promotes growth at a fast rate for sustainability (Negi and Saxena, 2011). In South African nurseries, rhizome cuttings and culm cutting are the main propagating techniques.

However, several concerns include the difficulty in transporting the propagating material and the bulkiness of the material. This has initiated the development of *in vitro* propagation (micro propagating through tissue culture) in order to promote sustainable production to meet market demands (Amlani et al., 2017).

2.4.2 Sweet bamboo (Dendrocalamus asper)

Economic and environmental factors play an essential role in the extensive bamboo cultivation throughout the world. For industries, the high return for bamboo plantations has changed perspectives causing a switch from other products to bamboo cultivation. Among the most, cultivated bamboo species on a commercial scale is *Dendrocalamus asper* (Schult.) Backer, a tropical sympodial bamboo with a pachymorph rhizome (Figure 2.7), native to Southeast Asia and Indonesia (Chandramouli and Viswanath, 2012). It comprises various cultivars which are important for the production of different products (Sujarwo et al., 2015). This species is used extensively for the reclamation of many previously abandoned agricultural lands. Lands previously cultivated with *Dendrocalamus* bamboo species are now protected and properly managed due to new industrial interest and high returns for growing the crop (Chandramouli and Viswanath, 2012).

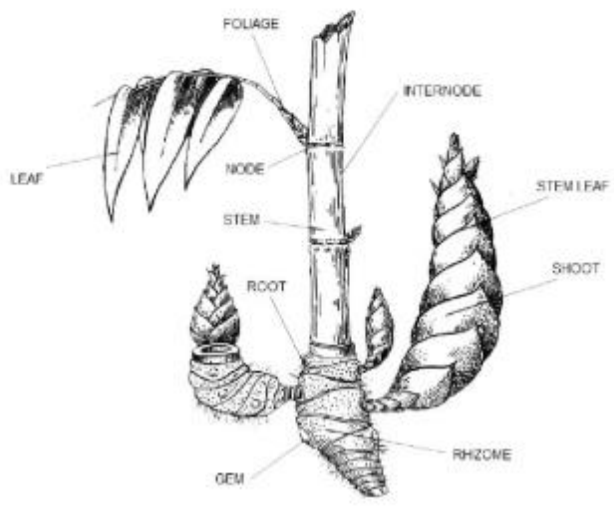

Figure 2.7 Pachymorph rhizome of sweet bamboo (Lahr et al., 2015)

Sweet bamboo has been introduced to the African continent and has been cultivated extensively in countries like Madagascar, the Democratic Republic of Congo, Kenya and Ghana. There is no information indicating its cultivation in South Africa. However, tropical regions in South Africa like northern KwaZulu-Natal, Limpopo and the Eastern Cape could have suitable climatic conditions for the cultivation of sweet bamboo.

Sweet bamboo is a worldwide accepted species, as a source of nutritious food to numerous rural households (Singh et al., 2012). Its use in the food industry has increased in the past decades (Shroti et al., 2012), because of its high crude fibre content in fresh shoots. The fibre extracted from the fresh shoots has been used to enhance the fibre content of yoghurt, bread, cheese, and the manufacture of pasta products (Felisberto et al., 2017). These products are exported to international markets. Felisberto et al. (2017) have also shown that sweet bamboo's fresh culms constitute 16g/100g starch, 79g/100g of fibre and less than 2% lipid content making them a highly nutritious food source.

Sweet bamboo is cultivated through rhizome and culm cuttings for commercial purposes (Shroti et al., 2012). However, modern techniques are being developed such as micropropagation using *in vitro* techniques (e.g. tissue culture, protoplast fusion, embryo rescue) (Shroti et al., 2012). These techniques are being used to optimize the level of production in order to meet the industrial demand.

However, currently it has been evaluated that cultivation of rhizomes as a planting stock gives a much better yield and carbon biomass. For example, in a study by (Sujarwo et al., 2015) it was concluded that rhizome propagation had much better yield than culm propagation. An efficient propagating technique is essential, especially because bamboo's propagating material is difficult to handle, transport is difficult and growth is slow using existing procedures. In addition, factors like soil conditions, rainfall, aspect, and altitude are important factors for biomass accumulation (Chandramouli and Viswanath, 2012).

There are other species suitable for South Africa's sub-tropical environmental conditions like *Bambusa bambos,* and *Bambusa nutans,* which can be cultivated for large scale commercial production. However, due to little available information about the species water use, mechanical properties, and plant behaviour, various research projects are being developed to address these knowledge gaps.

2.4.3 Small scale cultivated bamboo species in South Africa

Other species cultivated in South Africa are *Bambusa oldhamii* commonly known as giant timber bamboo, *Dendrocalamus hamiltonii* and Berg bamboo (Table 2.2). The latter is scientifically known as *Thamnocalamus tessellatus* and is endemic to South Africa and to the high mountains of Lesotho and Swaziland.

This species is the only African bamboo having the ability to grow in other parts of the world due to its hardiness. Apart from the Berg bamboo, each of the species mentioned above is commercially cultivated in South Africa, mostly in the Eastern Cape and KwaZulu-Natal. They are being grown for both industrial and ecological uses. Industrial uses include construction, paper, and furniture while ecologically they are grown for carbon sequestration, water quality and soil improvement.

Table 2.2 Indigenous bamboo species in South Africa and growing conditions in relation to adapted environments

Species name	Native	Growth form	Climate	Environmental conditions	Area adapted in SA
Emily van Rijswick sp.	Asia	Clumping	Tropical	Prefer poor soils	Eastern Cape (St. Albans)
Berg bamboo (*Thamnocalamus tesselatus*)	South Africa	Clumping	Temperate	Prefers river & cave edges Altitude 1200-2400 m	Drakensberg
Bambusa balcooa	Northern India	Clumping	Tropical	Heavy soils, 600 mm rainfall/year Altitude 700 m above sea level	Eastern Cape, Western Cape
Bambusa vulgaris	Unknown	Clumping	Tropical	Altitude 1000-1200 m	Across Africa
Dendrocalamus asper	Indonesia	Clumping	Subtropical, Tropical	Loamy, Black soils	PMB, DBN North Coast
Bambusa oldhamii	Taiwan (China)	Clumping	Tropical	Average water Clay, Loam & sand soils	
Dendrocalamus hamiltonii	Asia	Clumping	Subtropical, Tropical	Average water, Altitude 870-1800 m Well-drained loam soils	
Phyllostachys nigra	China	Runner	Temperate	Rich in nutrients topsoil	Cape Town

Acknowledgement
(https://www.brandsouthafrica.com/investments-immigration/economynews/bamboo-051211)
(https://www.arkive.org/berg-bamboo/thamnocalamus-tessellatus/)
(https://www.ecoplanetbamboo.za.com/)
(https://www.scribd.com/document/141583688/African-Bamboo-Species)
(http://www.brightfields.co.za/bamboo-plants-for-sale/)
(http://www.learn2grow.com/plants/bambusa-oldhamii/)
(http://nbm.nic.in/PDF/Manual_Bamboo_Plantations.pdf)
(http://plantinfo.co.za/plant/phyllostachys-nigra/)

2.5 Bamboo market in South Africa

In recent years, most African countries excluding South Africa, have engaged in working with the International Network for Bamboo and Rattan (INBR) to develop the market, establish large scale plantations and industrial processing in order to manufacture various bamboo products (Scheba et al., 2018). The bamboo industry and research in South Africa are still developing (Figure 2.8) with small exports to international markets. Most of the bamboo plantations, especially giant bamboo '*Bambusa balcooa*', grow naturally in the Eastern Cape, South Africa and about 13 million tons are exported to India and China industries for processing (Dunbar, 2018). The species is also economically important for paper pulp manufacturing industries (Dunbar, 2018).

There are also various South African industries and societies that promote bamboo cultivation and use the plants to manufacture various products to meet market demands (e.g. Bamboo Revolution is an industry that produces bamboo watches). It also has the potential to provide an environmentally friendly alternative to single use plastic and polystyrene as the products of processed bamboo are 100% biodegradable (Nurul Fazita et al., 2016). In addition, bamboo products such as flooring, furniture, charcoal and plywood are increasing in popularity. The Eastern Cape Development Corporation (ECDC) is a society promoting bamboo cultivation in South Africa.

The domestic market has the potential to increase in South Africa. For example, since bamboo plantations can be used to generate energy, industries that supply energy like Eskom can switch from the use of coal to a bamboo energy supply (Busani, 2011).

2.6 SFRA status and exotic bamboo distribution in South Africa

Since 1875, South Africa have been totally depending on alien forest species to meet up with the demand for timber (Van der Zel, 1995). These species have been densely distributed in the southern and eastern regions where there is high rainfall. With high rate of distribution, concerns over the stream flow reduction on water resources led to the formation of research network that aims at assessing the impact of such species on water resources through long term monitoring as back as 1935 (Dye and Versfeld, 2007).

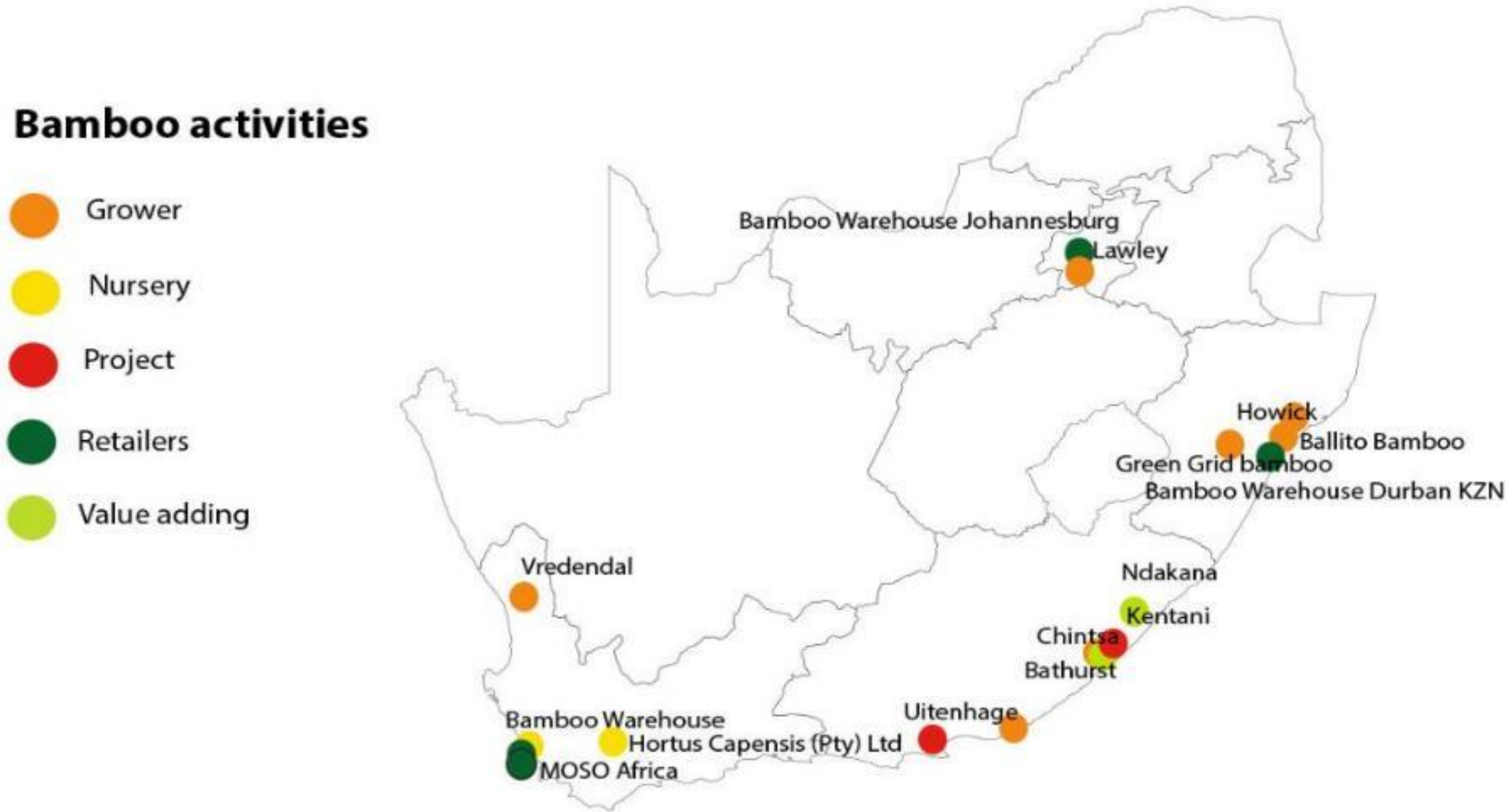

Figure 2.8 Bamboo activities in South Africa (Scheba et al., 2018).

Through advancement, studies involving monitoring forest, grassland and other vegetation transpiration and evapotranspiration using HRM and meteorological instruments were done.

Continuous cultivation of different bamboo species in South Africa due to the interest in bamboo properties has led to an alarming rate and concern for bamboo invasion just as it has been indicated in other part of the world (Canavan et al., 2021). There is very limited information on bamboo water-use globally, economic and environmental impact of these species. Therefore, understanding of alien taxa is critical in projecting the associated future risks and potential impacts of bamboo species in the hydrological cycle and invasions.

With high population of different types of bamboo species along the coast in South Africa, particularly KwaZulu-Natal (Durban) and in the Cape region, this cause a great concern (Figure 2.9). Also, as these areas are characterised by high rainfall and temperatures, studies on the water-use of these species are necessary. Tourism has been predicted as a major factor since many varities of bamboo species are used for ornamental purposes and art.

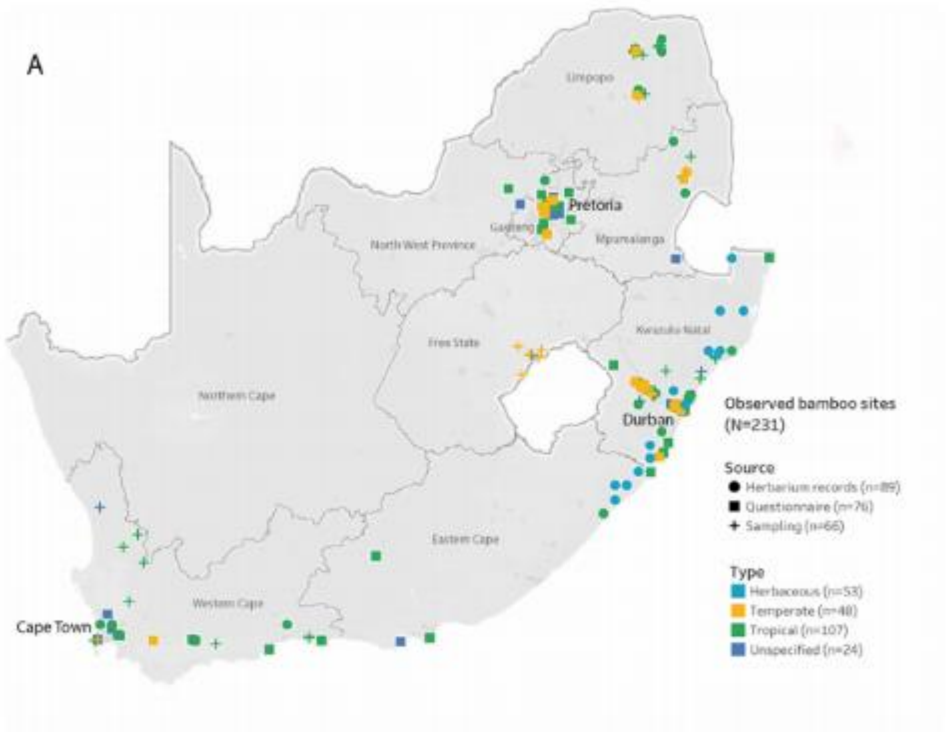

Figure 2.9 Distribution of different types of alien bamboo species in South Africa from 1896 to 2017 (Canavan et al., 2021).

2.7 Water-use and sap flow quantifying techniques

2.7.1 Understanding evapotranspiration and environmental effects

Water is essential for plant growth and development. Plants use water for metabolic activities and physiological processes. Therefore, soil moisture is absorbed by plants through fine roots and is translocated by the xylem tissue cells to leaves for photosynthesis and carbohydrate or sugar synthesis. Absorbed water can then be lost through stomatal openings in plant leaves (transpiration) due to changes in environmental conditions. Environmental conditions such as warm air temperatures, low relative humidity, soil moisture, wind and light play a crucial role in the rate of plant transpiration and soil evaporation (Figure 2.10). Therefore, quantifying the water-use of different plant species in relation to the environmental and human effect are very important aspects in understanding effect of biodiversity on water resources (Schmidt et al., 2009). Then, technological practices and techniques that measure and monitor plant water-use are required to understand the usage of available water. However, understanding and modelling the water-use of different plant species has been a great challenge for decades.

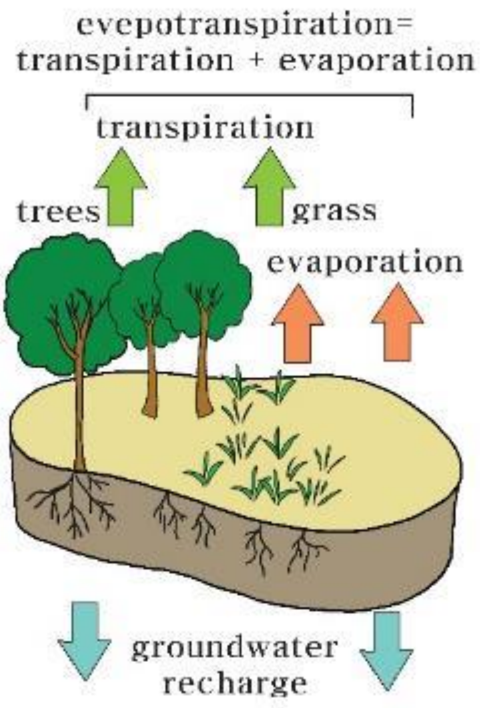

Figure 2.10 Schematic diagram for evapotranspiration (Muhammad, 2018)

Both indirect and direct methods have been used to measure transpiration and water-use of tree species. Indirect methods include the micrometeorological measurements of evapotranspiration, which can be used to estimate the plant water-use. An alternative approach is the indirect estimation of water-use based on of soil moisture balance calculations.

Major limitations of indirect methods may include factors such as soil type, time of measurement and the prevailing meteorological conditions. Therefore, setting up an automatic weather station (AWS) can be useful in data interpretation and referencing. However, water-use can also be measured directly using stem heat balance (SHB), trunk sector heat balance (THB), thermal/heat dissipation (HD), heat field deformation (HFD) and heat pulse method (HRM) techniques that measure sap flux density passing through a point in a stem (Smith and Allen, 1996).

2.7.2 Effect of bamboo structure on water-use

The fast growth rate of bamboo species necessitates research on its potential impact on South Africa's scarce water resources. Transpiration rate and evapotranspiration are essential components to assess their potential effect on water resources. These components affect the available water yield and through the catchment water balance. Therefore, various studies have been conducted to understand the effect of different forest species on the local water cycle (Tsuruta et al., 2016). However, there is very limited information regarding water-use of commercial bamboo species on the local water cycle. Since bamboo is a monocotyledonous grass and hollow within the stem structure (Figure 2.11), the vascular tissue arrangement differs from other forest species. Metaxylem (Mx) and phloem (P) tissues are not uniform and are located within fibre caps at the inner and outer part of the culm wall (Wang et al., 2012). This then makes it difficult to quantify the water-use using standard approaches.

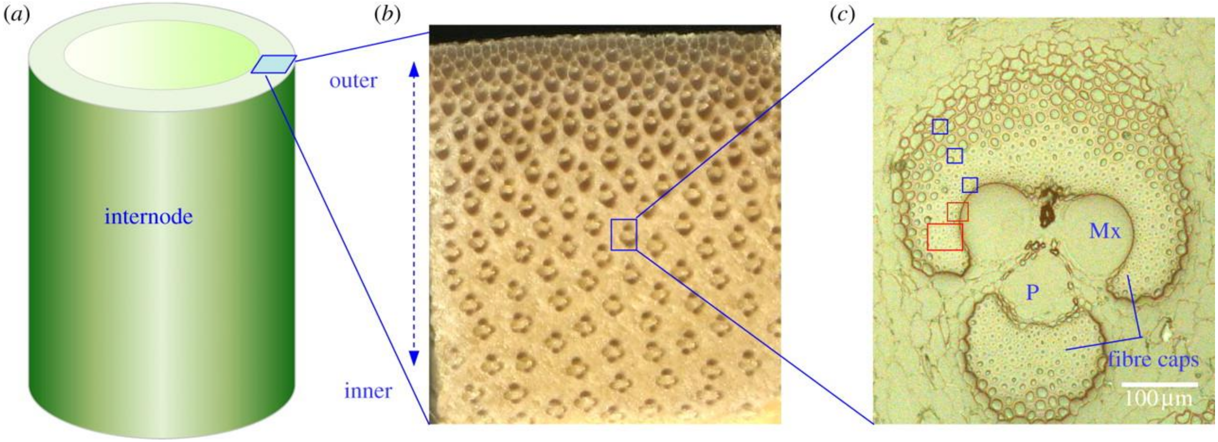

Figure 2.11 a) Cross-section of Phyllostachys pubescens bamboo species b) cross-section of culm wall showing vascular bundle arrangement and c) vascular bundle with metaxylem (Mx), phloem (P) and fibre caps (Wang et al., 2012).

However, the expansion of bamboo plantations is predicted to have an impact on water resources in the country, due to their reported high growth rates. Water resource managers are therefore concerned regarding the threat that bamboo expansion will have on South Africa's water security. This is, especially true for invasive monopodial bamboo species because of their high potential to aggressively spread, forming dense culms and thin rhizomes that extends horizontally under the soil surface over long distances to water sources (Tsuruta et al., 2016).

Sympodial species, with dense and numerous leaf structures, may also be high water users. In addition, the continuous rise in temperature due to global warming will increase transpiration. Transpiration in various species is a process that has been globally used to measure the amount of water uptake by different plant species and to evaluate their effect on the terrestrial water cycle (Laplace et al., 2017). It has been reported that bamboo species have higher transpiration rates when compared to other forest species (Laplace et al., 2017), however, the quantity of water used by bamboo plants differs among species. Also, factors like culm age, rhizome architecture (Tsuruta et al., 2016), climatic conditions (rainfall, solar radiation, air temperature, vapour pressure deficit and relative humidity), culm diameter (Tsuruta et al., 2016), and soil properties (thermodynamic potential) in relation to bamboo high root pressure (Yang et al., 2015) are factors which can affect the water uptake and subsequently transpiration.

A culm of bamboo is characterized by vascular bundles that lack secondary growth and do not regenerate after sprouting (Tsuruta et al., 2016; Yang et al., 2015). This characteristic promotes a high water uptake by the roots to supply the transpiration system of the plant during the day. A matured bamboo plantation has been estimated to have used on average 3.29 mm of water per day (Table 2.3) (Kleinhenz and Midmore, 2000). There are various sap flow measuring techniques that are used to measure the amount of water utilized by different plant species for growth and development.

Table 2.3 Estimated transpiration of mature bamboo species (Kleinhenz and Midmore, 2000).

Parameter	Value	Unit	Source
Leaf biomass (dry)	5	[t] [ha]$^{-1}$	overseas literature
Leaf dry/fresh weight	10	[%]	own measurements
Leaf biomass (fresh)	0.5	[t] [ha]$^{-1}$	own calculation
Specific leaf area	150	[cm leaf area]^{2} [g dry leaf]$^{-1}$	overseas literature
Specific leaf area	15	[cm leaf area]^{2} [g fresh leaf]$^{-1}$	own calculation
Leaf area index	7.5	[m leaf area]^{2} [m soil surface]$^{-2}$	own calculation
Transpiration rate	2.3	[mmol water] [m leaf area]$^{-2}$ [s]$^{-1}$	own measurements
Transpiration rate [a]	0.04	[ml water] [m leaf area]$^{-2}$ [s]$^{-1}$	own calculation
Water usage [b]	13	[l water] [m soil surface]$^{-2}$ [day]$^{-1}$	own calculation
Water usage [c]	9	[l water] [m soil surface]$^{-2}$ [day]$^{-1}$	own estimation
Water usage	3,285	[mm water]^{1}	own calculation

[a] Atomic weight of H_2O: 0.018 [g] [mmol]$^{-1}$
[b] ie Water usage at maximum transpiration rate for 12 [h] [day]$^{-1}$
[c] ie Water usage at estimated average yearly transpiration rate

2.7.3 Measuring bamboo water-use

2.7.3.1 Granier's thermal dissipation probe (TDP)

The thermal dissipation method is a continuous sap flow measuring technique that has been intensively used in forest hydrology to measure the amount of water a plant species utilizes (Lu et al., 2004). It is used to estimate the stand-scale transpiration of sampled trees and subsequently forest water-use. The method has been recommended and therefore adopted globally due to low costs and reliability (Yang et al., 2015). For example, in a study by Lu and Chacko (1998) the technique was recommended for the young mango trees, in Australia.

The technique measures the daily sap flow of trees which can be summed to the total monthly and annual transpirations.These values can then be used to justify the water-use of tree species in relation to changes of environmental conditions. However, bamboo culm structure and anatomy have proven to be the limiting factors in measuring precise water-use due to vascular cells arrangement and therefore careful selection of probe lengths in alignment to sapwood area is necessary so as to avoid underestimating the actual transpiration (Laplace et al., 2017).

The TDP system has been considered a sensitive sap flow system, senses the change in sap flux density caused by either girdling, excision or defoliation (Lu and Chacko, 1998). Although the sap flow techniques have been used extensively in temperate bamboo species, especially those with thicker culm structures, little work has been done for tropical bamboo species in measuring their transpiration rates (Laplace et al., 2017). Even though not much work has been done for tropical bamboo species there is some research which has applied technical instruments like the stem steady state heat balance gauge, heat pulse method and stem tissue heat balance system to various plant species to measure their transpiration rates.

2.7.3.2 Stem steady state (SSS)

A stem steady-state energy balance system is another alternative sap flow measuring technique that involves the application of constant continuous heat energy (J s^{-1}) around the portion of tree trunk instrumented (Figure 2.12) through a heater and thermocouples that measures energy loss both vertically upwards and downwards (as sap passes through) and the heat stored in the tree trunk or bamboo culm (Vellame et al., 2010).

Lascano et al. (2016) indicated that the system has been modified from a wire intensive system to a less intensive wiring system, which has a flexible heater and improved thermal contact between temperature probes and the tree trunk. The latter system (Figure 2.13) consists of a heater, thermocouples, and insulators and can also be used on species with smaller diameters (Lascano et al., 2016). The method involves measuring temperature differentials by two temperature sensors at different tree stem points in order to calculate the crop transpiration. The following equations describe calculation of crop traaspiration using the former and latter system:

Calculation of crop transpiration using former system (Figure 2.12):

$$P - q_a + q_r + q_c + S = 0 \quad 2.1$$

$$q_a = q_u + q_d$$

where P (heat flux) applied to the heater, q_a is the axial heat loss (W), q_r is radial heat loss (W), q_c is the convective heat loss (W), S being the storage term normally negligible for smaller plants (assumed to be zero), q_u is the heat along upward path of the heat flow (W) and q_d is the heat along downward (W).

$$P = \frac{E^2}{R} \quad 2.2$$

where P is the power of heater (W) is calculated from the Ohm's law using the input emf voltage (V) and resistance (Ohms) of the heat.

$$q_{u,d} = K_{st} \text{ x } A \text{ x } \frac{dT_{u,d}}{dx} \quad 2.3$$

where K_{st} is the thermal conductivity of the stem (W m^{-1} $^oC^{-1}$), A is the cross sectional area of the stem (m^2), dT_u and dT_d are temperature gradients (^{o} C) above and below heater and dx is the spacing between thermocouple junctions (m).

$$q_r = K_{sh} \text{ x E} \quad 2.4$$

where K_{sh} is the sheath conductance (W/V) obtained when sap flow rate F is assumed to be approximately equal to 0 (at dawn or before sunrise) and E is the output of the thermopile

$$q_c = C_p \text{ x } F \text{ x } (T_u - T_d) \quad 2.5$$

where C_p is the specific heat capacity of water (J kg^{-1} $^oC^{-1}$), F is the sap flow rate in the stem (kg s^{-1}) also equivalent to crop transpiration and T_u and T_d are average temperatures (^{o}C) of sap flow in and out of the system.

Therefore,

$$F = [\frac{P - (K_{st} \text{ x A x } \left(\frac{dT_u + d\,T_d}{d_x}\right) - K_{st} \text{ x } E}{C_p \text{ x } (T_u - T_d)} \quad 2.6$$

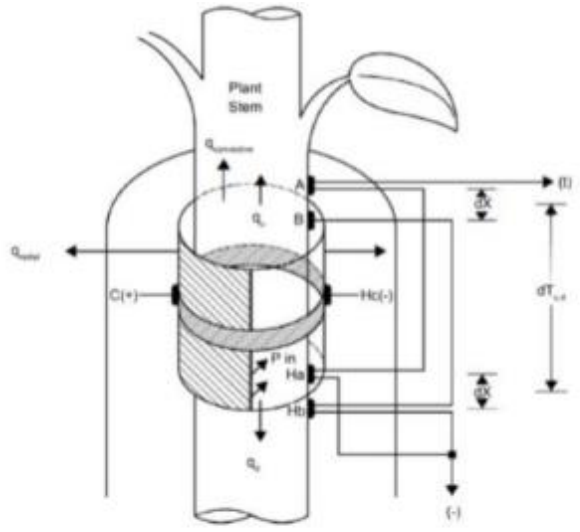

Figure 2.12 Schematic diagram of former stem flow sensor (Lascano et al., 2016).

Calculation of crop transpiration using EXO-Skin sap flow sensor (latter system) (Figure 2.13):

Equation (H) is based on the assumption that all energy losses through conduction are grouped into q_c calculated from radial thermopile. The axial (q_a) and radial (q_r) heat losses were combined into a single variable (q_f) results to valid energy balance. Therefore, $q_r = q_a + q_r$, then:

$$P = q_c + q_f \qquad 2.7$$

Ksh calculates the sheath conductivity (Ksh) assuming F is approximately equals 0,

$$K_{sh} = \frac{P}{E} \qquad 2.8$$

dT is calculated from mean temperatures (A_h and B_h) measured with the two thermocouples (type T-thermocouple, 0.040 mV $^oC^{-1}$)

$$dT = \left[\frac{A_h + B_h}{2}\right] \text{x } 0.040 \qquad 2.9$$

Therefore,

$$F = [\frac{p - q_c}{c_p}] \text{ x } dT \qquad 2.10$$

where F is the sap flux (kg/s), P is the power of heater (W), q_c is convective heat flux (W), Cp is the specific heat capacity of water (J/kg. °C) and dT is the average temperature measured with two thermocouples (°C).

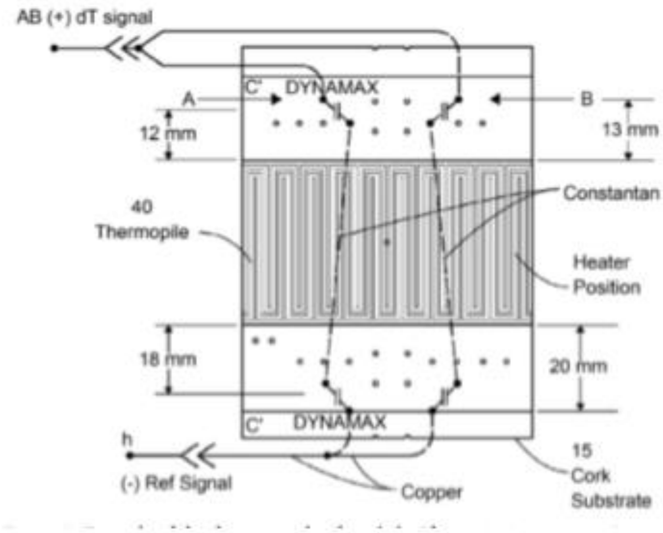

Figure 2.13 Schematic diagram of EXO-SkinTM Sap flow Model SGEX-13 (Dynamax Inc., Houston, TX) (Lascano et al., 2016).

Measurements can be done under steady state conditions by insulating a small stem portion and the intact thermocouple sensors from the sunlight and rainfall (Savage et al., 1993). The instrument is installed 200-700 mm above the soil surface (Savage et al., 1993), to prevent soil, water and insects from damaging the sensor. Water-use of mature bamboo culms can be estimated if total leaf biomass and specific leaf area are known. These values can be used to calculate the total leaf area and subsequently transpiration rate which are important parameters for estimating water-use (Kleinhenz and Midmore, 2000).

2.7.3.3 Heat ratio method (HRM)

The Heat Ratio Method is a heat ratio method technique used to measure sap flow. This technique has been successfully used worldwide to quantify water-use for different woody plant species and has been extensively used by researchers in South Africa (Gush, 2008). The technique uses a thermometric device to measure sap flow rates or water-use of woody plant species. The device is based on a three-probe configuration and is characterized by two temperature probes (downstream and upstream) that are inserted at an equal distance from a heater probe that discharges a short pulse of heat (Figure 2.14).

The heat acts as a tracer and is used for measuring the ratio of the downstream to upstream probe every sixty seconds following a heat pulse from the heater and this is used to calculate sap velocity (Burgess et al., 2001).

The HRM system was first proposed by Marshall (1958) to calculate heat velocity (V_h) in larger plants such as forest species whereas Hogg et al. (1997), developed it to calculate sap velocity (S) of smaller plants. The heat ratio method (V_h) is then calculated from Burgess et al. (2001):

$$V_h = \frac{k}{x} \ln\left(\frac{V_1}{V_2}\right) 3600 \qquad 2.11$$

where V_h is the heat velocity (cm hr^{-1}), k is a thermal diffusivity of fresh wood, x is the distance of each temperature probe from heater probe (cm) and V_1 and V_2 are temperature increases in upstream and downstream probe (^{o}C) at equidistant points.

The sap velocity is based on the following equation based on Hogg et al. (1997):

$$S = \frac{K_{cw} \ln(\frac{T_u}{T_l})}{X C_{pw} P_w} \qquad 2.12$$

where S is the sap velocity (cm hr^{-1}), K_{cw} is a thermal conductance, C_w is the specific heat of sap (4180 J/kg/^{o}C) and T_u and T_l are the temperature rises in upstream and downstream probe (^{o}C).

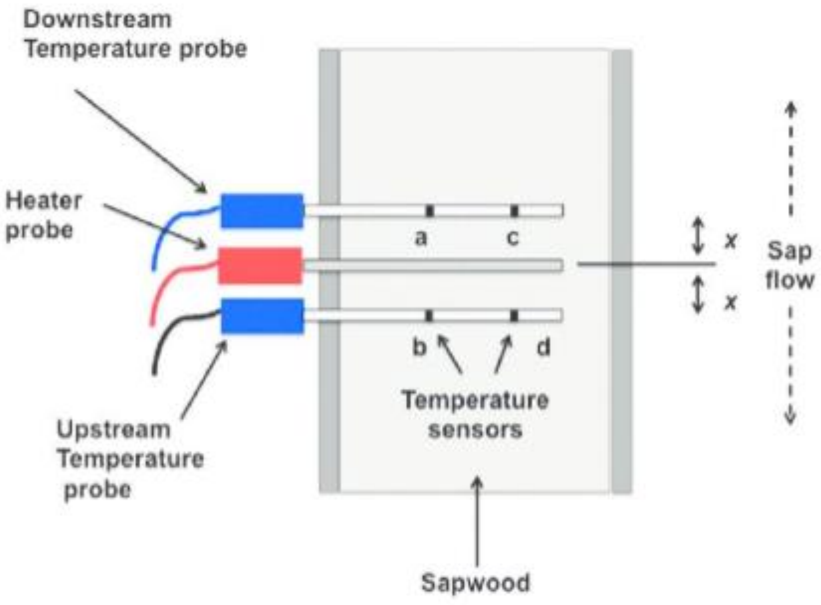

Figure 2.14 **Schematic diagram of Heat ratio method (Bayona-Rodríguez and Romero, 2016).**

2.8 Bamboo sap flow measuring challenges and limitations

The above thermoelectric technologies have been successfully used in dicotyledonous stems, which have a pith at the centre of the stem surrounded by vascular bundles. One of the challenges of determining the water-use of bamboo is that bamboo is a monocotyledonous grass species having stems with scattered vascular bundles near the outside edge of the stem and no pith region. These vascular bundles lack secondary growth and do not regenerate after sprouting (Tsuruta et al., 2016; Yang et al., 2015). This characteristic promotes a high amount of water uptake by the roots to supply the transpiration system of the plant during the day. By contrast, dicotyledonous stems have their vascular bundles in a ring porous. Therefore, the heat ratio methods that have been successfully developed to measure the water-use of dicotyledonous tree species, may not be suitable for bamboo species.

Other factors that need to be taken into account when measuring the water-use of bamboo are culm age and diameter (Tsuruta et al., 2016), and soil properties (Yang et al., 2015) which can affect the water uptake and subsequently transpiration. Since the heat ratio sensors quantify sap flow with respect to depth of temperature probes in a stem, it is necessary to determine the sapwood area of each culm in a bamboo clump.

2.9 Conclusion

There is still a gap in understanding the relationship between various bamboo species and the hydrological cycle, and how these components affect the quantity and quality of available water. This is particularly so in South Africa where bamboo water use has not been determined before. Therefore, understanding this relationship is crucial for optimizing the water resources in a drought prone country like South Africa.

3. Materials and methods

3.1 Meteorological station

3.1.1 Automatic weather station (AWS)

Meteorological data were required as input for calculations to determine total transpiration and interpret sap flow data (Allen et al., 1998). These data were obtained from the automatic weather station (AWS), which was installed in a nearby grassland site in August 2018 (Plate 3.1). The AWS was placed on a short uniform grassland area to meet the requirements of the FAO 56 reference evaporation (ET_o) calculations (Allen et al., 1998). A Campbell Scientific CR1000 datalogger recorded the air temperature (CS500, Vaisala Inc., Helsinki, Finland), the relative humidity (CS500, Vaisala Inc., Helsinki, Finland), the wind speed and direction (Model 03002, R.M. Young, Traverse City, Michigan, USA), the solar radiation (Kipp and Zonen CMP3) at 2 m and the rainfall (TE525, Texas Electronics Inc., Dallas, Texas, USA) at 1.2 m. Data from the station were downloaded at hourly intervals to the logger linked via a modem to the UKZN AIM server (Perdrial et al., 2020).

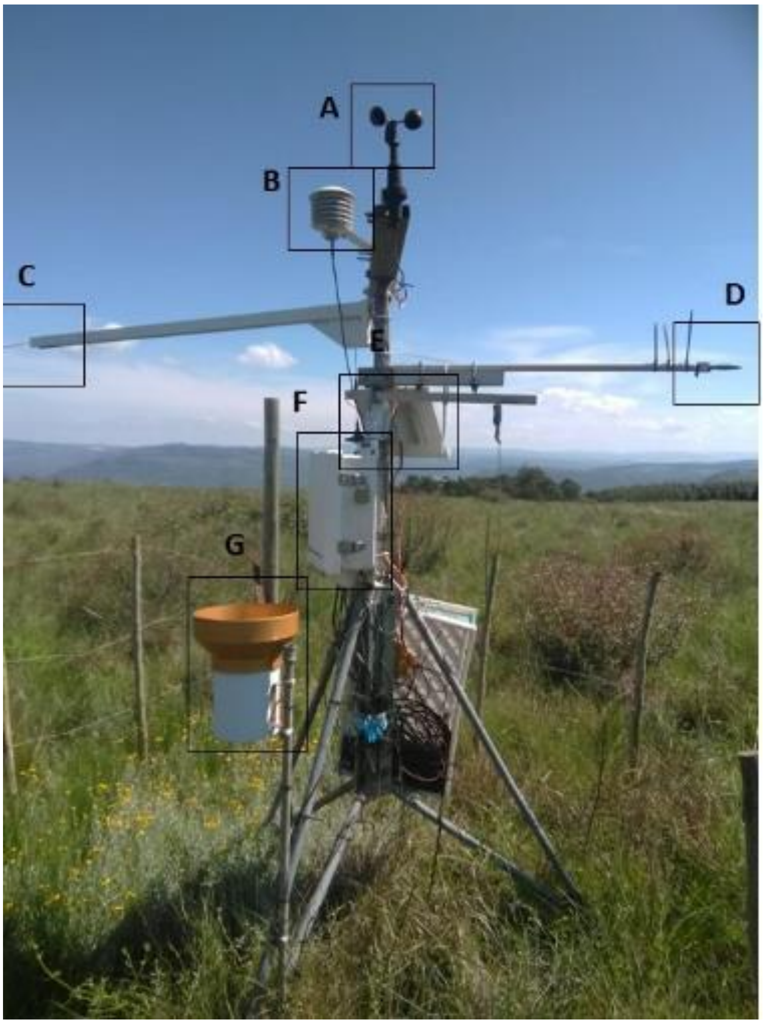

Plate 3.1 Automatic weather station A) anenometer, B) temperature and RH probe shield, C) thermocouple wire, D) NR lite net radiometer, E) solar panel, F) datalogger box and G) rain gauge at Shooters Hill, KwaZulu-Natal.

3.2 Volumetric water content (VWC)

Soil water content probes were placed at each site to measure the hourly volumetric water content (VWC). These measurements coincided with the hourly sap flow measurements of the HRM and Dynamax systems.

At each site, a pit was opened and three Campbell Scientific CS 616 TDR probes, connected to channels on the CR1000 data logger, were inserted horizontally at 0.2, 0.4 and 0.7 m, to ensure the soil water profile was monitored (Plate 3.2).

These consisted of two 0.3 m long stainless rods (wave guides) and electronics designed to measure the water content using the time domain frequency technique with a CR1000 datalogger (Kelleners et al., 2005).

The probes were positioned to measure total profile water content from the surface to 0.8 m depth. The depth was sufficient to cover the zone of active root water uptake since the species have predominantly dense lateral rhizome structures (Kumar and Divakara, 2001). This was confirmed by the absence of rhizome structure in deeper soil depths when CS 616 probes were installed (Plate 3.2). The sensors were installed within the 10 x 10 m^2 study area.

Plate 3.2 Installed soil water probes (CS 616) for measuring soil water content.

Total profile water content (equivalent depth of water) was calculated using the sum of the volumetric water contents measured at each depth multiplied by the depth of the soil profile to quantify the depth of water within the root zone:

$$W_{rz} = \theta_{v1} d_1 + \theta_{v2} d_2 + \theta_{v3} d_3 \qquad 3.1$$

where W_{rz} is the total profile water content in the root zone, Θ_{v1}, Θ_{v2} and Θ_{v3} are volumetric water contents, d_1, d_2 and d_3 are the three soil depths represented by each probe (Evett et al., 2006).

3.3 Bamboo selection

In KwaZulu-Natal, the study site was selected at a small commercial farm called Shooters Hill. The farm was located at Otto's Bluff in the uMgungundlovu District Municipality, KwaZulu-Natal, South Africa. It was approximately 980 m above sea level. Approximately 10 ha had been planted with bamboo including at least 15 different species (Plate 3.3). The site had reasonable security; this was essential due to the high value of research equipment installed. Two commercial cultivated species namely *Bambusa balcooa* var. balcooa and *Bambusa balcooa* var. beema were selected for the study.

Plate 3.3 KwaZulu-Natal study site at Shooter's Hill farm (29.43º S, 30.32º E).

3.4 *Eucalyptus grandis* (eucalyptus) selection

The Shooter's Hill farm comprised of other land uses such as grassland and *Eucalyptus grandis* plantations. To enable comparative measurements of other species, a healthy stand of three-year-old eucalyptus trees were identified and selected for monitoring water-use. In the 10 x 10 m^2 plot (within the eucalyptus plantation), diameters at breast height (DBH) from a total of 16 trees were measured.

Four trees with diameters of 118, 97, 121 and 116 mm were selected with respect to diameter size distribution to represent different diameter class sizes and these were instrumented with the HRM equipment.

The planting density of these trees was 3 x 3 m^2 and this was important for upscaling the total water-use in the larger compartments. Eucalyptus trees were instrumented from November 2018 to February 2020 with the HRM system to monitor the hourly sap velocity for later calculation of the water-use. In the Eucalyptus plantation, a total of 16 trees within the 10 x 10 m^2 were monitored and their diameter at breast height measurements were taken using diameter tape to study the radial increment. These values were used to support water use measurements with respect to trees growth.

3.5 *Acacia mearnsii* (wattle) selection

Four invasive wattle trees, with the diameters of 111, 133, 117 and 103 mm were identified within the beema plantation since there were no suitable commercial wattle plantation at Shooter's Hill. The selected wattle trees were estimated to be three-years-old (i.e. established at the time of planting of the beema bamboo). Their stem diameters were recorded and monitored monthly from April 2019 to January 2020. The DBH of the selected trees varied from 103 to 133 mm and were considered suitable for understanding the water-use of different size classes for subsequent upscaling to an "estimated" stand transpiration. Selected trees were then instrumented with the HRM system as described in section 2.6.3.3. The stand density was to 2222 trees ha^{-1}, and was important for upscaling to total water-use (Van Wyk et al., 2012).

3.6 Experimental design of the Beema and Balcooa sites at Shooter's Hill farm

At each site, a 10 m x 10 m plot was marked out to include representative plants and to avoid potential edge effects (Figure 3.1). To quantify (scale-up) the water-use of these multiple stemmed species it was necessary to measure the diameter of each culm of each clump. Vernier callipers were used to record the diameter of each of the culms of each bamboo clump (Plate 3.4).

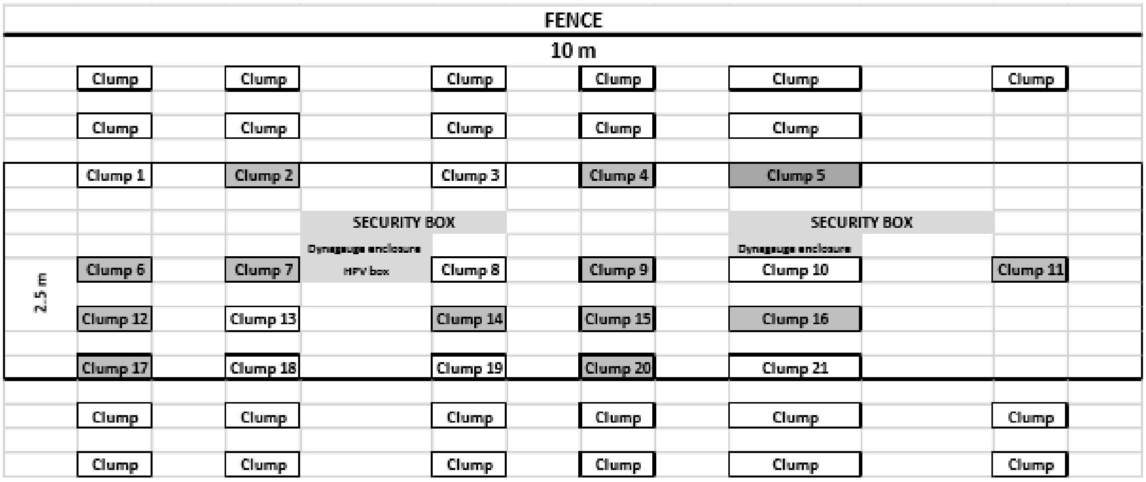

Figure 3.1 Site layout of bamboo clumps and equipment at the beema site, Shooter's Hill.

Plate 3.4 Measuring the culm diameters in the 10 X 10 m study plot with Vernier callipers.

3.6.1 Bamboo culms, eucalyptus, and wattle tree growth monitoring

Bamboo is recognised to have a very fast growth rate and therefore it is being promoted in South Africa to address the problem of fuel shortage, deforestation, and sustainable timber and as part of rural agricultural development (Gupta and Kumar, 2008). However, there is little information on the growth characteristics of the different species grown under the different climatic conditions in South Africa. The aim of the growth study experiments was to determine the growth of balcooa and beema at Shooter’s Hill in KwaZulu-Natal. Similar data from the commercial trees such as eucalyptus and black wattle were also considered essential to provide comparative data of the different land uses in the study.

3.6.1.1 Growth of *Bambusa balcooa* var. beema

At the *Bambusa balcooa* variety beema study site a total of 21 bamboo clumps in a 10 x 10 m plot were included in the growth study. A total of 251 culms were tagged and the DBH was measured with Vernier callipers. Measurements were taken at the start of the study on 13th of August 2018, and at the end of the study on 3rd February 2020 (Plate 3.4).

The selected *Bambusa balcooa* variety balcooa study site had one clump within a 3 x 2 m plot and 72 bamboo culms. This was used for the growth study. Bamboo culms were measured at the beginning of the study using Vernier callipers on the 24th August 2018 and at the end of the study on 26th February 2020.

3.6.1.2 Growth of eucalyptus and wattle

The diameters of four selected eucalyptus trees were recorded at the start of the study and subsequently monthly stem diameter measurements were taken. This was important in understanding the rate of tree growth and in predicting the growth of the heartwood for calculating the sapwood area for the HRM water-use measurements. The measurements were taken at the tree section where probes were installed. A similar approach was applied to the wattle trees.

3.6.2 Leaf area index (LAI)

Using a LI-COR LAI 2200 plant canopy analyser, leaf area index (LAI) measurements were collected from the balcooa, beema, eucalyptus and wattle sites. This provided an understanding of growth with respect to canopy cover and was an important variable regarding plant water-use (Jordan, 1969). A 45^{o} view cap was used in measuring the LAI data. The view cap selected was appropriate for blocking sunlight penetration caused by the planting spacing between clumps and to prevent the operator from blocking the sensor view.

Monthly measurements were performed to estimate the LAI from April 2019 to February 2020. However, owing to a calibration problem with the analyser, only the values from April to September 2019 are shown. The procedure involved taking one clear sky reading (the "above" measurement) and four below canopy measurements ("below" canopy) in a sequence programmed to give four replications per LAI measurement.

3.7 Bamboo anatomy

Fresh beema and balcooa culms were harvested at Shooter’s for bamboo anatomy analysis. This was done also to assess the pattern and distribution of vascular bundles in bumboo culms. These were stored in the ziplock reusable plastic sealer bags to keep out from mould and stored in a 5 ^{o}C laboratory fridge. The sample preparations were done within 24 hours after harvest.

3.7.1 Sample and blocks preparation

One square millimeter sections were cut (using stainless blade) from the wall of selected bamboo culms harvested at Shooter’s Hill, KZN (Plate 3.5). The samples were then fixed in 3% glutaraldehyde overnight to preserve quality and inhibit desiccation. A 0.05 M sodium cacodylate buffer was then used to wash the sample thoroughly by immersing twice for 30 minutes. The, samples were fixed with 2% osmium tetroxide (7:3 ratio of 2% osmium tetroxide and 0.05 M sodium cacodylate buffer) and left overnight. Samples were then washed in a 0.05 M sodium cacodylate buffer sample by immersing twice for 30 minutes.

The sodium cacodylate was then extracted using a Pasteur pipette and samples were dehydrated with 30% ethanol for 20 minutes then left overnight in 50% ethanol. The 50% ethanol was extracted using a Pasteur pipette and samples were dehydrated with 70% ethanol for 10 minutes, 90% ethanol for 15 minutes, and 100% ethanol twice for 15 minutes each time, 100% propylene oxide for 15 minutes subsequently and 100% propylene overnight. Propylene was then extracted using a Pasteur pipette and samples were immersed in a 1:1 Spurr’s resin (a low viscosity hydrophobic resin that contributes to its penetration in plant tissue) and propylene oxide for 60 minutes. Samples were immersed in 100% Spurr’s resin twice for 120 minutes then immersed in 100% Spurr’s resin. Samples were put in an oven and cured at 60-70 ^{o}C for 24 hours.

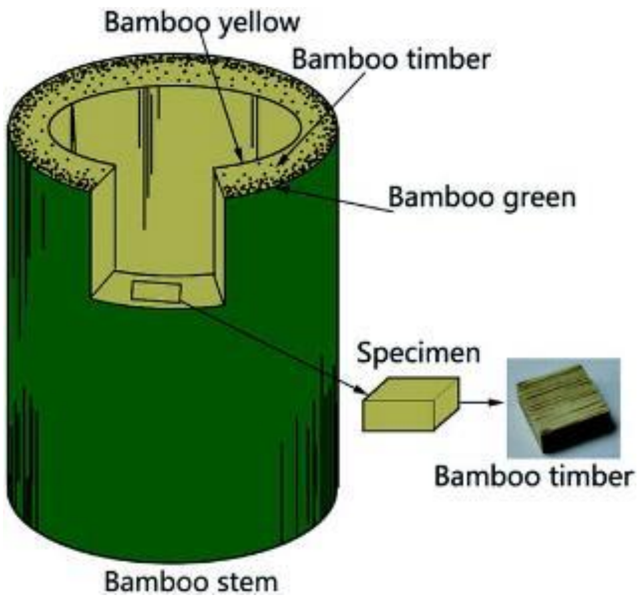

Plate 3.5 Anatomical structure of bamboo stem (Li et al., 2015).

3.7.2 Sample blocks trimming and viewing

A LKB 7800 knife-maker was used to make glass knives to cut the cured sample blocks into smaller blocks of approximately 60 mm^2 and 1 mm thick for trimming the samples into slices for analysis. The prepared blocks were then trimmed using an Ultramicrotome (Reichert-Jung Ultracut E) into approximately 0.03 mm thinner segmented pieces. Sectioned segments of the samples were then transferred into a drop of water on a glass slide to hydrate. Using a heater stirrer plate, the slide was warmed to evaporate the distilled water. Then 0.1 % Toluidine blue was used to stain the sample for 10 seconds after which it was washed through with distilled water.

The slide was reheated to drive out the stain and viewed and captured using a Nikon DS-Ri1 high resolution camera microscope at different magnifications and an Olympus AX 70 fluorescence microscope through Nikon NIS software version 4.1.

3.8 HRM water-use measurements at Shooter's Hill farm

The HRM system consisted of an 18-gauge hypodermic needle, with a 1 cm constantan wire heater at the distal end. The needle with the heater was 1.8 mm in diameter and 35 mm long. The needle heater was inserted into a 2.5 mm outside diameter brass tube, which was inserted into the sapwood area. The thermocouples, made of type T copper-constantan, were embedded in PTFE tubing (outside diameter 2 mm) and were equidistant (5 mm) from the central needle heater (Plate 3.7). They were inserted to the predetermined depths of in 2,4,6 and 8 mm in the beema and 4,6,8 and 10 mm in the balcooa. The depths were determined based on the full sapwood depth of the bamboo culms.

A single culm installation consisted of four pairs of probes (with each pair consisting of a needle heater and an upper and lower thermocouple), which were inserted radially to varying depths in the stem. The system was controlled, and data were collected using a CR1000 data logger (Campbell Scientific Inc., Logan, Utah, USA) connected to an AM 16/32B multiplexer (Campbell Scientific Inc., Logan, Utah, USA). This system was programmed to measure the hourly sap flow velocity.

The selected plants were monitored over an18-month period (September 2018-February 2020), allowing for an understanding of the seasonal variations in bamboo water-use. To ensure that the data were not affected by outside variables, such as incoming solar radiation or heat loss, insulation foam was placed around the line heater and temperature probes, which also assisted in holding the probes in place.

Sensors were connected to CR1000 data loggers and multiplexers which were housed in a locked logger enclosure. Batteries to power the system were placed in safe boxes for security (Plate 4.8).

3.8.1 Assessing the culm area of beema and balcooa culms

In order to understand the relationship between culm diameter and the hollow diameter for installing HRM instrumentation a survey was undertaken of cut culms that had been harvested for use by the farmer. Vernier callipers were used to record the diameter and hollow diameter of each of the culms (Plate 3.6). These measurements (Table 2.1) were done to estimate the culm wall depth for installation of the HRM probes. For the Beema plants no significant relationship ($R^2 = 0.22$) between culm diameter and hollow diameter was found (Figure 3.2).

The data indicated an almost constant hollow diameter size of approximately 11.5 mm with a SE of ± 0.5 mm. These data were therefore used to estimate the HRM thermocouple probe insertion depths at 6.0 mm mm.

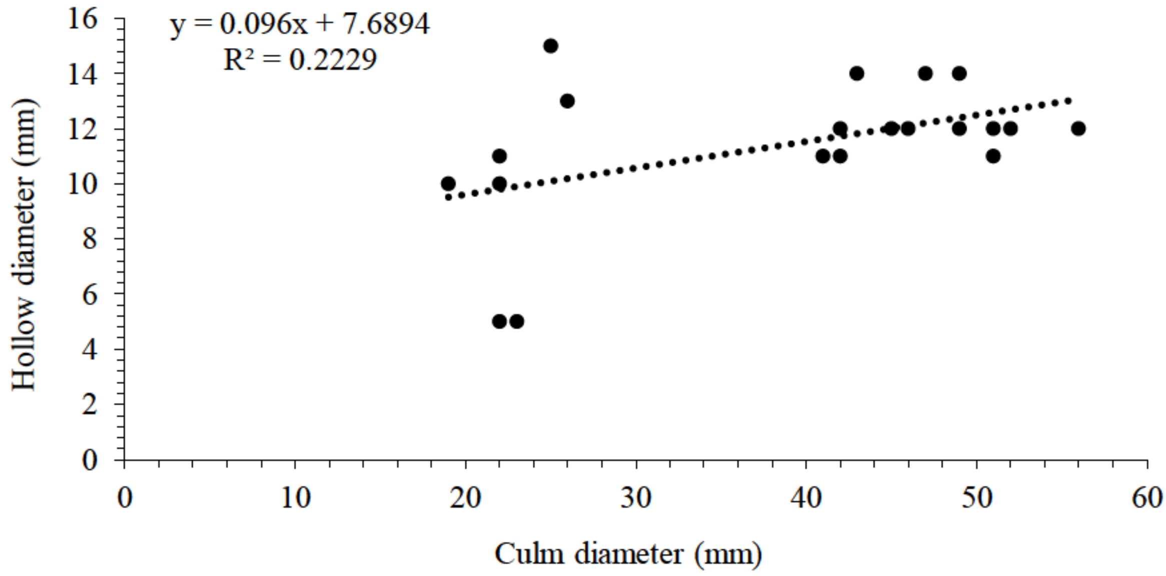

Figure 3.2 Regression of culm diameter vs hollow diameter for Beema.

Table 3.1 Stem diameters and areas of Beema and Balcooa bamboo at Shooters Hill, KZN.

Bamboo sp.	Culm diameter (mm)	Culm area (mm^2)	Hollow diameter (mm)	Hollow diameter (mm^2)	Actual bamboo area
Beema	56	2461.8	12	113.0	2348.7
Beema	52	2122.6	12	113.0	2009.6
Beema	51	2041.8	12	113.0	1928.7
Beema	51	2041.8	11	95.0	1946.8
Beema	49	1884.8	14	153.9	1730.9
Beema	49	1884.8	12	113.0	1771.7
Beema	47	1734.1	14	153.9	1580.2
Beema	46	1661.1	12	113.0	1548.0
Beema	45	1589.6	12	113.0	1476.6
Beema	43	1451.5	14	153.9	1297.6
Beema	42	1384.7	12	113.0	1271.7
Beema	42	1384.7	11	95.0	1289.8
Beema	41	1319.6	11	95.0	1224.6
Beema	26	530.7	13	132.7	398.0
Beema	25	490.6	15	176.6	314.0
Beema	23	415.3	5	19.6	395.6
Beema	22	379.9	5	19.6	360.3
Beema	22	379.9	10	78.5	301.4
Beema	22	379.9	11	95.0	285.0
Beema	19	283.4	10	78.5	204.9

Balcooa	130	13266.5	105	8654.6	4611.9
Balcooa	130	13266.5	41	1319.6	11946.9
Balcooa	122	11683.9	78	4775.9	6908.0
Balcooa	121	11493.2	102	8167.1	3326.0
Balcooa	118	10930.3	92	6644.2	4286.1
Balcooa	115	10381.6	102	8167.1	2214.5
Balcooa	113	10023.7	94	6936.3	3087.4
Balcooa	111	9672.0	89	6218.0	3454.0
Balcooa	111	9672.0	86	5805.9	3866.1
Balcooa	110	9498.5	70	3846.5	5652.0
Balcooa	108	9156.2	58	2640.7	6515.5
Balcooa	107	8987.5	83	5407.9	3579.6
Balcooa	102	8167.1	82	5278.3	2888.8
Balcooa	102	8167.1	52	2122.6	6044.5
Balcooa	94	6936.3	74	4298.7	2637.6

Plate 3.6 Measuring different stem diameters and wall thickness of A) balcooa and B) beema bamboo sp.

3.8.2 HRM setup of beema and balcooa

Heat ratio method systems were installed at the two bamboo sites, following the principles of the heat ratio measurements, as detailed in Burgess et al. (2001). A total of eight culms were instrumented with HRM sensors for long-term monitoring in the beema and balcooa sites. Selected instrumented stems were 25 mm and 50 mm in diameter for beema (Plate 3.7) and 70 mm and 100 mm for balcooa (Plate 3.8).

Plate 3.7 Heater probes connected to a data logger and multiplexer.

Plate 3.8 HRM installation in the balcooa clump at Shooter's Hill.

HRM probes were installed initially at 2, 4, 6 and 8 mm for beema and at 4, 6, 8 and 10 mm for balcooa and these were located to represent four different concentric rings of the conducting area. When 3-month data was collected, all probes for beema were repositioned to 6 mm following sap data assessing which showed very low sap flow in the other respective depths. This was necessary for up-scaling the water-use of a single stem to the whole plant, as sap velocities can vary radially across the xylem and with variation in culm circumference.

However, there was no prior information on which to base the approach (as bamboo represents a completely different anatomy to normal trees with heartwood), and it was necessary to adjust the probes depths once a time-series of sap velocity data was analysed. The data collected from the HRM system was also analysed using information described in Table 8.1.

Plate 3.9 Safe boxes for batteries (grey boxes) and the logger enclosure (white box) in the Beema site.

3.8.3 Water-use of Eucalyptus grandis (eucalyptus)

Four three-year-old *Eucalyptus grandis* trees were instrumented with HRM systems for monitoring sap-flow (Plate 3.10). The probes were initially inserted to 5, 15, 25 and 35 mm. When 10-month data was collected, probes at 25 mm and 35 mm were relocated at 15 mm and 20 mm, respectively due to growth in the heart wood resulting in very low or no sap flow data. Three CS616 probes were added to the eucalyptus site as described in section 3.2 to determine soil water content. The data collected provided comparative estimates with the bamboo water-use under similar climatic conditions.

Plate 3.10 Eucalyptus plantation at Shooter’s Hill, KwaZulu-Natal.

3.8.4 Water-use of Acacia mearnsii (black wattle)

Four three-year-old wattle trees were selected within the beema plantation site and were instrumented with HRM systems at 5, 15, 25 and 35 mm for monitoring sap-flow (Plate 3.11). No additional CS616 probes were installed around the wattle at the site as the wattle trees were within the beema site. It was assumed that the difference in water content between the beema and wattle plants was therefore the same on average due to their proximity to each other. The, the soil water content data collected from the beema plantation was therefore presumed to be the same for the solitary wattle trees within the beema plantation (Plate 3.11).

Plate 3.11 Black wattle trees at Shooter’s Hill, KwaZulu-Natal.

3.9 Stem steady state (SSS)

Bamboo sap velocity was monitored using HRM and SSS sensors to assess whether HRM can be used as an alternative technique in monitoring the water-use of bamboo species. This would be beneficial as the SSS sensor have a high cost of maintenance, high system power consumption, are expensive, are difficult to install and are not easily serviceable in the field.

The Dynagauge collar is a precision thermodynamic electronic sensor that measures water flow rates and the accumulated daily totals of water lost through transpiration. The sensor is designed to convert transpiration to a mass flow rate when ancillary plant data (e.g. stem area) are combined in the logger software (i.e. the data are in g hr^{-1}) (Savage et al., 2000). The stem gauges have soft foam insulation that surround the electronics. The units were installed on a stem having an axial length of at least the gauge height.

One Dynamax Flow 32-1K sap flow system with a Flow 32B-1K expansion unit having the capacity to monitor 16 gauges (Dynamax, Houston, TX, USA) was installed at the Beema site in KZN (Table 3.3). At the Balcooa site, a single Flow 32-1K Sap Flow Base System was installed with two SGA100 gauges with diameters of 98.6 and 99.4 mm.

Each of these systems, which is comprised of a CR1000 data logger and an AM16/32B multiplexer (Plate 3.12) were powered by two 12V 100Ah RR2 deep cycle batteries, installed in high-security safe boxes to prevent theft.

A voltage control unit regulated the voltage output depending on the number of collars and the size of the collars. The specification of the gauge diameter is the determining factor for the selection of a gauge. Thus, at both the Beema and Balcooa sites culms with matching diameters to the gauges were selected from the growth survey data.

At the Beema site the selected gauges included one SGA70, six SGA50s, one SGA 40, four SGB25s, three SGEX25s and two SGB19s (a total of 16 gauges). At the Balcooa site two large SGA100 gauges were installed. The mechanical specifications of these gauges and the gauges selected with their constants are shown in Table 3.2 and Table 3.3, respectively.

Plate 3.12 The wiring of the Dynamax system with a CR1000 data logger and AM16/32B multiplexer with two adjustment potentiometers of the AVRD in the centre.

Table 3.2 List of gauges used at the Beema site and the inital program constants and parameters used to measure sap flow.

Box number	Sensor number	Sensor type	Diameter of instrumented culm (mm)	Resistance (Ohms)	Culm area (mm^2)	K_{st}	dTmin	K_{sh}
Enclosure 1: Base	1	SGB 50	51.5	25.1	186.5	0.28	0.2	0.8
	2	SGB 50	52.5	26.9	186.5	0.28	0.2	0.8
	3	SGB 50	49.0	25.3	186.5	0.28	0.2	0.8
	4	SGB 70	67.0	20.6	636.0	0.28	0.2	0.8
	5	SGB 50	50.0	25.4	186.5	0.28	0.2	0.8
	6	SGB 50	47.5	26.4	186.5	0.28	0.2	0.8
	7	SGB 50	50.0	26.4	186.5	0.28	0.2	0.8
	8	SGA 40	36.5	39.7	114.4	0.28	0.2	0.8
Enclosure 2: 8 Gauge expansion	9	SGB 50	48.0	41.7	41.3	0.28	0.2	0.8
	10	SGEX 25	26.0	41.2	41.3	0.28	0.2	0.8
	11	SGEX 25	22.5	39.5	41.3	0.28	0.2	0.8
	12	SGEX 25	27.0	41.7	41.3	0.28	0.2	0.8
	13	SGEX 25	26.0	41.0	41.3	0.28	0.2	0.8
	14	SGB 19	18.5	64.7	20.1	0.28	0.2	0.8
	15	SGB 19	20.0	62.7	20.1	0.28	0.2	0.8
	16	SGEX 25	26.0	41.1	20.1	0.28	0.2	0.8

Table 3.3 Mechanical specifications of the Dynamax gauges used at the Beema site.

Flow gauge type	Sensor type	Shield height (mm)	Stem diameter (mm)			TC gap dX (mm)	Input voltage (V)	Input power (W)
			Min.	Typ.	Max.			
Stem flow gauge	SGA9-ws	180	8.0	9.0	10.0	4.0	4.0	0.1
	SGA10-ws	180	9.5	10.0	13.0	4.0	4.0	0.1
	SGA13-ws	180	12.0	13.0	16.0	4.0	4.0	0.2
	SGA16-ws	200	15.0	16.0	19.0	4.0	4.5	0.2
	SGA19-ws	250	18.0	19.0	23.0	5.0	4.5	0.3
	SGA25-ws	280	24.0	28.0	32.0	7.0	4.5	5.0
Trunk flow gauge	SGB35-ws	460	32.0	41.0	45.0	10.0	6.0	0.9
	SGB50-ws	505	45.0	50.0	65.0	10.0	6.0	1.4
	SGB70-ws	610	65.0	70.0	90.0	13.0	6.0	1.6
	SGB100-ws	660	100.0	110.0	125.0	15.0	8.5	4.0
	SGB150-ws	1129	125.0	150.0	165.0	20.0	9.0	4.0

3.9.1 Preparation of bamboo culms for Dynagauge installation

Normal trunk preparation requires a reasonably smooth stem since good thermal contact is key to obtaining the temperature of the xylem and heat flow into the xylem. In general, the least amount of disturbance is best and for bamboo, this was easily facilitated by the already smooth shiny outer surface of the culm which obviated careful sanding of any loose or rough bark. Another advantage of bamboo is that the culm diameter is essentially constant in the first few meters from the base, making the selection of the median diameter relatively easy.

Once the culm position was selected for a suitable gauge, the culm was cleaned to remove any dust and grit and then sprayed around the circumference with Canola release spray in the region of the expected heater position to prevent the sensor sticking to the stem and to prevent damage to the gauge due to daily expansion and shrinkage of the stem (Plate 3.13).

Plate 3.13 Preparation and installation of the dynamax collars.

During installation the following precautions were made:

- The gauge was orientated in the correct direction to measure flow
- The gauge was the correct size to prevent damage to the components
- The heater strip was carefully tucked inside the insulation foam
- The Velcro straps were tightened to ensure a snug fit

- The stem gauge heater resistance was recorded for use in the program
- The sensor cable was attached and sealed with insulation tape.

Finally, the aluminium bubble wrap was wrapped around the sensor and secured with cable ties (Plate 3.13) and then the upper opening was sealed with plastic wrap to prevent moisture ingress from above (Plate 3.14). Once all the gauges were installed and the electrical cables connected, then the battery power was applied and the AVRDs were adjusted using a voltage meter to match the recommended voltages for the relevant gauge. The program was then launched with the entered user constants for each gauge as shown in Table 3.3.

Plate 3.14 A) Securing the sensor and B) Completed Dynamax collar installation.

3.9.2 Automatic zero set

In the CRBasic program, the flag for automatic zero set was set using the K_{sh} values between 04h00 and 06h00. K_{sh} is the sheath conductance and is calculated when the plant has established a non-flow condition. The data were monitored and the apparent K_{sh} measured.

The data were then retrieved from the logger and updated with the user constants. K_{sh} proportionally relates the radial heat thermopile voltage (C_h signal), directly to the radial heat q_r. The calculation for K_{sh} was determined by solving the energy balance equation 2.1 to 2.4 discussed above and equation 3.2, when setting F approximately equals 0.

$$q_r = K_{sh} \text{x } \Delta T_{Ch} \qquad 3.2$$

where ΔT_{Ch} is the temperature difference measured in channel Ch.

After computing P and q_v to the usual sap flow computation, the thermopile signal ΔT_{CH} (mV) was divided into the remaining heat flux. The minimum apparent K_{sh} value was obtained at a minimum flow rate, the zero-set point. Each of the Dynamax sensors were then calibrated and the K_{sh} was updated.

3.9.3 Data output

The data output from the Dynamax systems is in g hr^{-1} (using the specific heat of water). The conversion to L day^{-1} is as follows:

- Convert g hr^{-1} (x) to latent heat flux:

$$L_v F(W\ m^{-2}): (\frac{1000x}{3600}) \qquad 3.3$$

Convert ƛ ET (W m^{-2}) to ET (mm day^{-1}) where ƛ = 2454000 J kg^{-1} :

$$\frac{x}{245400} \text{ x } 3600 \qquad 3.4$$

- 1 kg m^{-2} of water is equal to 1 mm
- Therefore, sap flow is in mm.hr^{-1} × area of the stem provides L hr^{-1}
- Summed for the day provides L day^{-1}.

3.10 Transpiration coefficient (K_{cb})

Transpiration coefficient refers to the ratio of measured crop transpiration (T_{crop}) over reference grass evapotranspiration (ET_0), when transpiration is not limited by soil water. It is denoted as K_{cb} (Kang et al., 2003). The K_{cb} is affected by the crop characteristics, management practices and environmental aspects (Savva and Frenken, 2002). Other factors may include ground cover and planting density. Mature crops are characterised by K_{cb} > 1 (Allen et al., 1998).

The purpose of calculating the crop coefficient lies in its effectiveness in irrigation planning and design as well as management (Savva and Frenken, 2002). In this study, K_c was calculated for crop water demand modelling. Transpiration coefficient was calculated as:

$$K_{cb} = \frac{T_{crop}}{ET_0} \qquad 3.5$$

where T_{crop} is the transpiration of the crop (mm day^{-1}), K_{cb} transpiration coefficient (dimensionless) and ET_0 is the reference grass evapotranspiration (mm day^{-1}).

3.11 Root mean square error (RMSE)

RMSE refers to the standard error of the residuals, a measure of relationship between the actual data from the regression line (best fit). This was used to validate the relationship between SSS and HPV techniques in the estimation of water-use in bamboo species. RMSE was calculated as:

$$\sqrt{\sum_{i=1}^{n} \frac{(y - \widehat{y})^2}{n}} \qquad 3.6$$

where n is the number of observations, y is the actual y variable (mm) in the data set for a given x, ŷ is the estimated y variable (mm) and i is an index.

4. Results

4.1 Meteorological data

From September 2018 to March 2019, daily total incoming solar radiation increased markedly from 15 to ~ 28 MJ m^{-2} especially in January-February 2019 (summer) when most days exceeded 25 MJ m^{-2} (Figure 4.1). High incoming solar radiations were accompanied by high VPD values that exceeded 2 from early spring to late summer. Most highest VPD values ~ 3.0 were recorded in spring-early summer as oppose to mid-late summer. However, in mid-summer (22nd January 2019), when maximum reading of incoming VPD was ~ 2.2, solar radiation reached 27 MJ m^{-2} at Shooter's Hill (Figure 4.1). By contrast, in winter (May-August 2019), when solar angles were lower, the average minimum incoming solar radiation and VPD recorded were 13 MJ m^{-2} and ~ 1.2, with a few clear warm days reaching 16 MJ m^{-2} (Figure 4.1). The lowest incoming solar radiation and VPD recorded were ~ 2.4 MJ m^{-2} and 0.09 on 21th May 2019 on a cold cloudy winter day.

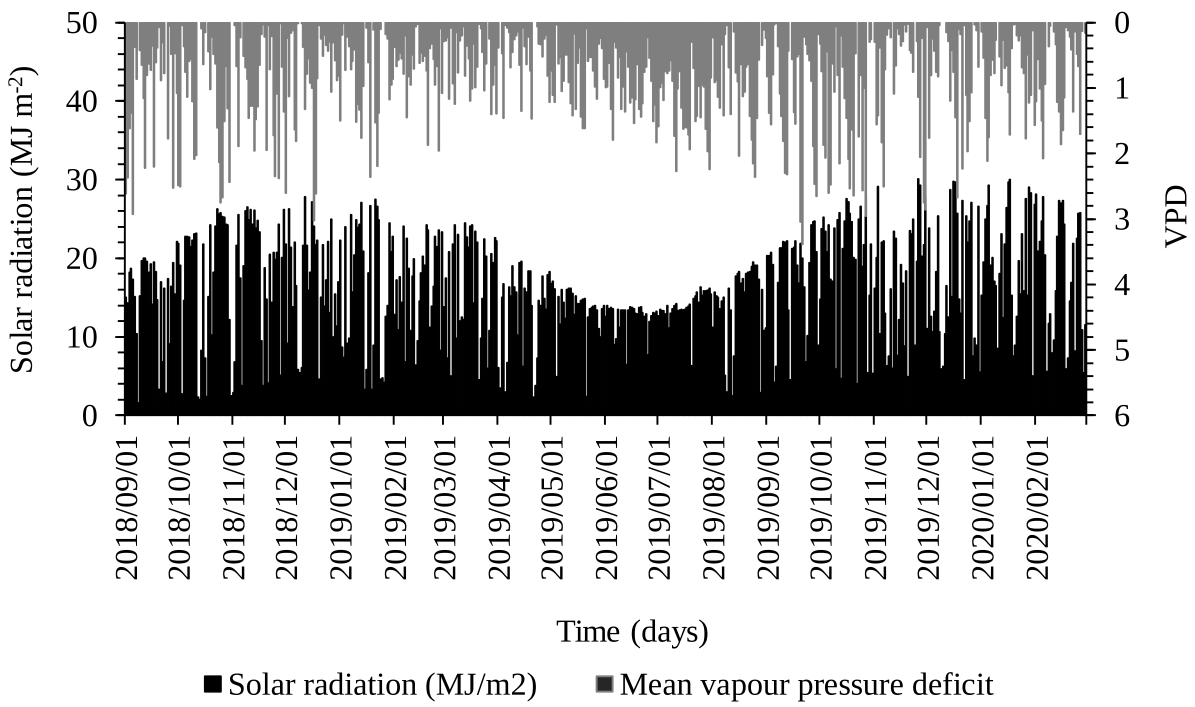

Figure 4.1 Daily total incoming solar radiation and mean vapour pressure deficit from September 2018 to February 2020 at Shooter's Hill, KwaZulu-Natal.

Average daily air temperatures exceeding 22 ^{o}C were regularly recorded from September 2018 to March 2019 and from September 2019 to February 2020, spring-summer (Figure 4.2) and are indicative of the warm summer conditions in the Pietermaritzburg district, coinciding with the high daily total incoming radiation conditions (~ 27 MJ m^{-2}) and VPD exceeding 2.0 described above. Minimum average temperatures of < 20 ^{o}C were also noted from May-August 2019 (winter), with temperatures ~ 15 ^{o}C in July-August 2019 (Figure 4.2).

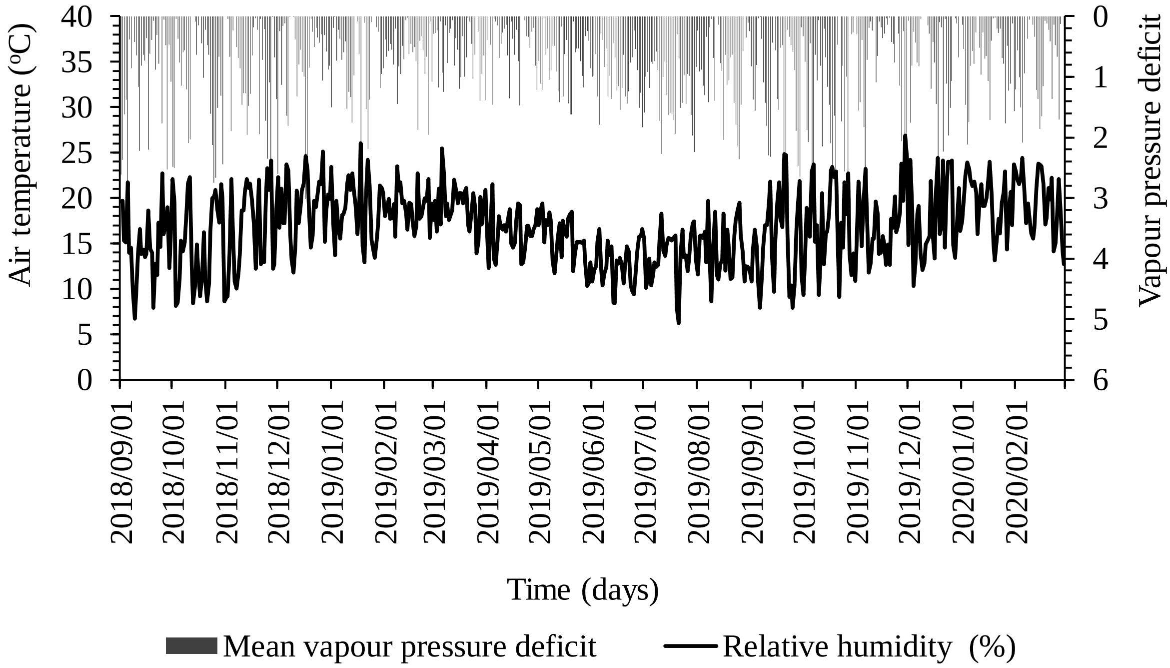

Figure 4.2 Daily average ambient air temperature and vapour pressure deficit from September 2018 to February 2020 at shooter's Hill, KwaZulu-Natal.

With an increase/decrease in solar radiation, air temperature also increased/decreased at Shooter's Hill. For example, in August 2019, solar radiation was recorded to be ~ 14 MJ m^{-2} increasing to ~ 28 MJ m^{-2} in November 2019 while average air temperatures recorded in August and in November 2019 were ~ 14 ^{o}C and 22 ^{o}C, respectively (Figure 4.2). During the same period, average VPD decreased from ~ 1.3 to 0.8. The decrease of solar radiation from 17 to 13 MJ m^{-2} from March-June 2019, air temperature showed a concomitant decrease from ~ 19.1 to 12.7 ^{o}C. However, an increase in the average VPD from 0.6 to 0.9 was measured in the same period.

Daytime (06h00-18h00) rather than daily relative humidity (RH) data are presented here due to the bias caused by the saturated conditions at night (dew) when RH was generally 100%. Daytime relative humidity > 70 % were observed from September 2018 to March 2019 and September 2019 to February 2020 (spring-summer period) (Figure 4.3). Maximum RH of 100% were frequently reached from September 2018 to February 2020 on moist rainy days. During the period, in the days when RH had decreased by < 80%, VPD values increased and exceeded 2.0.

During the dry winter period from May-August 2019, the RH and VPD recorded were generally < 60% and ~ 1.6 (Figure 4.3). Minimum RH and reasonable VPD were assumed to be caused by dry air. However, Shooter's Hill was considered humid in summer and dry in the winter seasons during the study period.

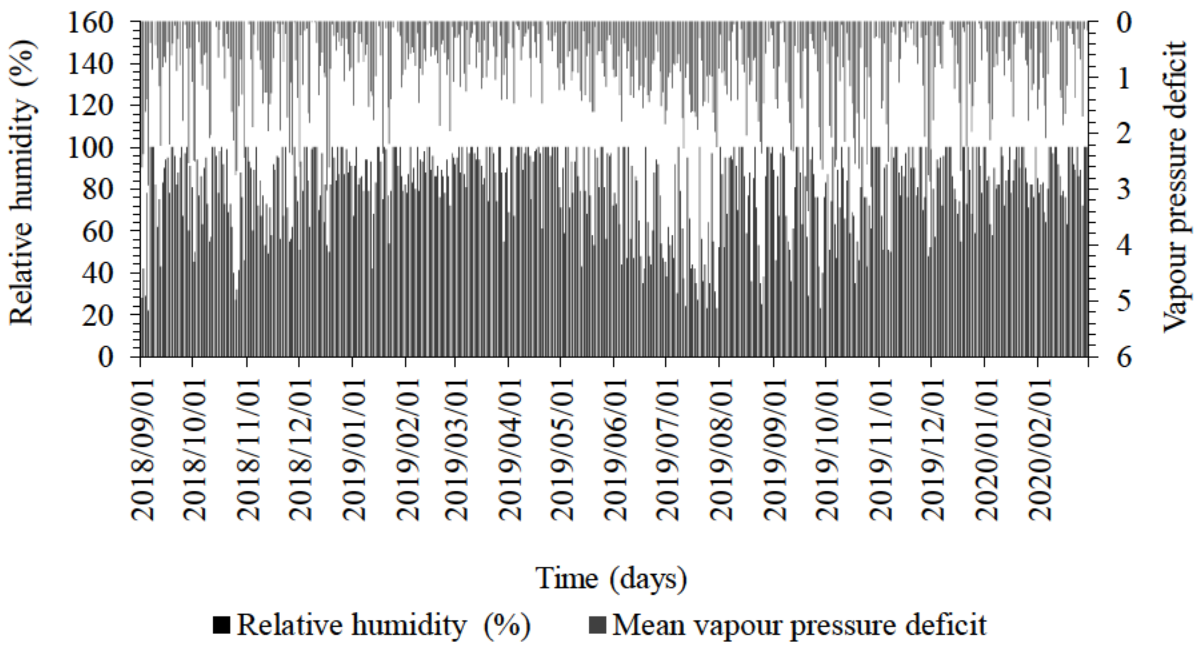

Figure 4.3 Daily relative humidity (%) and vapou pressure deficit measured at Shooter's Hill grassland site from September 2018 to February 2020.

From September 2018 to April 2019 frequent daily rainfall events exceeding 15 mm were recorded at Shooter's Hill, with the highest rainfall of 46 mm being recorded between February and March 2019 followed by 40 mm in 21st April 2019 (Figure 4.4). The highest monthly recorded summer rainfall was 160.2 mm in December 2019 followed by 151.0 mm in November 2019 and 133.6 mm in January 2020 (Table 4.1).

With the onset of winter, the rainfall ceased with only a few rain events (< 4 mm) recorded between June-August 2019. From September 2019, regular rainfall events of > 10 mm were recorded (Figure 4.4). During the 2018/19 hydrological year (September 2018 to October 2019) 853.0 mm was recorded at the site. A further 567.2 mm was recorded for the period from November 2019 to February 2020. With a total of 1420.2 mm for the 18-month study period the site was therefore considered "wet".

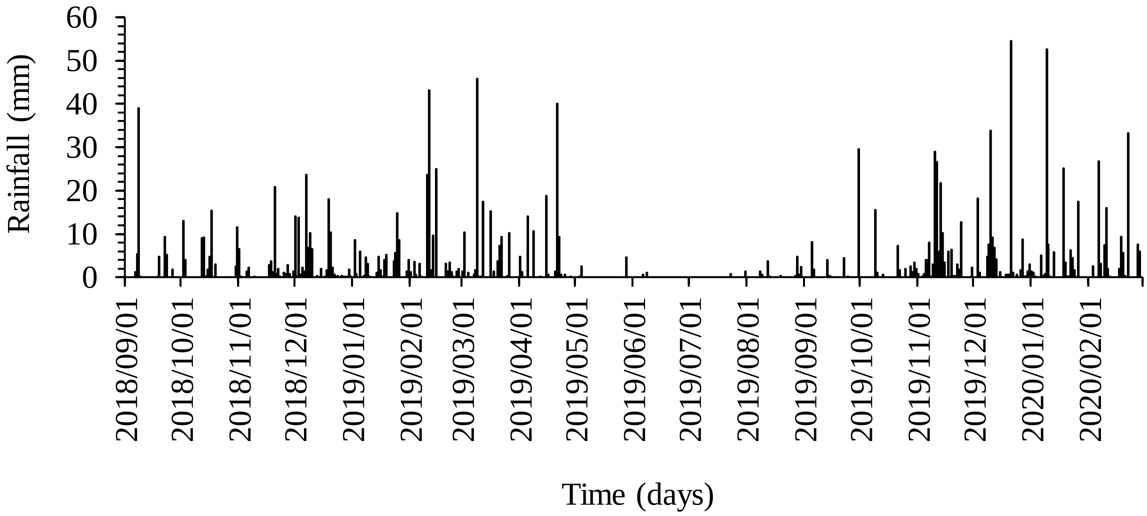

Figure 4.4 Daily rainfall measured at Shooter's Hill grassland site from September 2018 to February 2020.

Wind velocity monitored at Shooter's Hill showed no noticeable or seasonal daily patterns with daily average wind speeds generally < 10 m s^{-1} (Figure 4.5). However, some days experienced high wind speeds. For example, in September-December 2018 a high average wind speed of ~ 8.21 m s^{-1} (29.6 km hr^{-1}) was recorded (Figure 4.5). On the 13th of November 2019, maximum average daily wind was 18.4 m s^{-1} (66.2 km hr^{-1}). Therefore, the effect of wind speed as a driver of transpiration was considered to be small in the assessment of the evaporation rate of the various land-uses studied.

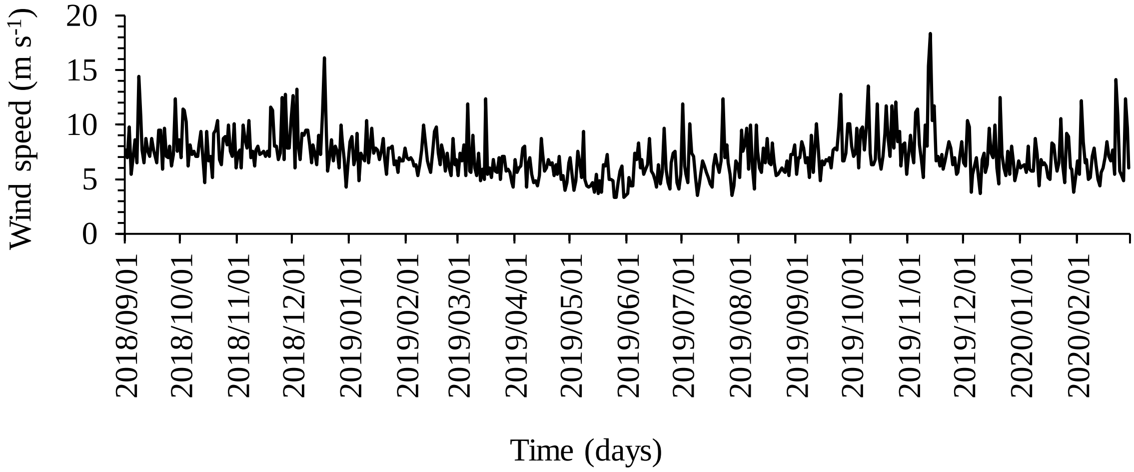

Figure 4.5 Average daily windspeed measured at Shooter's Hill grassland site from September 2018 to February 2020.

Table 4.1 Total monthly measurements of realtive humidity, air temperature and rainfall at Shooter's Hill.

Timestamp	**Relative humidity**			**Air temperature**			**Rainfall**
	Maximum	**Mean**	**Minimum**	**Maximum**	**Mean**	**Minimum**	
Sep-18	99	76	40	23.3	14.8	9.2	67.2
Oct-18	95	76	47	22.3	15	9	74.6
Nov-18	99	81	52	23.7	16.6	11.1	49
Dec-18	100	86	56	26.6	19.2	14.6	118.4
Jan-19	100	87	58	25.6	18.8	14.3	78.8
Feb-19	100	89	57	26.1	19	14.4	124.6
Mar-19	100	90	61	25.7	19.2	15	126.2
Apr-19	100	90	62	22.6	16.3	12.3	102.4
May-19	97	78	44	22.9	15.4	10.5	7.4
Jun-19	88	62	31	20.8	12.7	6.8	1.6
Jul-19	79	50	22	22.2	13.7	7.2	2.2
Aug-19	93	72	41	22.1	14.3	8.7	14.6
Sep-19	94	68	33	23.7	15.4	9.3	48.8
Oct-19	97	76	42	25.4	16.7	10.8	37.2
Nov-19	99	86	56	25.1	17.5	12.8	151
Dec-19	100	88	63	24.5	17.7	12.9	160.2
Jan-20	100	88	57	26.8	19.6	14.9	133.6
Feb-20	99	87	59	25.9	19.4	15	122.4
Total							**1420.2**

4.2 Soil profile water content

At the Beema site, the equivalent soil water content (SWC) measured at different soil depth levels was recorded with the top soil (0-200 mm) > 40 mm from October 2018 to February 2020. Other SWC values recorded were frequently > 60 mm (January –May 2019) corresponding with high rainfall events exceeding 15 mm. From January to May 2019 the water contents in the intermediate soil depth (> 300 to < 500 mm) was > 30 mm meanwhile deeper soil depths (500-800 mm) were generally > 35 mm and remained wetter than the top soil during the dry period (Figure 4.6). In the topsoil low rainfall of < 4 mm recorded from June-August 2019, resulted in a reduction in SWC from > 80 mm in May 2019 to < 35 mm in July 2019. However, from November 2019 to February 2020 peaks exceeding 60 mm were noted with the continuous increase in daily rainfall events from ~ 15-40 mm (Figure 4.6). It was also noted that from May-November 2019, low rainfall only increased the soil water content only in the topsoil from 19 to 34 mm, while the SWC in the intermediate and deeper depths (>300-800 mm) remained constant until rain infiltrated, as the rainfall accumulated by the end of October 2019. It is important to note that the plant available water (water between field capacity (FC) and permanent wilting point (PWP)) was not determined through soil characteristics studies, which were beyond the resources of this study. Therefore, conclusions on differences in plant soil water content availability between horizons are preliminary.

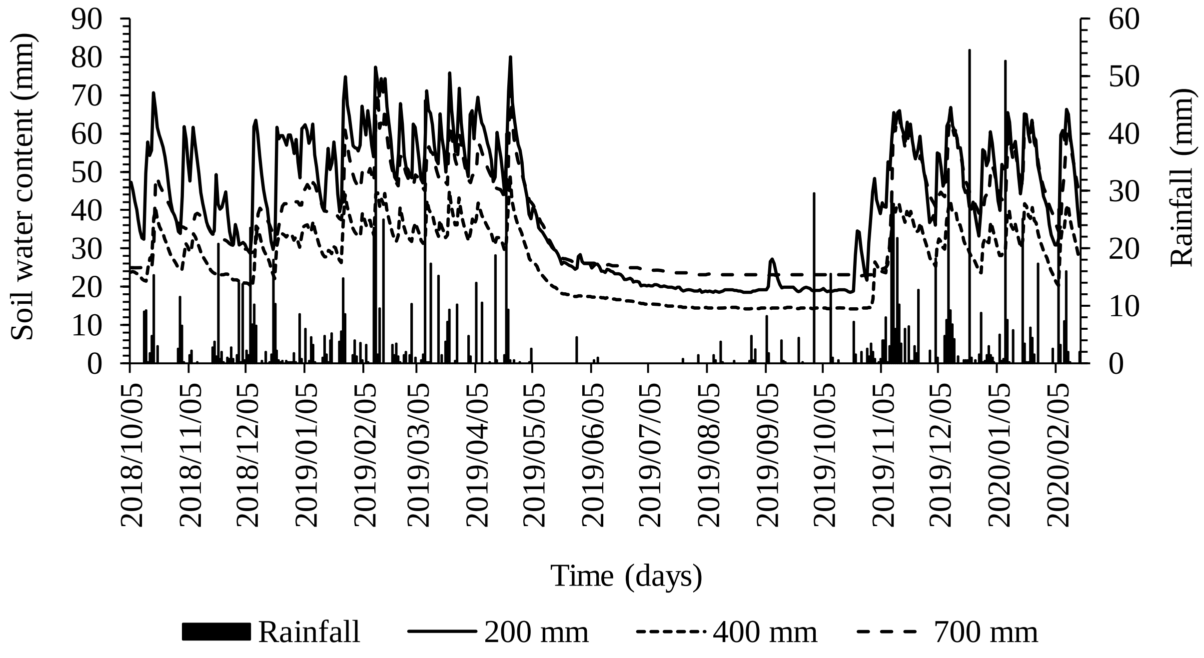

Figure 4.6 Rainfall and soil water content with respect to soil depth at Beema site, KwaZulu-Natal.

Total soil profile water content (TSPWC) for the 800 mm deep soil profile varied from 60-190 mm from October 2018 to February 2020 (Figure 4.7). Irregular rainfall events > 15 mm caused large fluctuations of ~ 80-190 mm in TSPWC from October 2018 to May 2019. TSPWC of ~ 190 mm was recorded from February-April 2019, with a total of 353.2 mm rainfall recorded during this period (Figure 4.7). In contrast, the reduction in TSPWC from 160 mm in May 2019 to < 90 mm from June-October 2019 was associated with the decrease in rainfall from 7.4 mm in May 2019 (Figure 4.7) to a low of 3.8 mm total rainfall recorded in June and July 2019 (Table 5.1). Total soil profile water content at the Beema site remained constant at ~ 60 mm from September to October 2019 (Figure 4.7) even when a total rainfall of 86.0 mm was recorded during this period. Assuming the wetter conditions corresponded with field capacity (FC) and driest with permanent wilting point (PWP), the maximum plant available water (PAW) was ~ 120 mm in the summer.

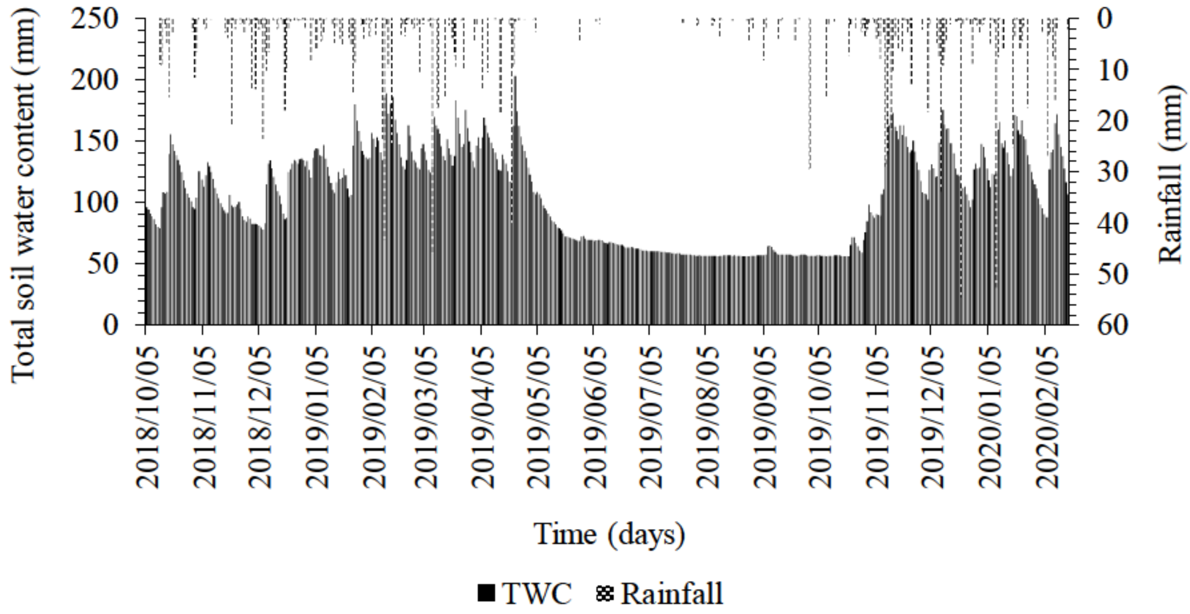

Figure 4.7 Total soil water content and rainfall at the Beema site, KwaZulu-Natal.

SWC data were collected in the Balcooa site from September 2018 to February 2020. Rainfall events > 10 mm day^{-1} occurred frequently between September 2018 and April 2019, resulting in an increase in soil water content from 59 mm in September 2018 to > 78 mm in November 2019 (Figure 4.8). By contrast, rainfall < 4 mm fell at the study site between May-August 2019 and resulted in a decrease of SWC from 80 mm in April 2019 to < 40 mm in June-July 2019 (Figure 4.8).

The SWC was higher (> 50 mm) in the deepest soil depth (500-800 mm) than in the shallower (0-200 mm) and intermediate soil depth (> 200 to < 500 mm), which was < 50 mm and < 41 mm from May-August 2019 (Figure 5.8) when rainfall was low (< 4 mm). Therefore, the increase in rainfall by a total of ~ 653.2 mm from September 2019 to February 2020 caused the deepest depth (700 mm) to accumulate > 80 mm of TSPWC by December 2019 (Figure 4.8).

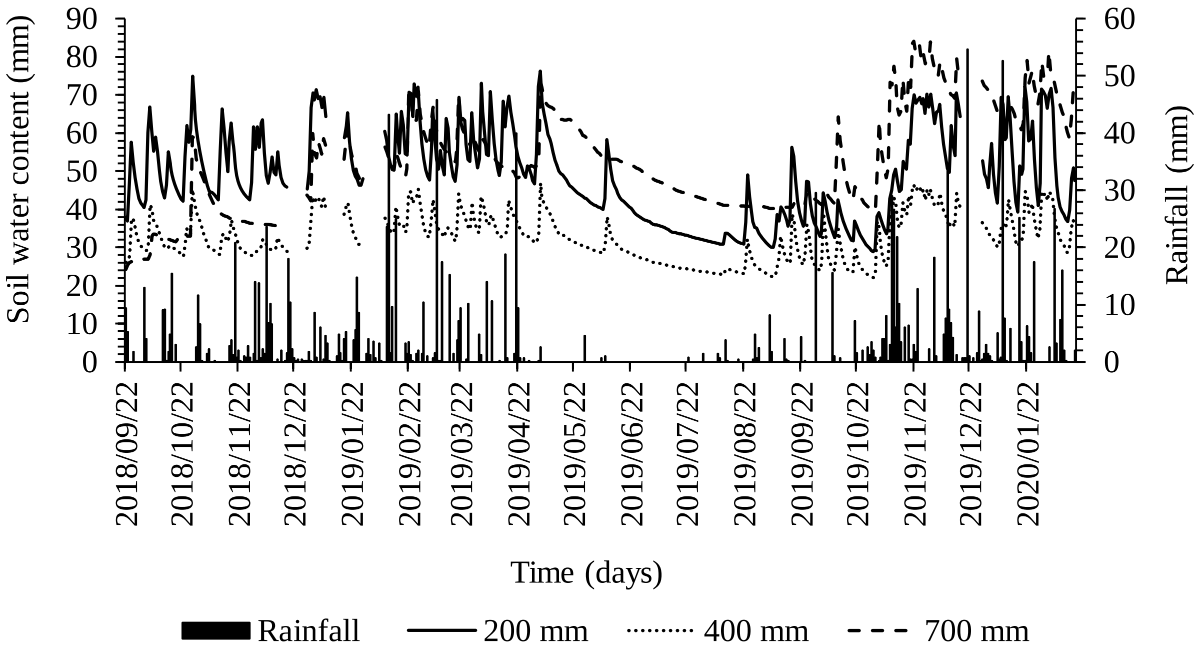

Figure 4.8 Rainfall and soil water content with respect to soil depth at the Balcooa site, KwaZulu-Natal.

Over the study period, total profile soil water content ranged between 80-190 mm in the 800 mm soil profile at the Balcooa site. For example, TSPWC increased from ~ 122 mm in September 2018 to 170 mm in October 2018 when rainfall exceeded 10 mm (Figure 4.9). With the cessation of rain in winter (June to July 2019), when only 3.8 mm of rain fell, there was a rapid decrease in the TSPWC from 150 mm in May 2019 to < 100 mm in July 2019 (Figure 4.9). Assuming the wetter conditions corresponded with volumetric water content at FC and driest with PWP, the maximum PAW was ~ 150 mm in the summer.

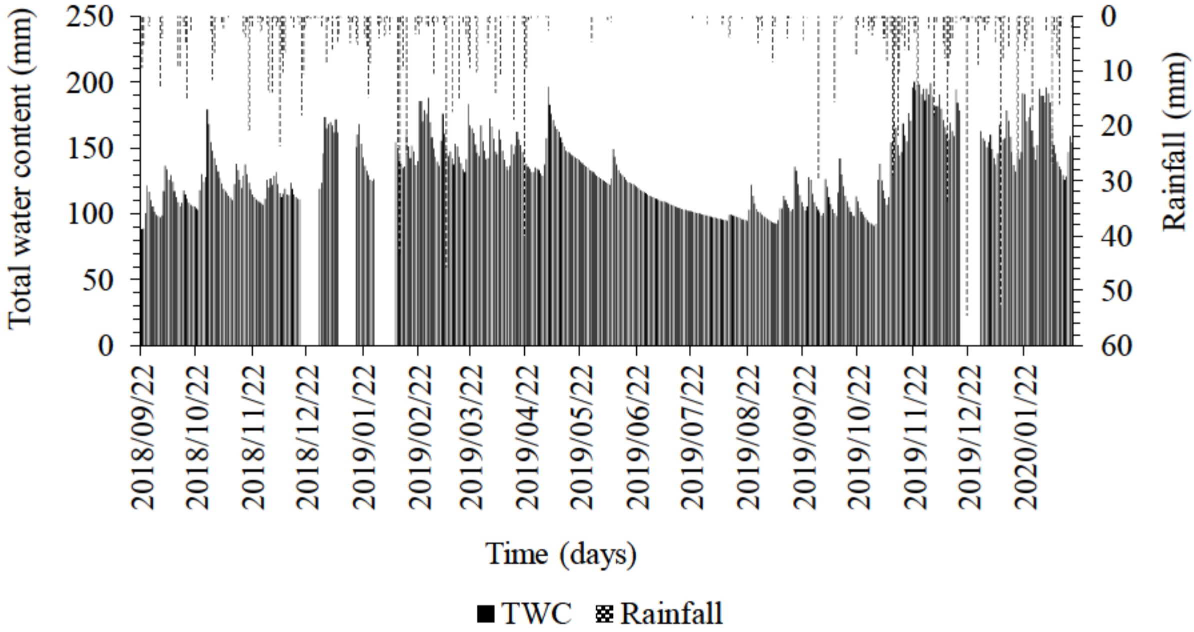

Figure 4.9 Total soil water content and rainfall at the Balcooa site, KwaZulu-Natal.

SWC data for the Eucalyptus site were collected from May 2019 to February 2020. There was a constantly decreasing SWC in the topsoil between May-October 2019 from 69 mm to 45 mm coinciding with the low rainfall events (< 6.0 mm). Increasing daily rainfall from ~ 10 mm to 30 mm from November 2019 to February 2020 caused an increase in SWC to > 60 mm, with top soils reaching 80 mm when high summer (November) daily rainfall events of ~ 45 mm were recorded (Figure 4.10).

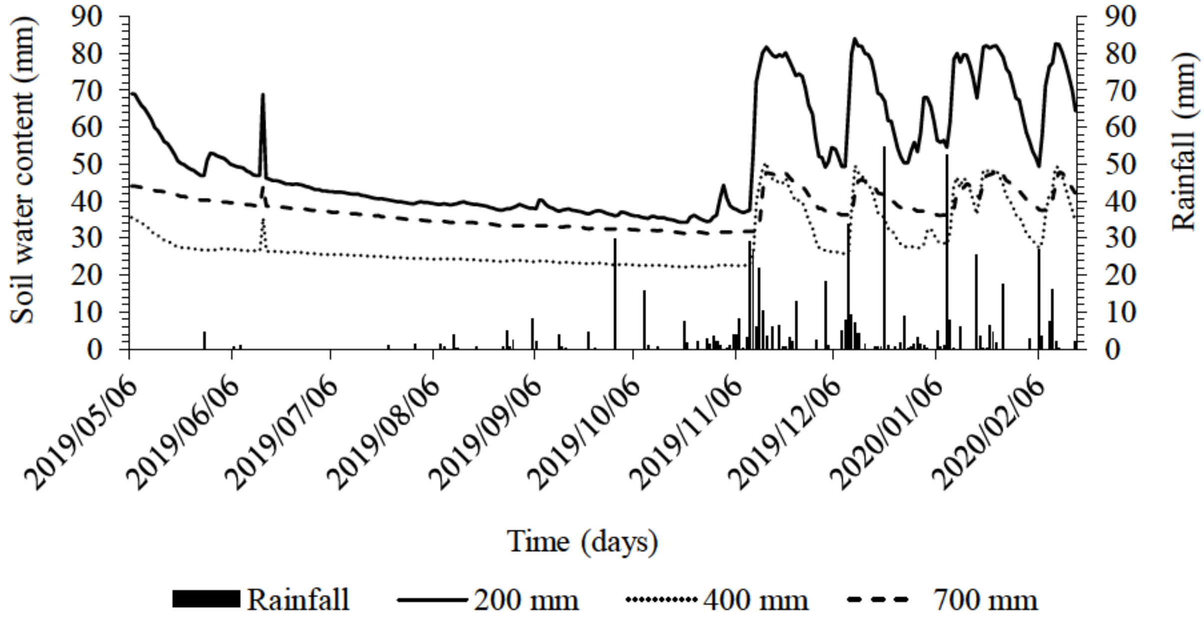

Figure 4.10 Rainfall and soil water content with respect to soil depth at the Eucalyptus site, KwaZulu-Natal.

A total rainfall of only 3.8 mm between June and July 2019 resulted in a steady decline in TSPWC from 150 mm to ~ 100 mm from May-November 2019 (Figure 4.11). However, high summer daily rainfall of > 10 mm recorded frequently in November 2019 to February 2020 caused the TPSWC to exceed 170 mm (Figure 4.11). Assuming the wetter conditions corresponded with FC and driest with PWP, the maximum PAW was ~ 100 mm in the summer.

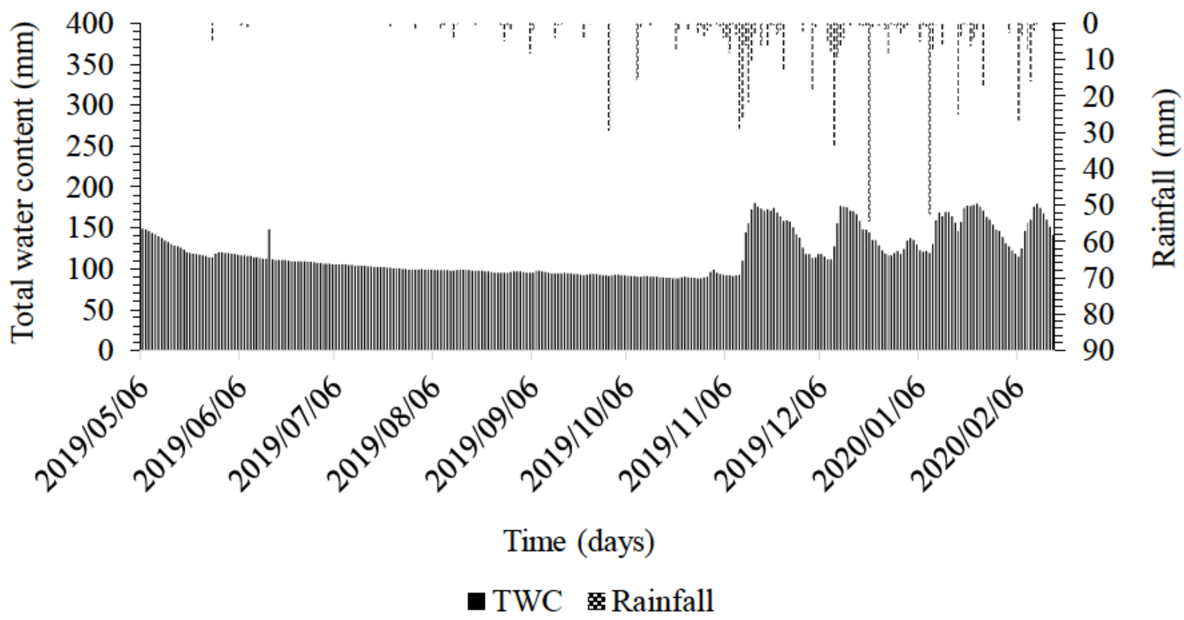

Figure 4.11 Total soil water content and rainfall at the Eucalyptus site, Shooter's Hill, KwaZulu-Natal.

4.3 Growth of *Bambusa balcooa*

There was a notable difference between the culm diameters measured at breast height (DBH) between balcooa and beema plantations. With the DBH ranging from 10-69 mm (in the beema plantation) and 30-109 mm in the balcooa plantation, the data showed that balcooa bamboo had large culm diameters than the beema culms (Figure 4.12). Therefore, these culms were classified according to different size classes to understand the distribution of diameter sizes. The data had a normal distribution with 54 % of the 251 beema culms measured falling into the 30-49 mm size class. Likewise, 54% of the 63 beema culms measured fell into 80-99 mm size class (Figure 4.12). The balcooa culms were characterized by a lower number of culms but significantly higher culm diameters. Optimal growth may be attributed to the high rainfall events (2104.5 mm) recorded at Shooter's Hill.

The bamboo culms of beema at Shooter's Hill had an 8.0 % increase in diameter from a mean of 34.0 ± 5.6 mm to 37.4 ± 9.5 mm over the 18-month study period (Table 4.2). There was an increase of 38 beema culms over the study period from 213 total number of culms measured in September 2018 (Table 4.2). The high standard deviation in the beema plantation indicated the high variability of culms.

Balcooa culms had only 4.0 % increase in diameter from a mean of 77.30 ± 14.49 mm to 79.33 ± 14.91 mm, over the same period (Table 4.3). The standard deviation in the balcooa plantation was also high showing high variability of culms. When assessing the growth of bamboo and its potential for biomass production for rural areas, additional growth parameters such as soil nutrition, texture and soil water retention may be considered.

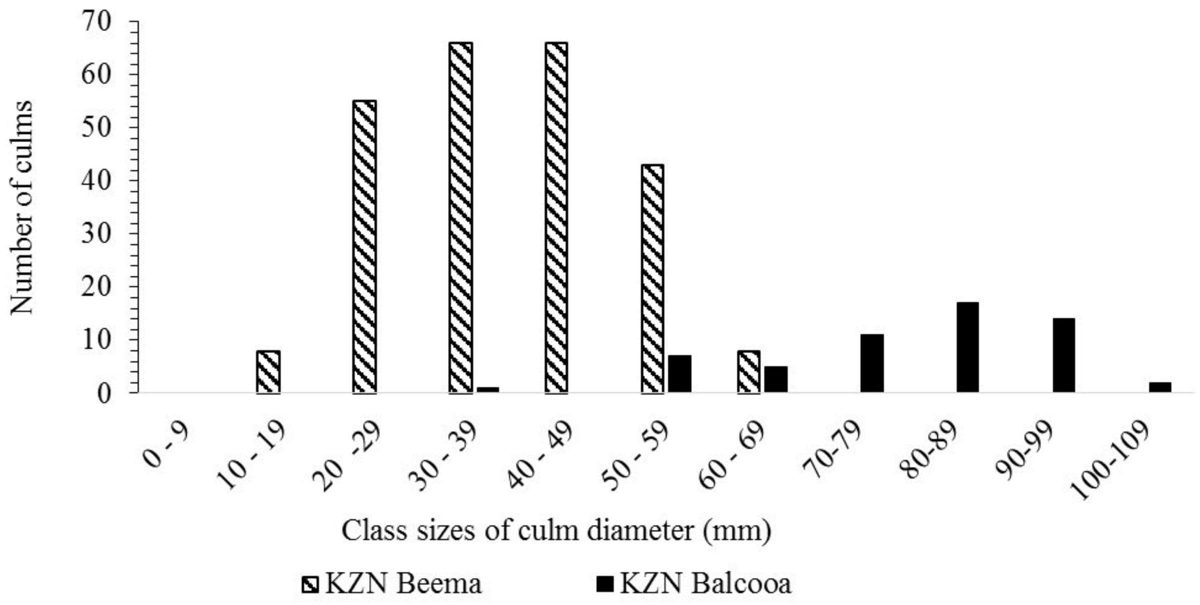

Figure 4.12 Frequency size classes of beema and balcooa.

Table 4.2 Culm diameter measurements (mm) of beema.

Clump	Total culms/clump 13/08/2018	Total culms/clump 03/02/2020	Clump mean diameter (mm) 13/08/2019	Clump mean diameter (mm) 03/02/2020
1	17	20	34.4	36.4
2	9	9	33.4	34.7
3	14	14	33.3	33.5
4	6	6	27.7	23.8
5	19	21	36.1	40.8
6	24	24	42.5	47.9
7	6	9	40.6	42.3
8	5	6	26.7	30.0
9	20	22	38.6	41.2
10	5	7	32.5	35.3
11	1	2	19.0	19.5
12	14	16	35.1	37.2
13	11	12	28.6	31.1
14	7	8	30.9	33.4
15	14	18	40.2	43.1
16	9	11	37.2	40.3
17	8	11	32.9	38.3
18	2	4	32.0	39.8
19	17	24	41.1	66.8
20	2	3	34.8	29.2
21	3	4	37.3	40.5
Total number of culms	**213**	**251**		
Mean culm diameter			**34.0**	**37.4**
Standard deviation			**5.56**	**9.46**

Table 4.3 Summary of culm diameter (mm) measurements of balcooa.

Clump	Total culms/clump 13/08/2018	Total culms/clump 25/02/2020
1	56	63
Mean culm diameter (mm)	**77.3**	**63**
Standard deviation	**14.49**	**14.91**

The Li-Cor plant canopy analyser was used to estimate LAI for the bamboo plantation, *Eucalyptus grandis* (Eucalyptus) and *Acacia mearnsii* (black wattle) trees. Data were collected from April to December 2019. However, due to calibration problems, only data from April to September 2019 was usable. The LAI of a plant canopy is defined as leaf area per unit ground surface area (Breda, 2003). It is an important parameter in water-use studies as it is a measure of the photosynthetic active area and the area subjected to transpiration.

Increase in the LAI from 4.8 in the dry winter (April) to 7.2 in early summer (September) showed the contribution and effects of moisture and solar energy on beema bamboo growth (Figure 5.13). By contrast, approximately 5.2 was recorded in the Balcooa site in April 2019, slightly higher than the initial LAI in the beema plantation. The balcooa culms were characterised by extensive leaf and culm structure. Therefore, high LAI's were recorded at the beginning of August (> 6.4) in the Balcooa site with a maximum value of 7.0 recorded in September when rainfall and temperatures were higher.

Low LAIs (~ 4.0) were recorded in the eucalyptus plantation in April 2019, compared to other land-uses at Shooter's Hill in the same month (Figure 4.13). Fluctuating LAI were recorded in winter, ranging from 3.8-4.8 (April-July) followed by increasing rates of 5.0 and 7.0 from August to September, respectively.

Winter LAIs of ~ 5.0 were recorded in April to June in the wattle trees, and these were 18% higher than the value in the eucalyptus. There were similar values between beema and wattle since the trees were located within the beema plantation. High summer values reaching 7.0 were recorded in August-September (Figure 4.13).

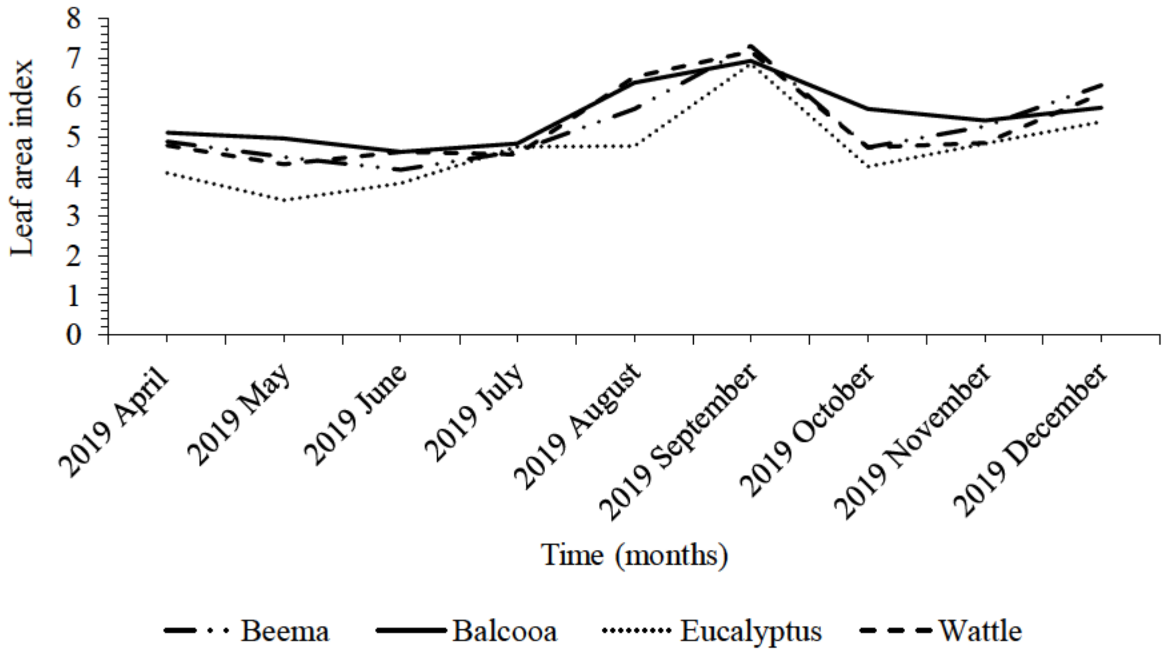

Figure 4.13 Leaf area index of beema, balcooa, eucalyptus and wattle at Shooter's Hill.

Increases in average stem diameters from ~ 102.2 mm in April 2019 to 151 mm in January 2020 were observed in the eucalyptus trees (Figure 4.14). Eucalyptus stems were increasing at an average of ~ 2 mm month resulting in a maximum average diameter of 151 mm in January 2020 (Figure 4.14).

Canopy measurements of the wattle trees were not possible since the results were compromised by the dominant beema canopy (wattle trees were within the vicinity of the beema). An increase in average wattle stem diameters from an initial 116 mm in April 2019 to 164 mm in January 2020 showed ~ 48 mm growth within the 10- month period (Figure 4.14). The rates of tree growth for wattle and eucalyptus were ~ 2-3 mm month.

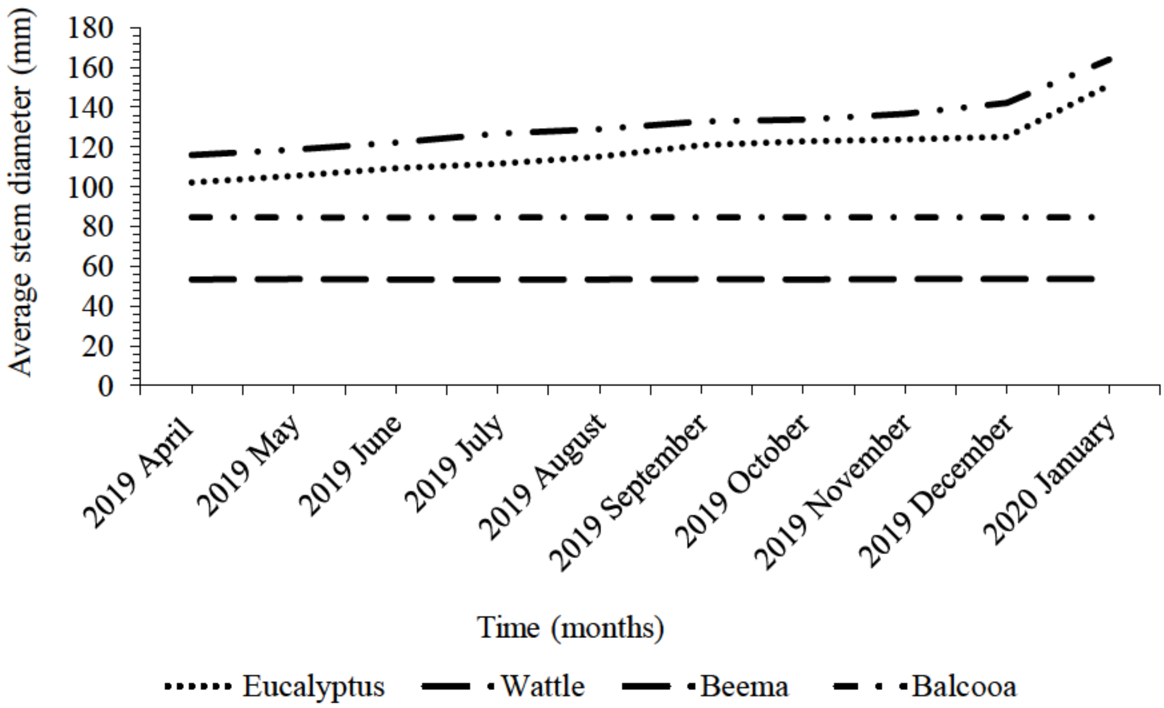

Figure 4.14 Average stem diameters of beema, balcooa, eucalyptus and wattle trees at Shooter's Hill.

4.4 Bamboo anatomy

Bamboo culms were viewed with a scanning electron microscope (SEM) and under 10 and 40 X magnification with a light microscope to identify key cellular contents such as xylem tissues and the vascular tissue arrangement. The SEM images showed four rings of vascular bundles, fibre sheath and parenchyma cells (Plate 4.1). The xylem cells were associated with phloem cells to form the vascular bundle (Plate 4.2). At least three vascular bundles were observed in the 1 x 1 mm^2 culm section (Plate 4.1).

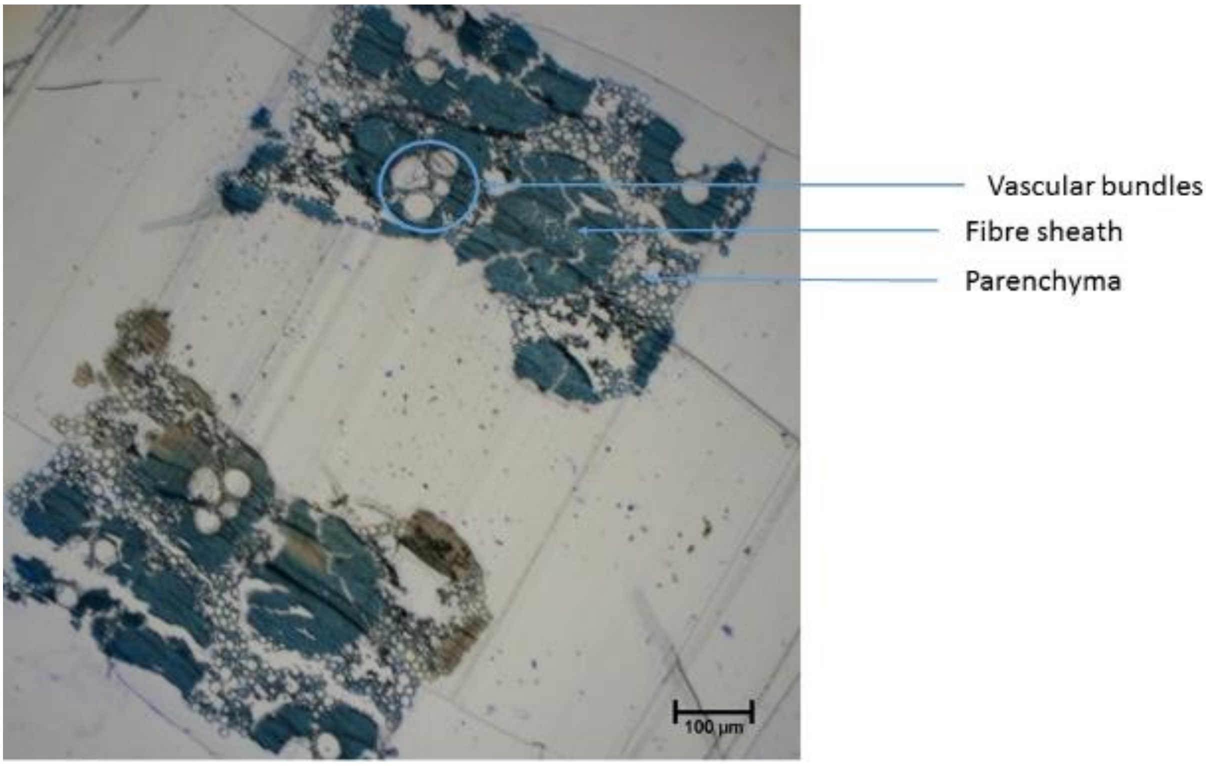

Plate 4.1 Cross-sectional layout of beema cellular structures.

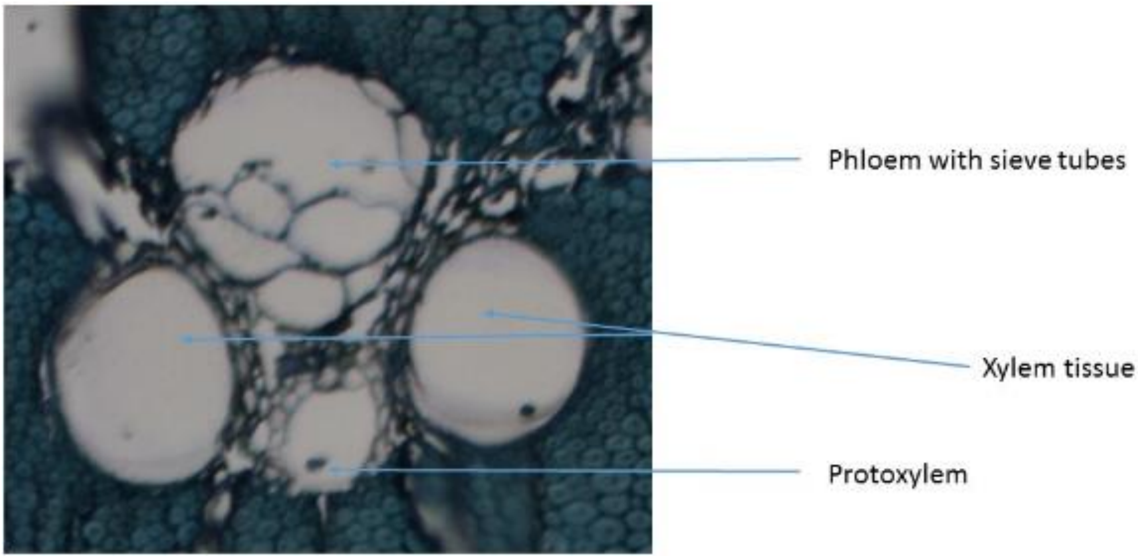

Plate 4.2 Anatomical structure of a vascular bundle of beema.

The 6 x 4 mm^2 beema cross-sectional area was viewed under a light microscope and at least 41 vascular bundles were identified (Plate 4.3). Therefore, the 44.9 mm beema culm harvested at Shooter's Hill had ~ 1163 vascular bundles.

The average vascular bundle diameter and the area were ~ 0.03 mm and 42.4 mm^2 respectively. Approximately, 128 mm^2 in the 680.78 mm^2 (44.9 mm culm diameter) was occupied by the vascular bundles. Most vascular bundles (73%) in the 6 mm thick wall were concentrated between the 2-5 mm depth zone (Plate 4.3). Vascular bundles were compacted towards the culm the surface and dispersed deeper in the culm, which was important for identifying high sap flow regions within the culm.

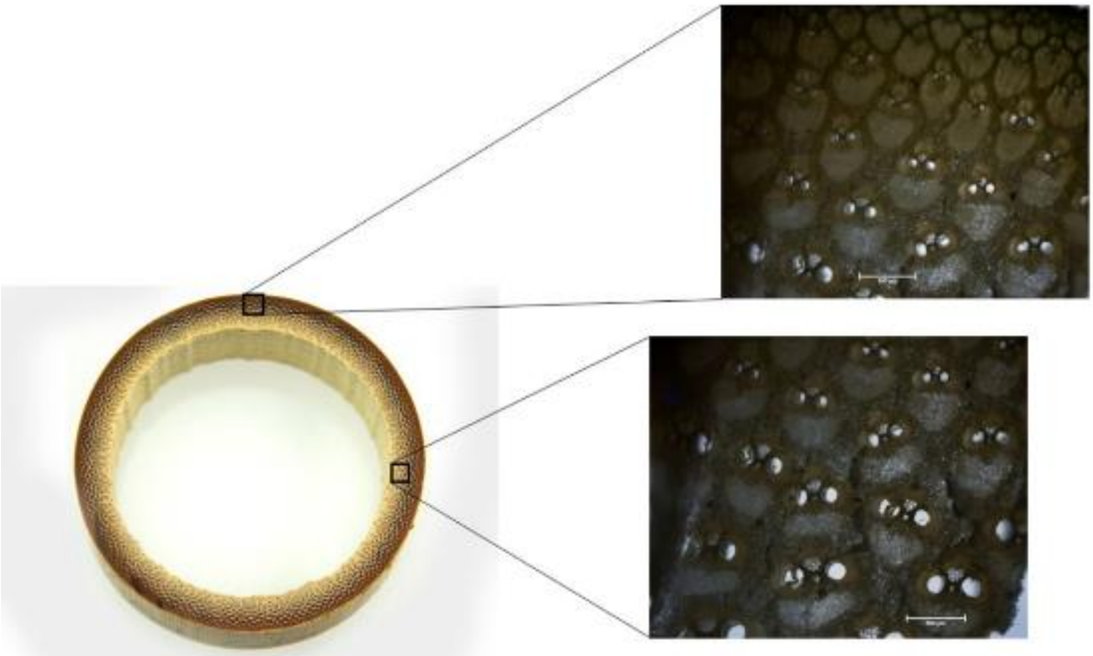

Plate 4.3 Cross-section of beema culm and vascular bundles distribution.

The SEM captured images showed 3-4 vascular bundles in the 1 x 1 mm^2 balcooa culm cross-section (Plate 4.4). The total number of vascular bundles in the 1 x 1 mm^2 in both beema and balcooa were the same.

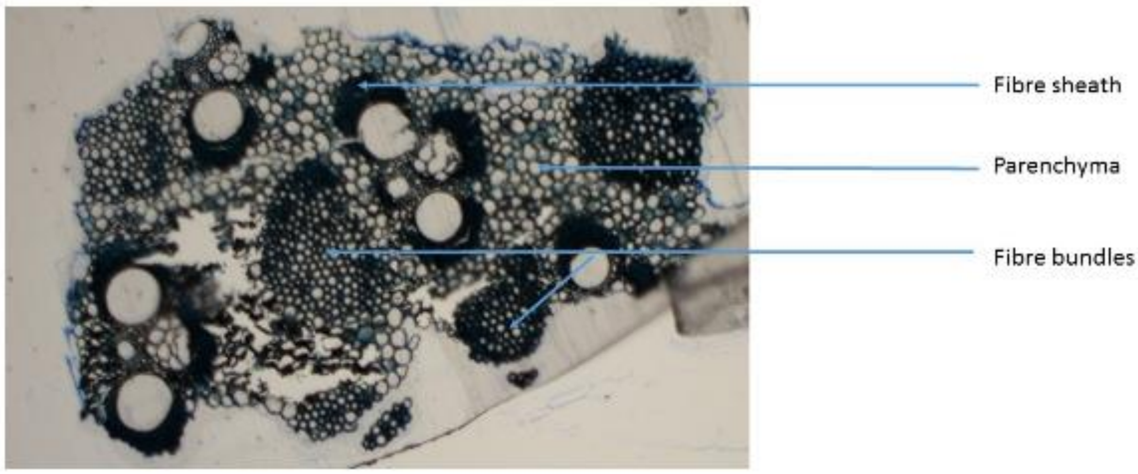

Plate 4.4 Balcooa bamboo culm cross-section.

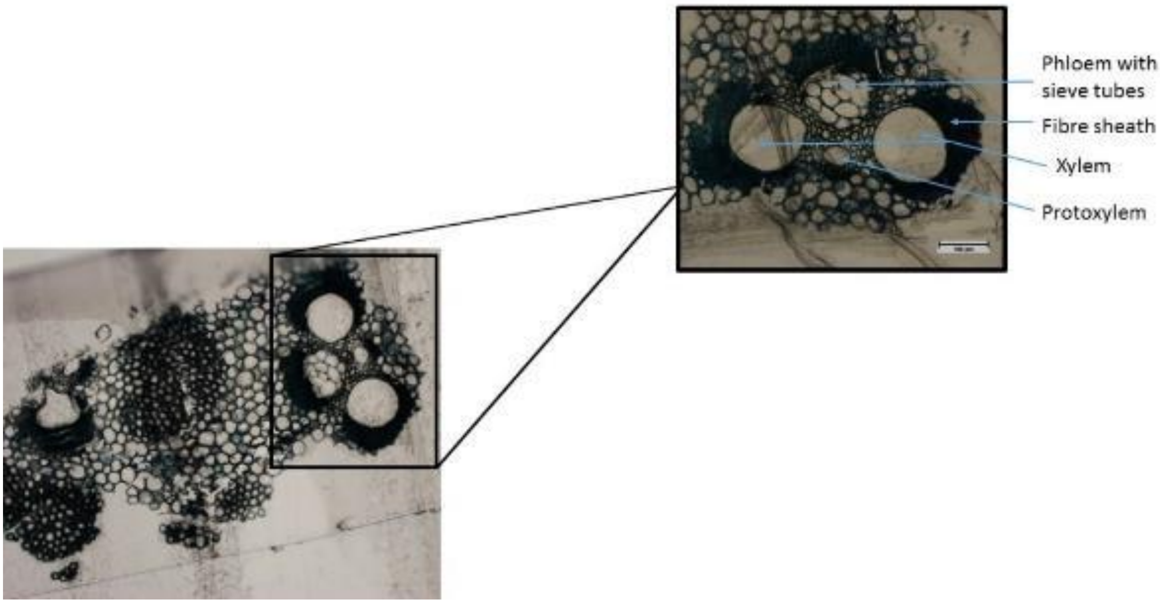

Plate 4.5 Balcooa bamboo vascular bundle structure.

There were approximately 33 balcooa vascular bundles identified in the 20 mm^2 culm under the light microscope. Therefore, the 54.5 mm balcooa culm had at least 2542 vascular bundles of which 65% of the 5.3 mm thick culm were located within the 2-4.5 mm depth region (Plate 4.6). The average vascular bundle diameter and the area were ~ 0.03 mm and 42.4 mm^2 respectively. Approximately, 562 mm^2 in the 1848.8 mm^2 (54.5 mm culm diameter) were occupied by the vascular bundles.

An overall comparison of the anatomy of balcooa and beema indicated that balcooa had higher number of vascular bundles per mm of culm (46.6) when compared to beema (25.9).

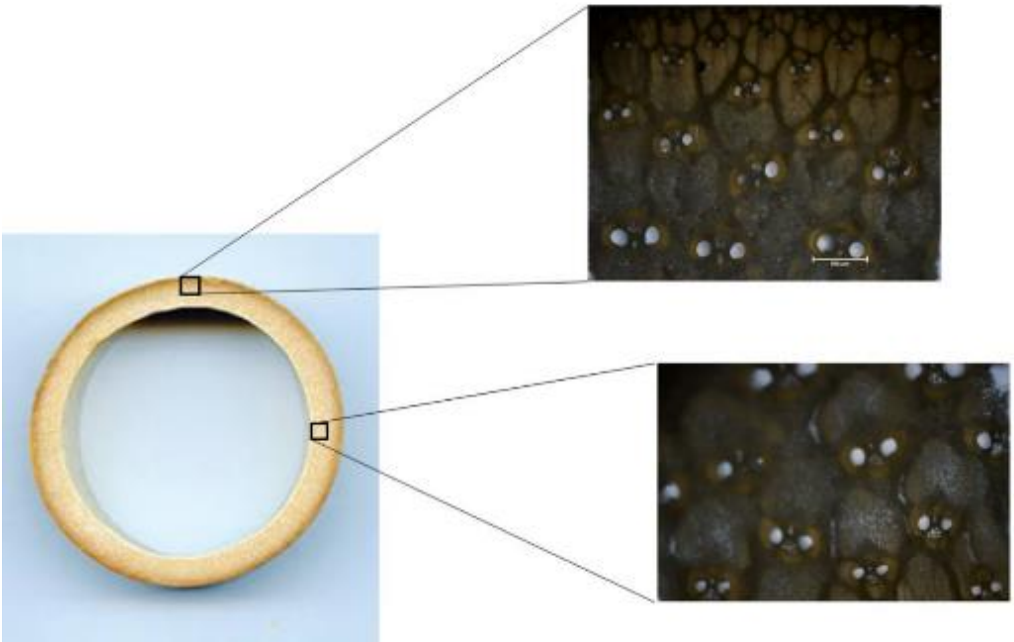

Plate 4.6 Cross-section of balcooa culm and vascular bundle distribution.

4.5 Water-use estimates using the HRM sensors

Four beema culms were monitored from October 2018 to February 2020. The data were used to provide a combined water-use estimate of the beema site based on the four culms monitored and the frequency size classes of all the culms (stand-scale transpiration) measured in the 10 m x 10 m plot (Figure 4.12).

High daily sap flows reaching on average 300 L day^{-1} (average water-use of four instrumented culms) were recorded on warmer days in summer for the beema plot (December-March), except on cool cloudy days when only ~ 170 L day^{-1} were recorded (e.g. 15-30 December 2018) (Figure 4.15). By contrast, consistently low sap flows < 150 L day^{-1} were recorded in winter (May-July 2019) with a few warmer days reaching 170 L day^{-1} in July 2019. Increasing sap flows from ~ 200 L day^{-1} to > 300 L day^{-1} were recorded from September 2019 to February 2020 (Figure 4.15).

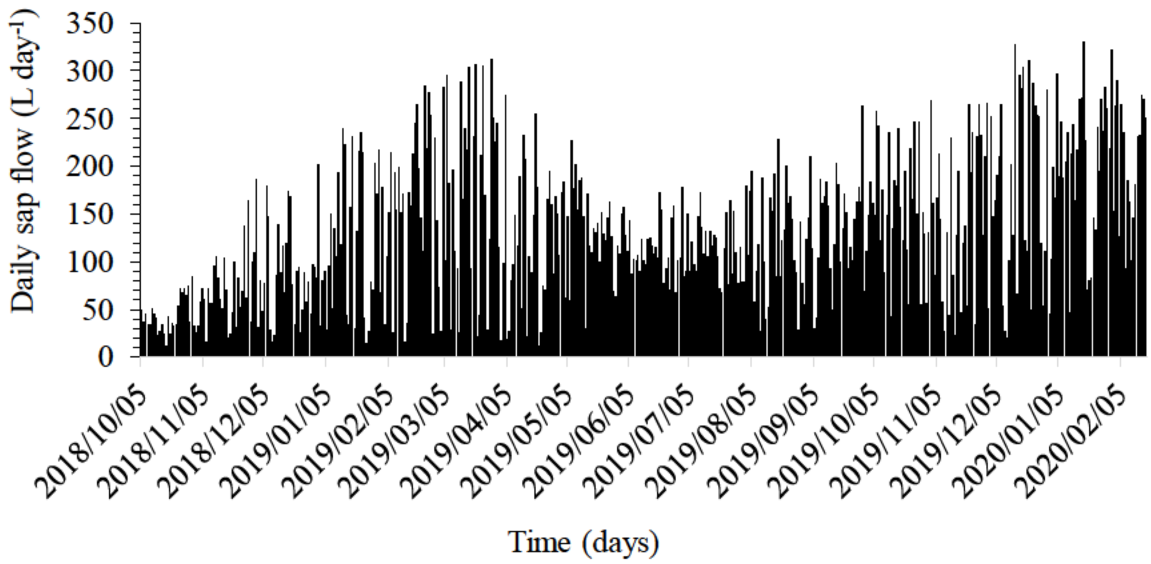

Figure 4.15 Total daily sap-flow (L day^{-1}) of the beema stand for different seasons at Shooter's Hill from 2018 to 2020.

Daily water-use (stand transpiration) was ~ 1.6-3.4 mm day^{-1} in summer (November 2018/2019 to February 2019/2020) with ~ 1.0-1.6 mm recorded in winter (May-July 2019) (Figure 4.16). For the 2018/19 hydrological year (12-month period, from 1 October to 30 September) this resulted in an annual water-use of ~ 422.1 mm yr^{-1}.

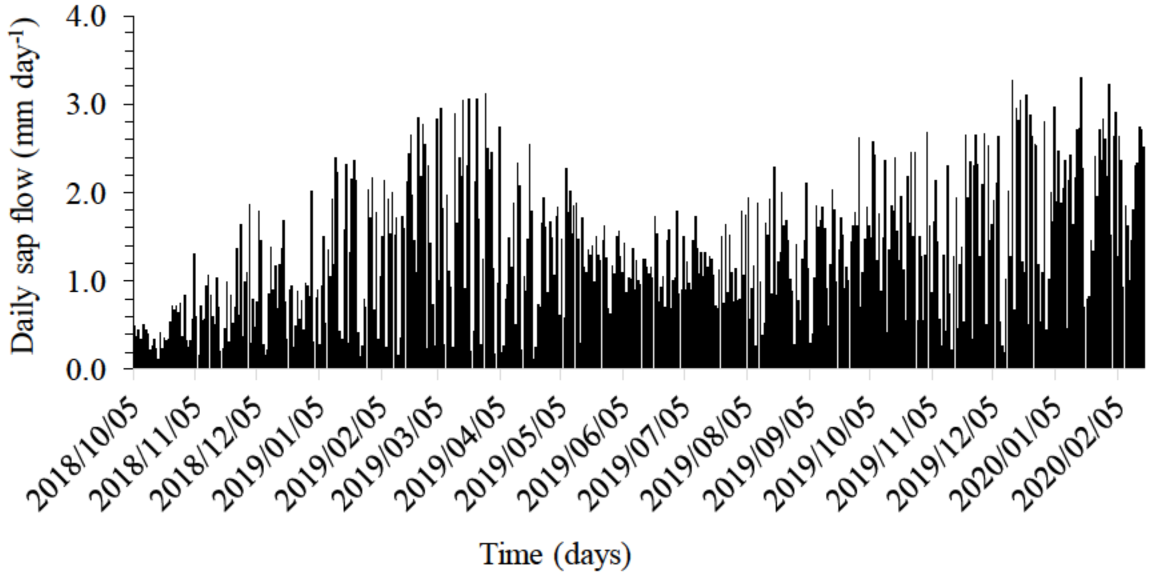

Figure 4.16 Total daily sap-flow (mm day^{-1}) of the beema stand for different seasons at Shooter's Hill from 2018 to 2020.

There was a positive correlation (R^2 = 66%) between the solar radiation and sap flow in beema culms a Shooter's Hill. This indicated that high solar radiation values in summer corresponds to high sap flows in the Beema plantation (Figure 4.17 A). These high water-use rates were therefore achieved also when both energy and moisture were not limiting transpiration.

When conditions were humid (RH ~ 89.6%) in February 2019, VPD and average solar radiation (MJ m^{-2}) were ~ 0.63 and 16.2 MJ m^{-2}. Therefore, the estimated sap flows were only 1.2 mm day^{-1} (Figure 4.17 B).

A

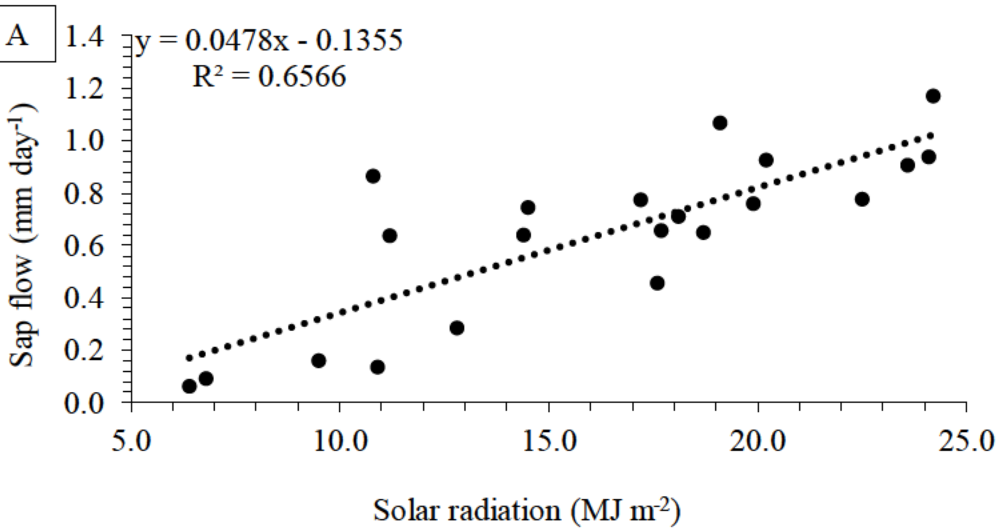

B

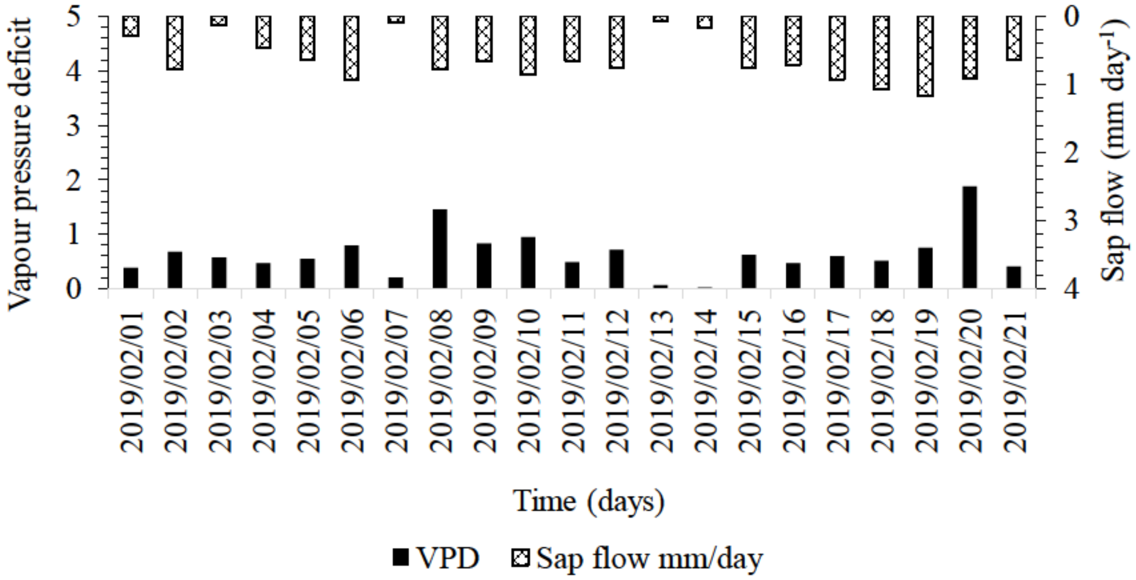

Figure 4.17 Daily sap-flow (mm day^{-1}) of the beema stand in the summer period in relation to A) solar radiation (MJ m^{-2}) and B) VPD using HRM.

By contrast, when incoming energy was < 14 MJ m^{-2}, sap flows were < 0.8 mm day^{-1} in winter (June 2019) (Figure 4.18 A). There was a weak correlation between these variable (R^2 = 6.43%). Dry winter air of RH < 69% and low incoming energy resulted in low sap flows of ~ 0.6 mm day^{-1} during the period (Figure 4.18 B).

A

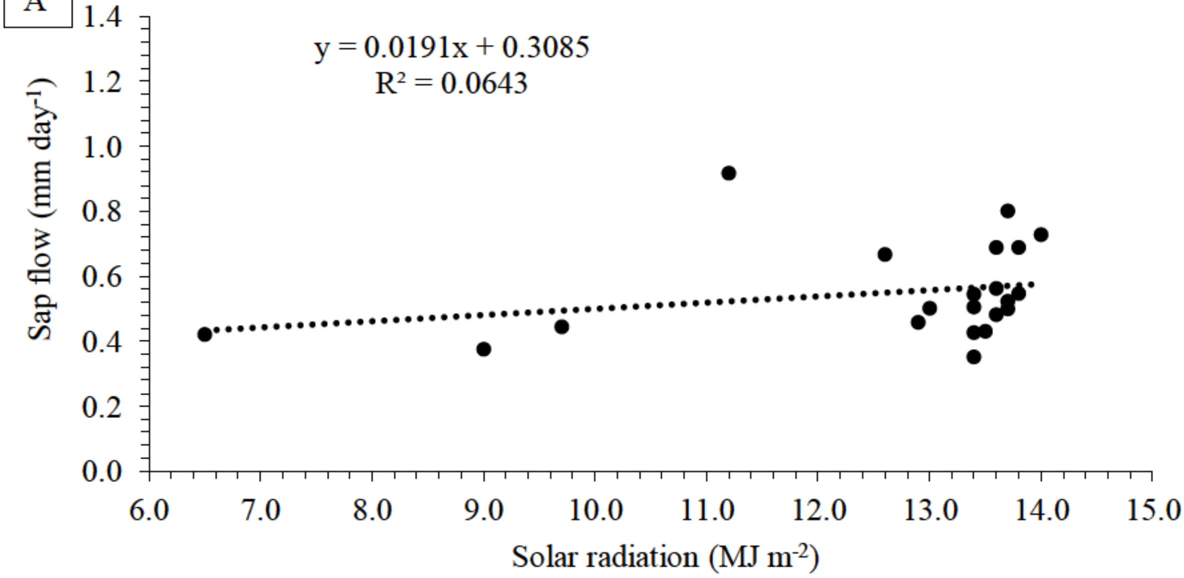

B

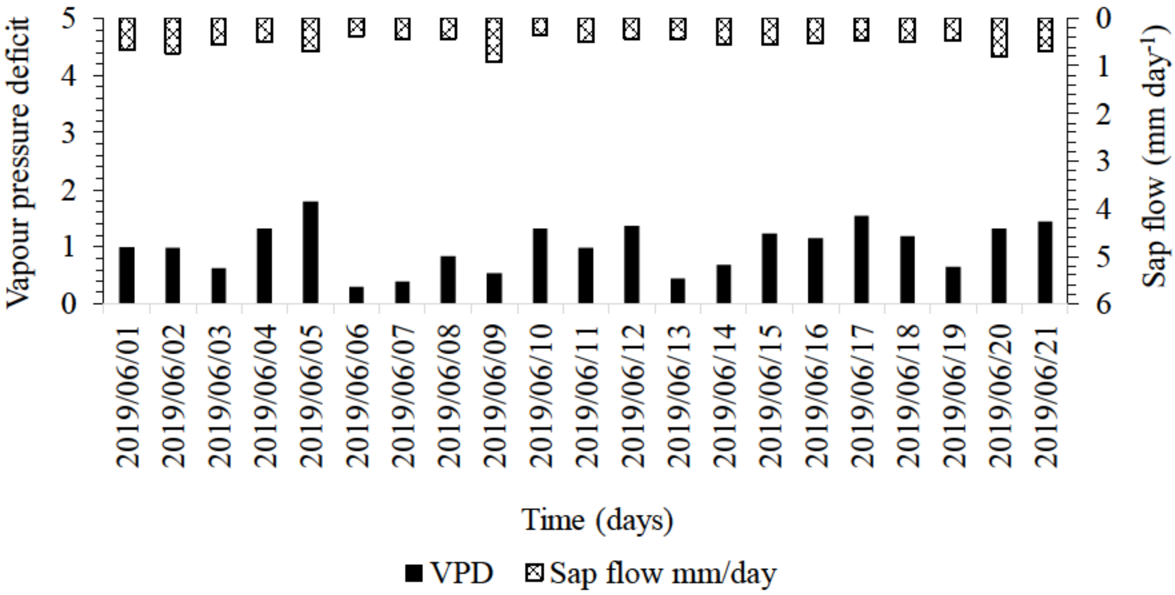

Figure 4.18 Daily sap-flow (mm day^{-1}) of beema stand in winter period in relation to A) solar radiation (MJ m^{-2}) and B) VPD using HRM.

Water-use of balcooa culms were recorded from January 2019 to February 2020. Plot/stand sap flows ≥ 150 L day^{-1} were recorded in summer (January-March 2019) with a maximum sap flow of ~ 220 L day^{-1} in February 2019 (Figure 4.19). Low plot sap flows of ≤ 70 L day^{-1} were recorded in winter (May-July 2019) with the exception of 80 L day^{-1}, which was recorded on the warmer days of 19-20th July 2019 (Figure 5.19). Increasing sap flows from ~ 100 L day^{-1} to > 200 L day^{-1} were recorded from September 2019 to January 2020 (Figure 4.19).

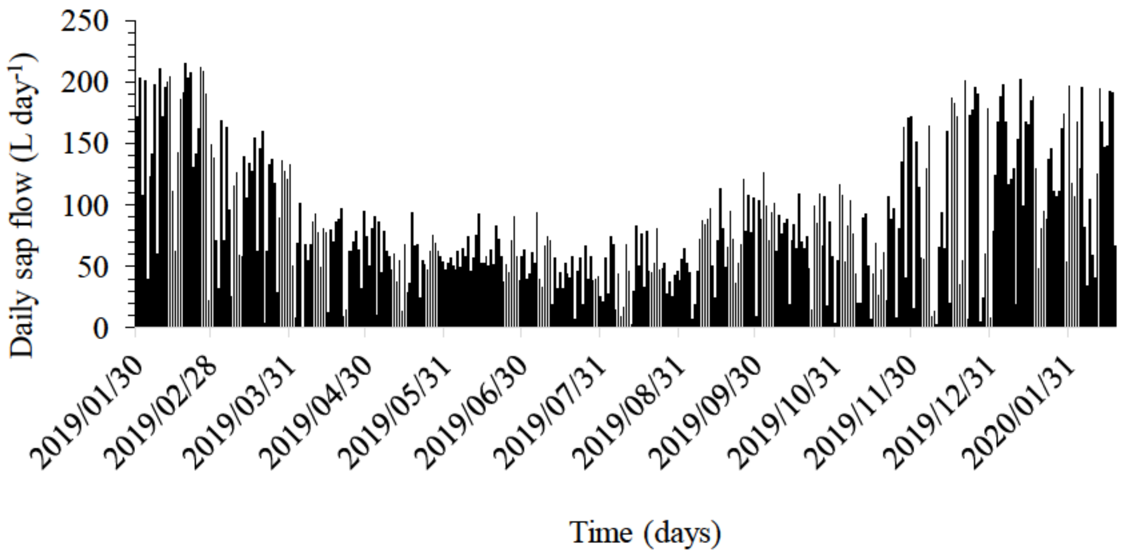

Figure 4.19 Total daily sap-flow (L day^{-1}) of the balcooa stand for different seasons at Shooter's Hill from 2018 to 2020.

Using the size class data and a projected canopy area of 6 X 6 m (36 m^2) the daily transpiration was estimated to be ~ 3.8-5.6 mm day^{-1} in summer and ≤ 2.4 mm in winter (Figure 4.20).

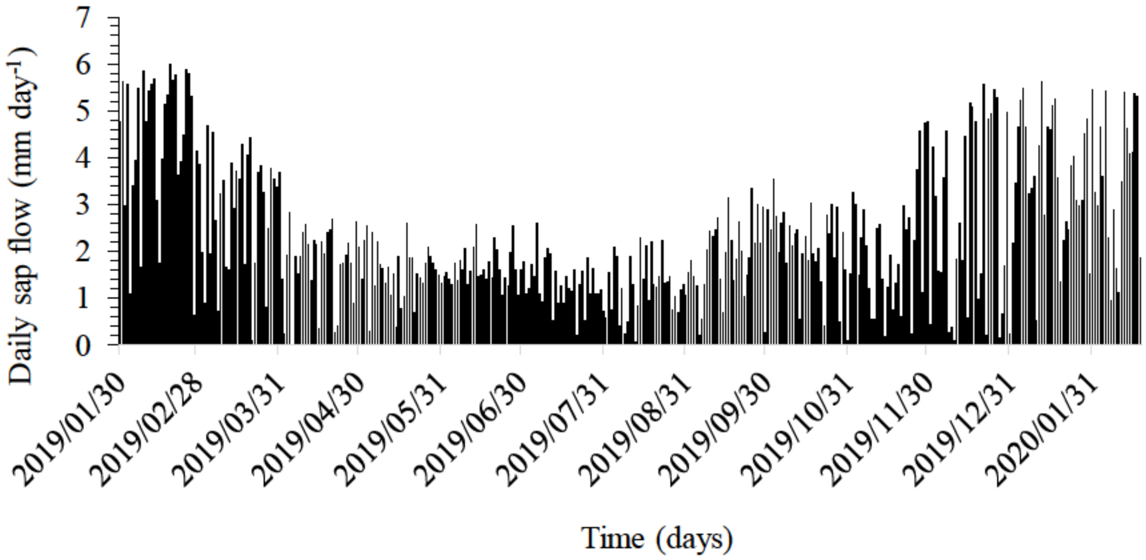

Figure 4.20 Total daily sap-flow (mm day^{-1}) of the balcooa stand for different seasons at Shooter's Hill from 2018 to 2020.

Maximum incoming solar radiation ~ 24.2 MJ m^{-2} and rainfall of 116.4 mm (01st -21st February 2019) resulted to high sap flows reaching 6.00 mm day^{-1}. There was a positive correlation (R^2 = 62%) between solar radition (MJ m^{-2}) and sap flow (mm day^{-1}) at Shooter's Hill (Figure 4.21 A). These high sap flows were mainly caused by high energy and rainfall even though RH were > 89.6% and average VPD ~ 0.63 (Figure 4.21 B).

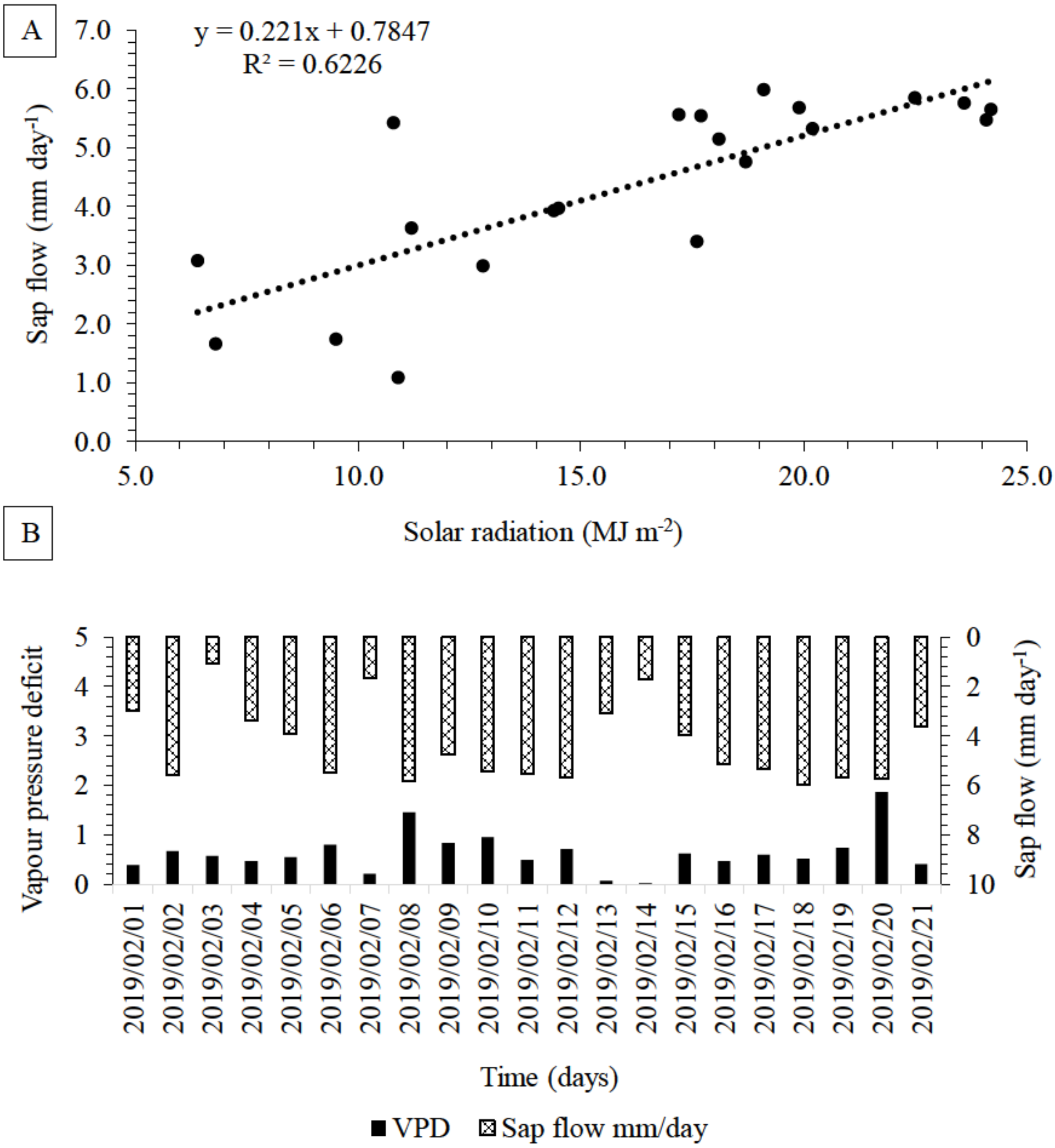

Figure 4.21 Daily sap-flow (mm day^{-1}) of the balcooa stand in the summer period in relation to A) solar radiation (MJ m^{-2}) and B) VPD using HRM.

By contrast, reasonably dry winter air (RH ~ 69.1 %) and low incoming energy < 14.0 MJ m^{-2} resulted to low sap flows < 2.5 mm day^{-1} at Shooter's Hill. The correlation was only 19.6% betweethe energy and water-use of balcooa culms (Figure 4.22 A). Average VPD during the period was ~ 1.00 except few days when the measured RH was 35% low, VPD increased to 1.54 (Figure 4.22 B).

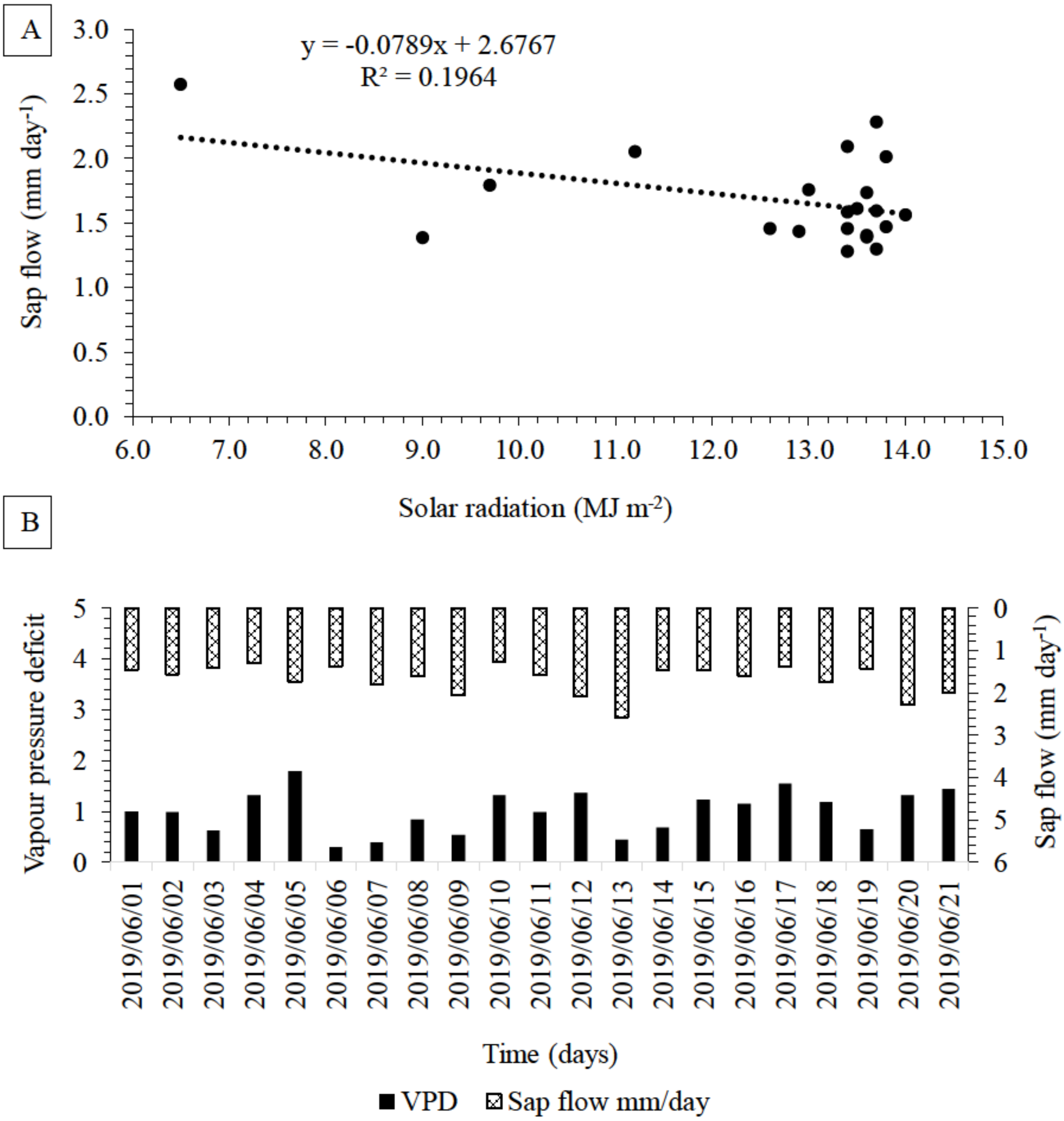

Figure 4.22 Daily sap-flow (mm day^{-1}) of the balcooa stand in the winter period in relation to A) solar radiation (MJ m^{-2}) and B) VPD using HRM.

Daily stand sap flow in the eucalyptus trees showed a high variation of between 700 and 310 L day^{-1} in summer and winter respectively (Figure 4.23). These results were based on a 12 x 12 m (144 m^{2}) plot.

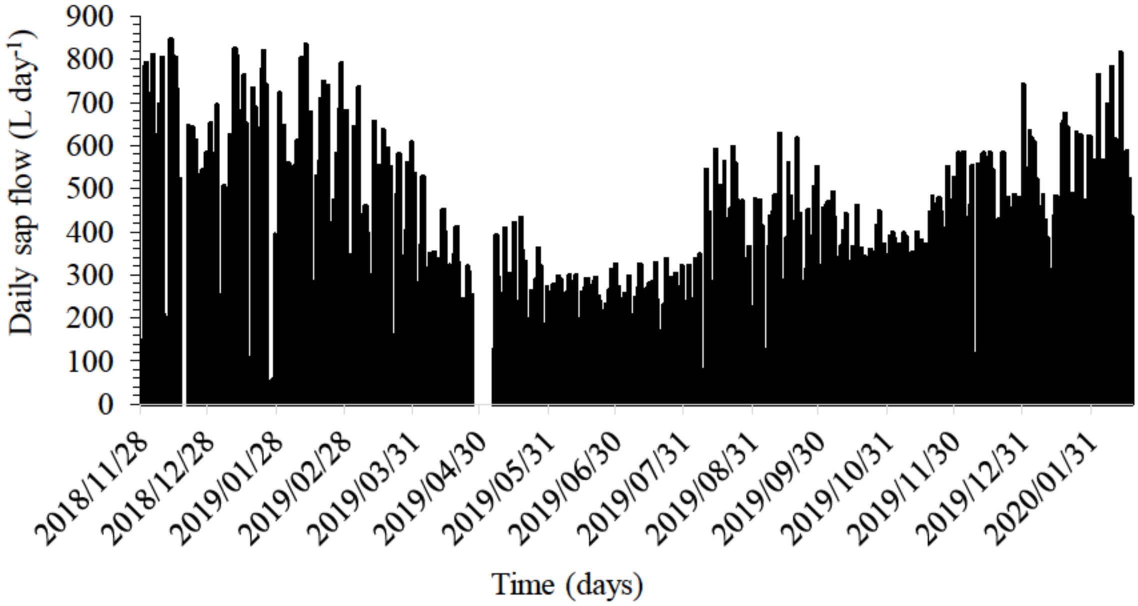

Figure 4.23 Seasonal daily sap-flow (L day^{-1}) at the eucalyptus plantation in Shooter's Hill from 2018 to 2020.

This converts to a daily transpiration of 6.0 and 3.2 mm day^{-1} during summer and winter respectively. From December 2018 to November 2019 the estimated total water-use of the young eucalyptus trees was ~ 906.4 mm (Figure 4.24).

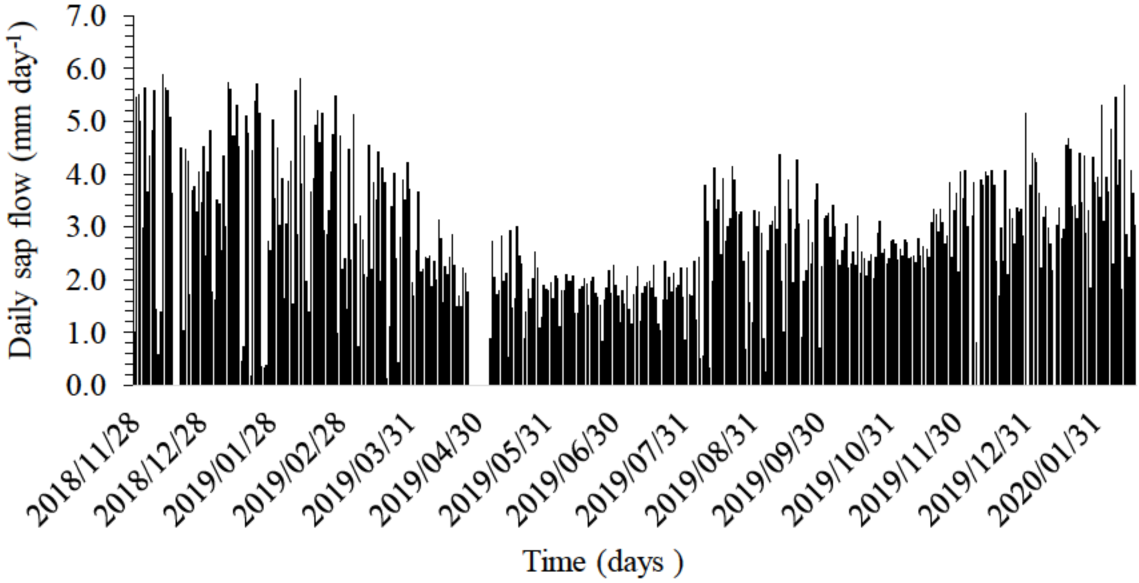

Figure 4.24 Seasonal daily transpiration (mm day^{-1}) of the eucalyptus plantation at Shooter's Hill from 2018 to 2020.

High estimated sap flows > 5.0 mm day^{-1} were measured from the eucalyptus trees when incoming solar radiation reached maximum of 24.2 MJ m^{-2} during the period (Figure 4.25 A). These high sap flows of ~ 6.0 mm day^{-1} were also caused by high VPD reaching 1.87 during the period (Figure 4.25 B).

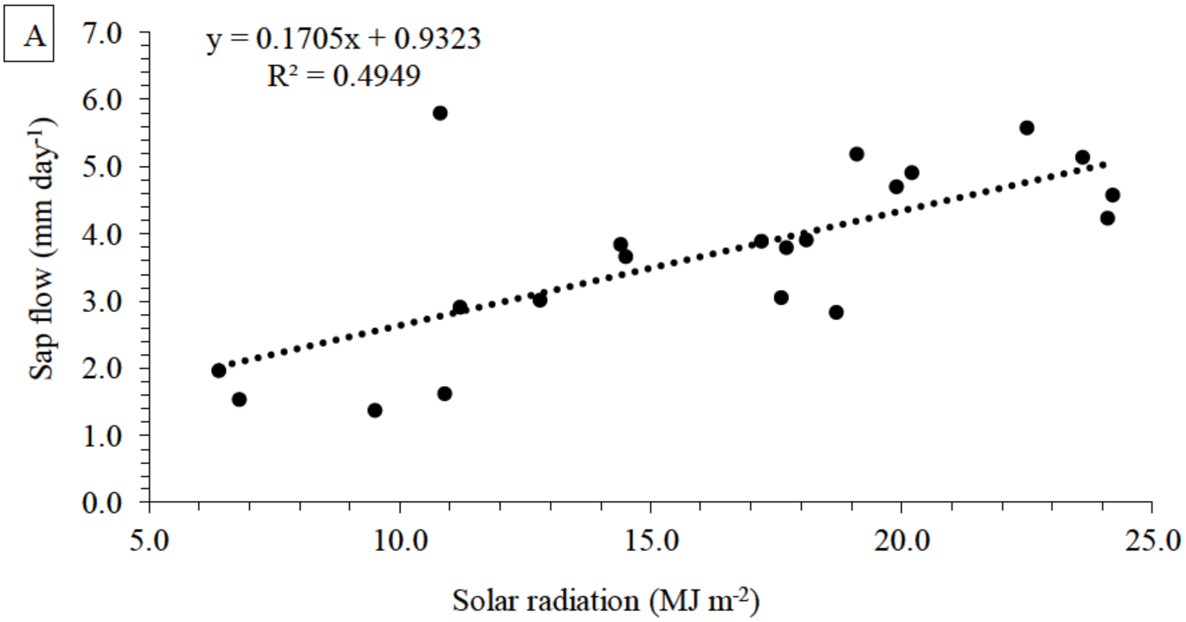

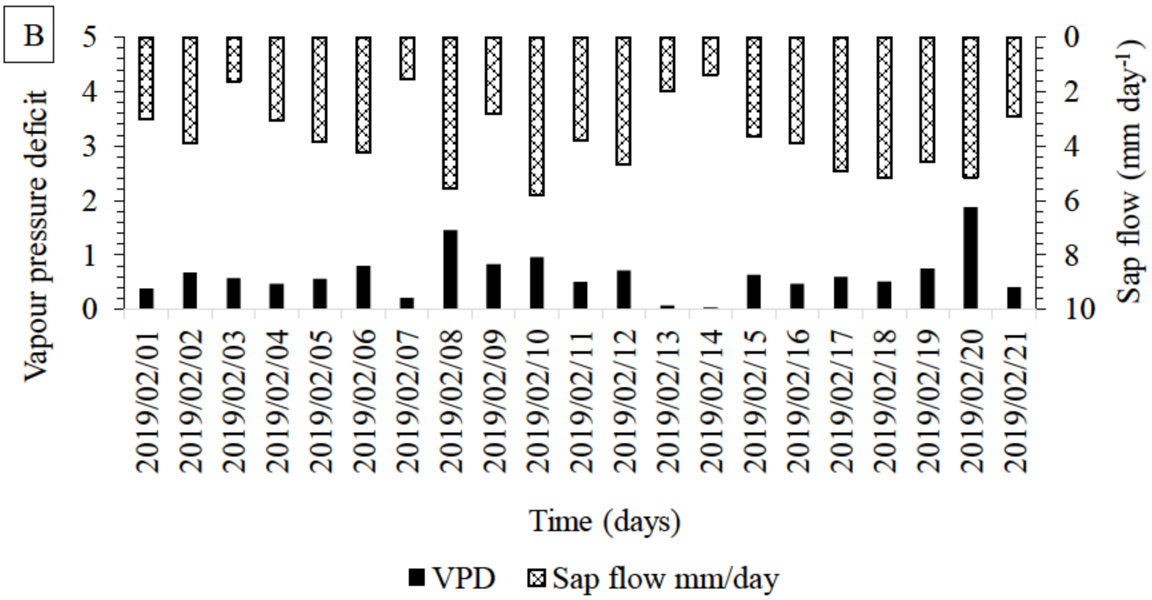

Figure 4.25 Daily sap-flow (mm day^{-1}) of the eucalyptus trees in the summer period in relation to A) solar radiation (MJ m^{-2}) and B) VPD using HRM.

By contrast, minimum energy < 14.2 MJ m^{-2} were measured when the estimated sap flow was ~ 1.8 mm day^{-1} (Figure 4.26 A). The was a poor correlation (R^2 = 34.1%) between these variables. With dry winter air and minimum RH of < 69.1%, high VPD values were measured in the warmer winter days resulted to sap flows reaching ~ 2.1 mm day^{-1} (Figure 4.26 B).

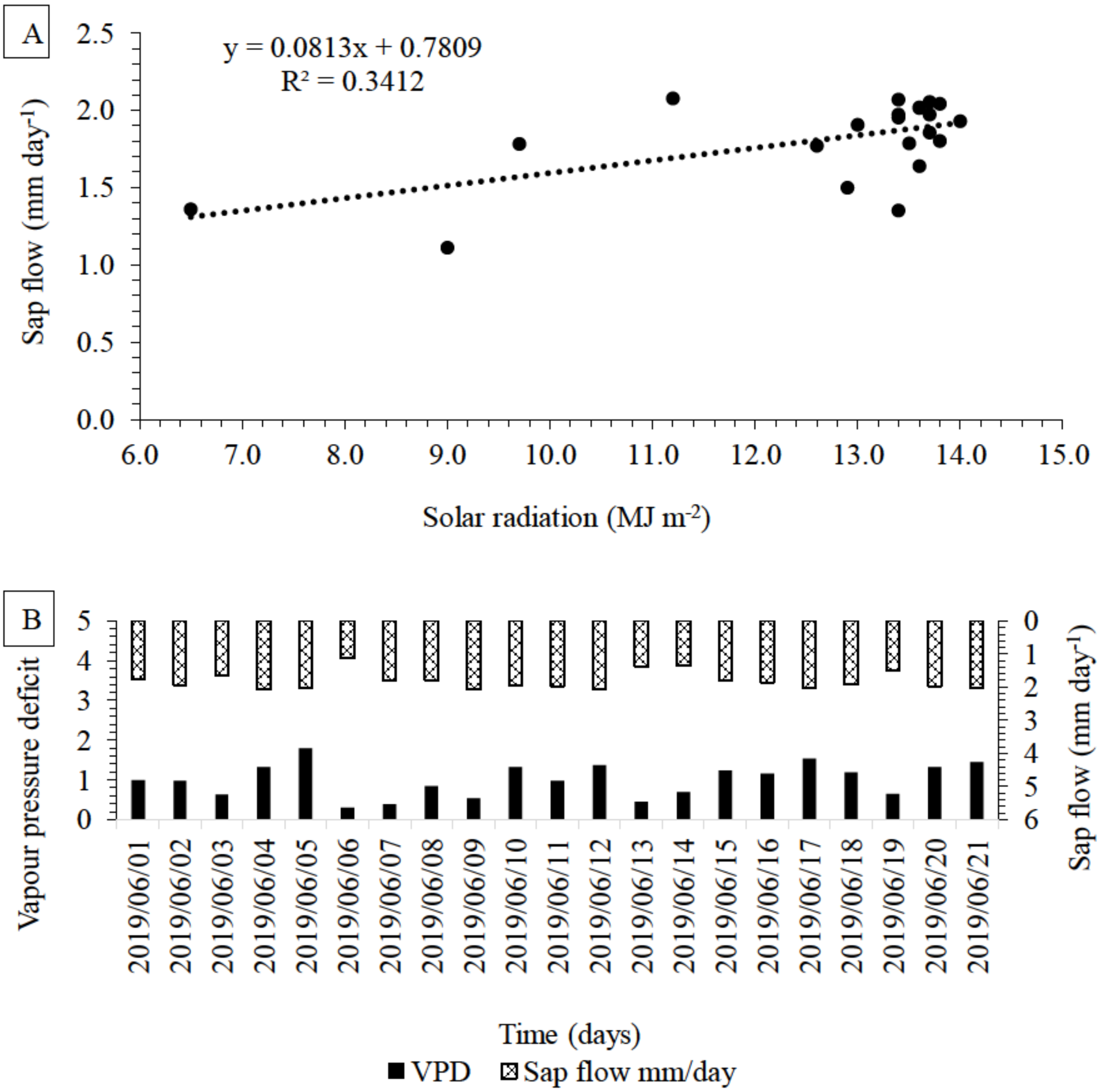

Figure 4.26 Daily sap-flow (mm day^{-1}) of the eucalyptus trees in the winter period in relation to A) solar radiation (MJ m^{-2}) and B) VPD using HRM.

Four *Acacia mearnsii* (wattle) trees were instrumented and measured and compared at the Shooter's Hill site. The average water-use of the four instrumented trees showed that wattle was using ~ 15.0-23.0 L day^{-1} in both winter and summer (Figure 4.27). This was based on a planting espacement of 3 x 1.5 m (4.5 m^2).

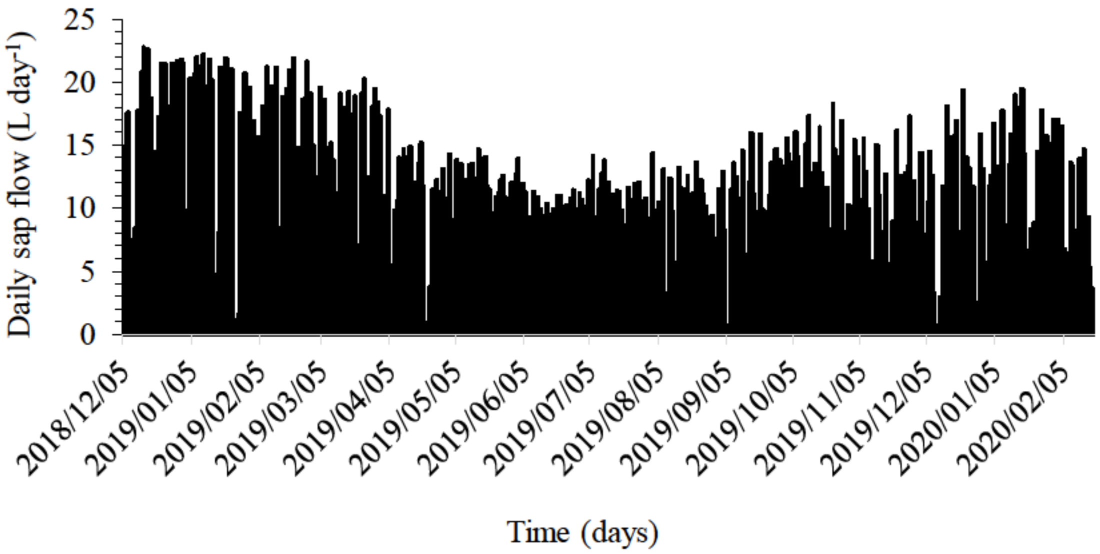

Figure 4.27 Seasonal sap-flow (L day^{-1}) of the black wattle trees at Shooter's Hill from 2018 to 2020.

This translated into ~ 4.0-5.0 mm day^{-1} in summer and 2.4-3.2 mm day^{-1} in winter (Figure 4.28). The total water-use of wattle trees from December 2018- February 2020 was 1132.59 mm whereas 878.17 mm was measured during the hydrologic year (December-October 2019).

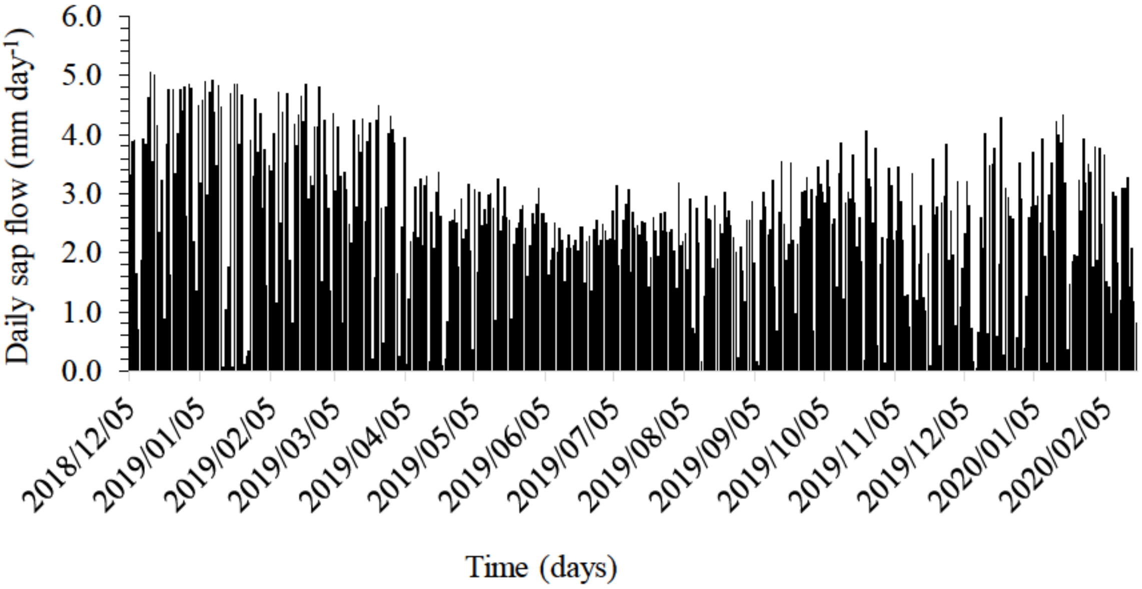

Figure 4.28 Daily transpiration (mm day^{-1}) of black wattle trees for different seasons at Shooter's Hill from 2018 to 2020.

High summer sap flows in wattle trees were exceeding exceeding 4.0 mm day^{-1} when solar radiation was > 23.6 MJ m^{-2}. There was a positive correlation between these variables with R^2 = 59.0 (Figure 4.29 A). Maximum sap flows were corresponding to maximum incoming solar energy VPD ~ 1.87. Also, with high mean air temperatures (> 22.7 ºC) and wind speed 8.15 m s^{-1}, sap flow values recorded in summer were high (Figure 4.29 B).

A

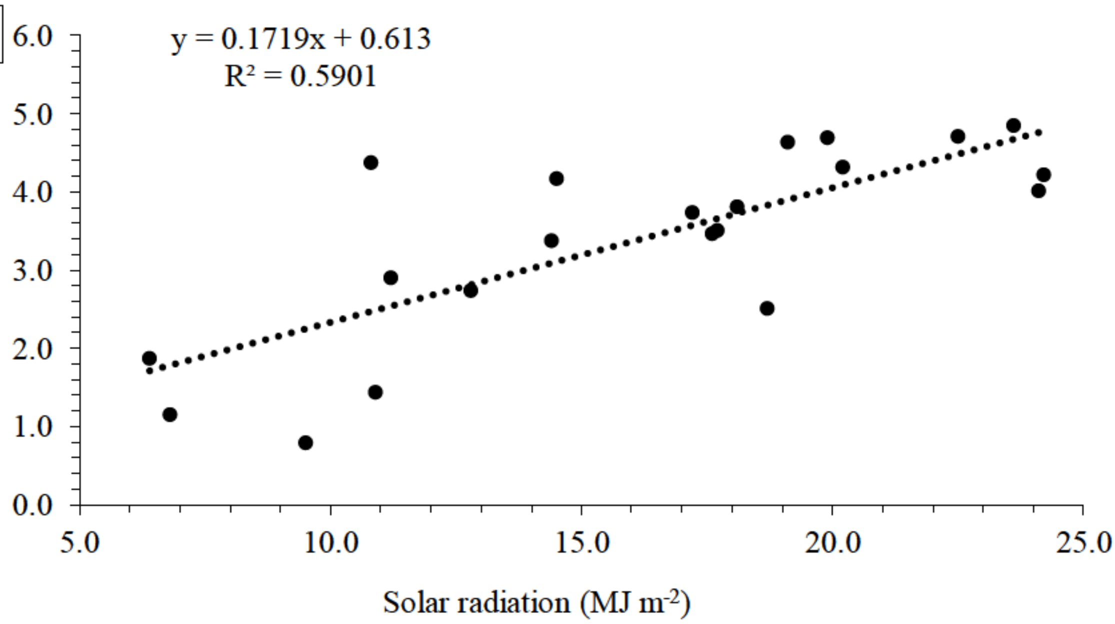

B

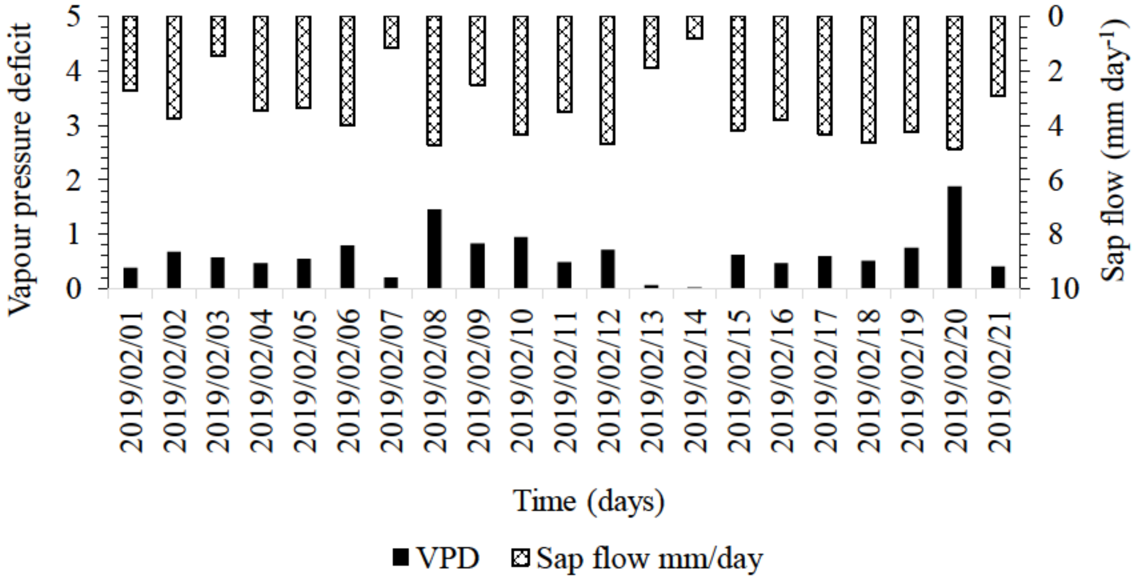

Figure 4.29 Daily sap-flow (mm day^{-1}) of the wattle trees in summer in relation to A) solar radiation (MJ m^{-2}) and B) VPD using HRM.

By contrast, low sap flows < 2.5 mm day^{-1} were measured in winter (June 2019) when solar radiation was ~ 13 MJ m^{-2} and rainfalls < 1.6 mm at Shooter's Hill (Figure 4.30 A). Also, due to dry winter air, measured VPD values were ranging between 1.0-1.7 (Figure 4.30 B).

A

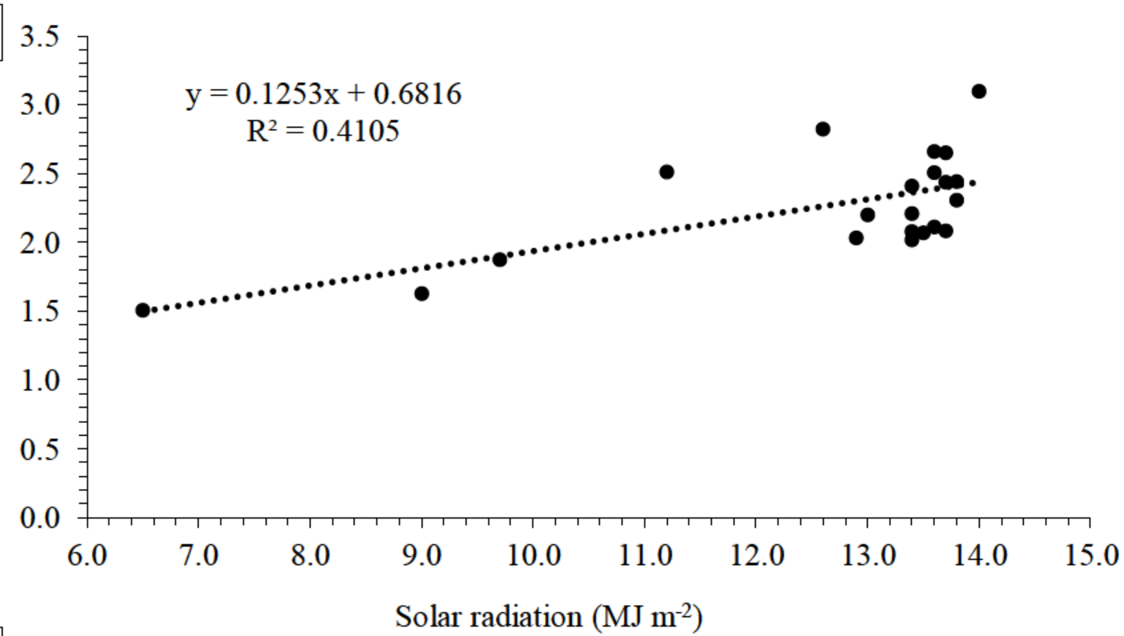

B

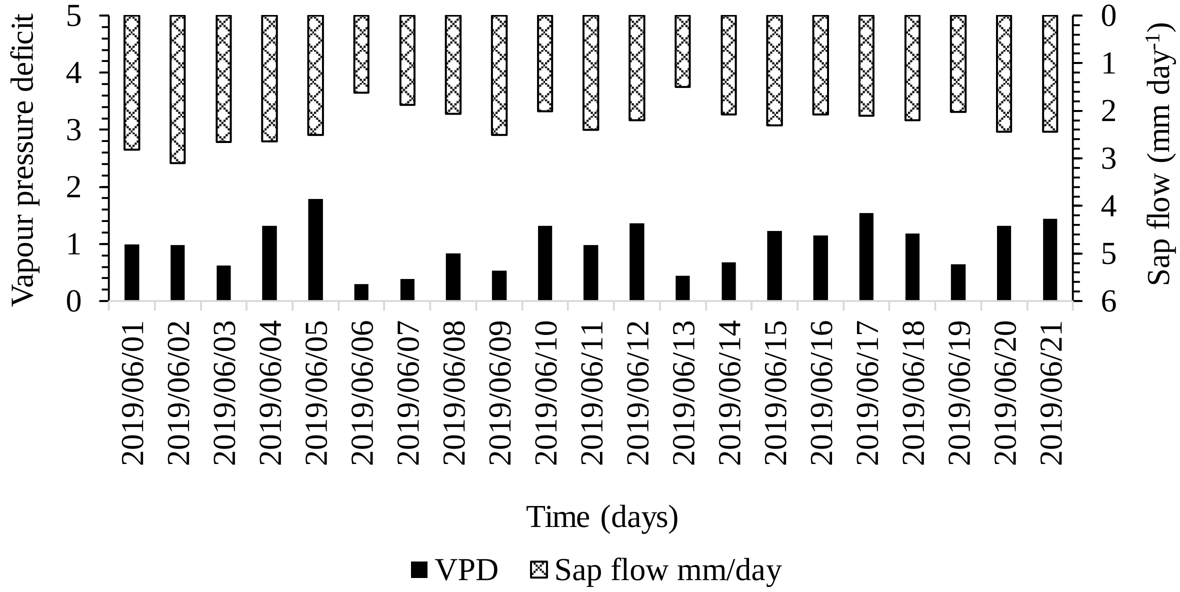

Figure 4.30 Daily sap-flow (mm day^{-1}) of the wattle trees in winter in relation to A) solar radiation (MJ m^{-2}) and B) VPD using HRM.

4.6 Water-use estimated using SSS

Hourly and daily water-use data were collected for the 25 and 50 mm beema culms diameters using SSS from September 2018 to January 2020 (Figure 4.31). The data were used to provide a combined water-use estimate of the beema stand based on the six culms monitored and the frequency size classes of all the culms measured in the 10 X 10 m (100 m^2) plot.

Higher stand sap flows of > 250 L day^{-1} were recorded in summer (November 2018 to March 2019), following low sap flows of ~ 190 L day^{-1} in spring (September-October 2018) (Figure 4.31). By contrast, low sap flows of < 170 L day^{-1} were recorded in winter (May-July 2019) with flows approximately 190 L day^{-1} in the fewer warmer days of winter (May and July 2019) (Figure 5.31). Increasing sap flows of > 200 L day^{-1} were observed in the spring and summer season (September 2019 to January 2020) following low sap flows of ~ 80 L day^{-1} measured in July and August 2019. These were then followed by higher rates in spring and summer recorded in September-December 2020 (Figure 4.31).

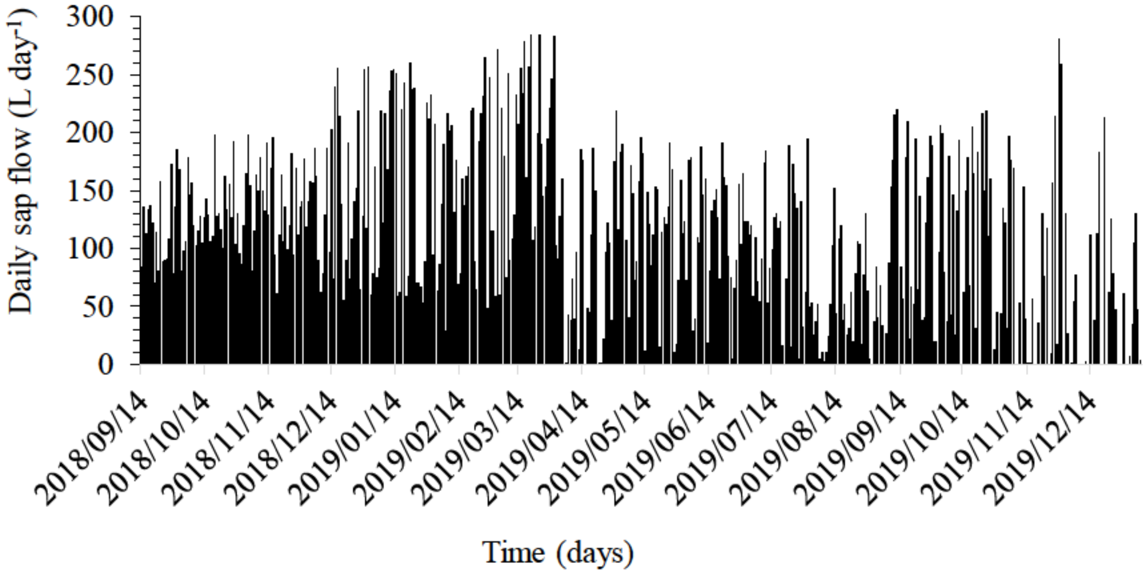

Figure 4.31 Seasonal daily sap-flow (L day^{-1}) of the beema stand at Shooter's Hill.

Upscaling various size classes within the plot gave daily sap-flow rates approaching 2.8 mm day^{-1} in summer and < 1.7 mm day^{-1} in winter (Figure 4.32). This resulted in an average transpiration rate of approximately 1.0-2.7 mm day^{-1} for the monitoring period of 17 months.

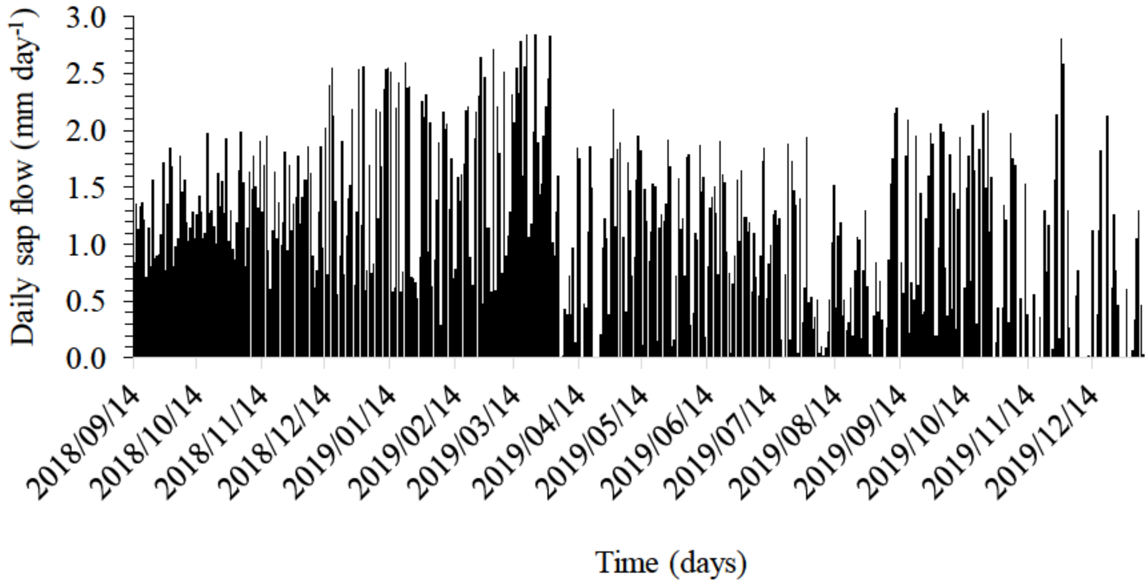

Figure 4.32 Daily transpiration (mm day^{-1}) of the beema stand for different seasons at Shooter's Hill.

There was a positive correlation (R^2 = 61.0%) between the solar radiation and sap flow for the wattle trees following increase in sap flow with te increase in solar radiation (A) at Shooter's Hill in summer. High sap flows exceeding 2.0 mm day^{-1} were measured when solar radiation were ~ 23.6 MJ m^{-2} and VPD > 1.7 in February 2019 (Figure 4.33 A-B).

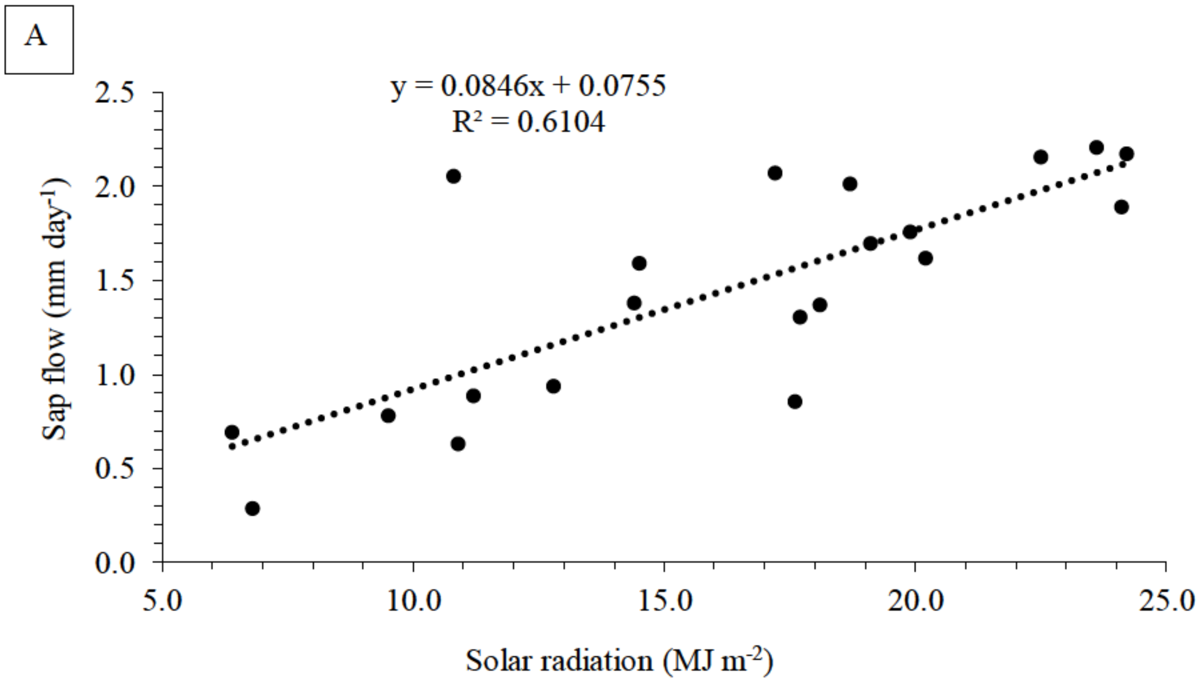

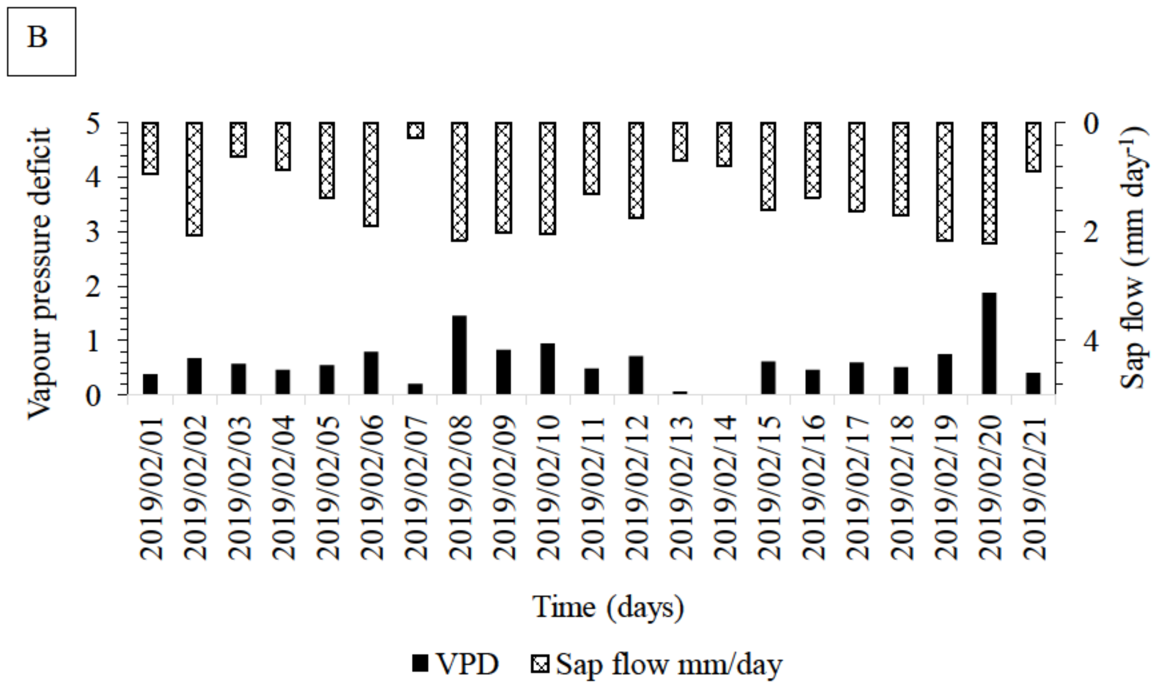

Figure 4.33 Daily sap-flow (mm day^{-1}) of the beema stand in the summer period in relation to A) solar radiation (MJ m^{-2}) and B) VPD using SSS.

By contrast, sap flows < 2.0 mm day^{-1} were measured in winter when average solar radiation was 13.7 MJ m^{-2}. The positive correlation between the variables was 58% (Figure 4.34 A). Due to dry winter air (relative humidity was ~ 69%), the estimated VPD was < 1.3 in most days (Figure 4.34 B).

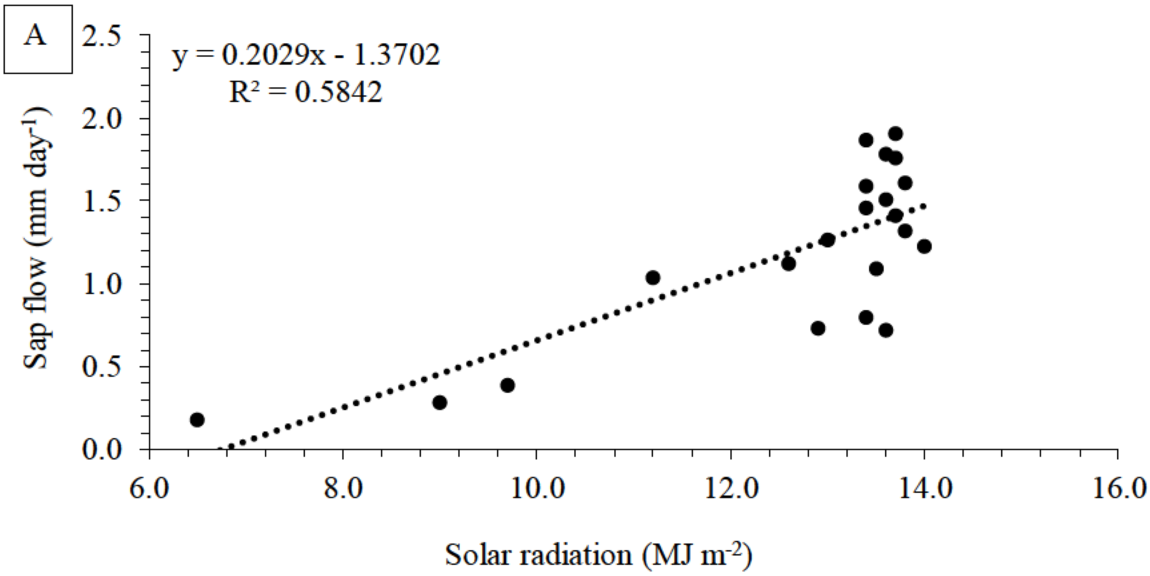

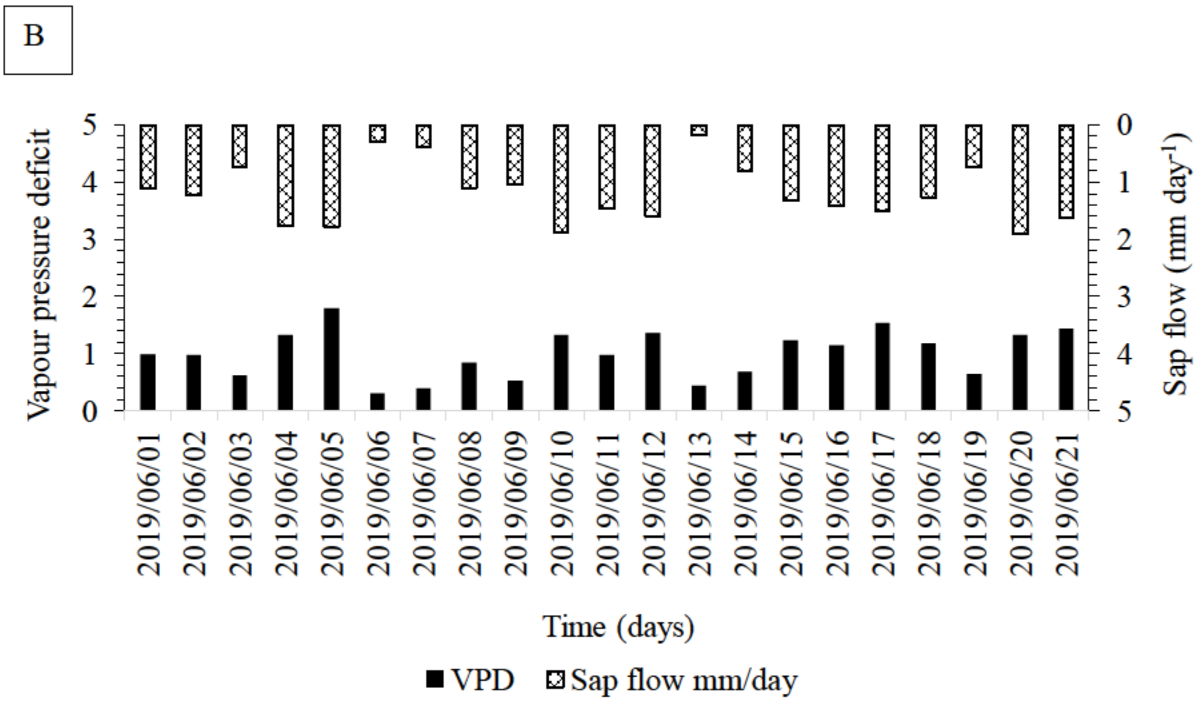

Figure 4.34 Daily sap-flow (mm day^{-1}) of the beema stand in winter in relation to A) solar radiation (MJ m^{-2}) and B) VPD using SSS.

Hourly and daily water-use for the 70 and 100 mm balcooa culms were monitored from September 2018 to January 2020. The data collected were used to provide a combined water-use estimate of balcooa plantation based on four culms monitored and the frequency size classes of all culms measured within the 6 X 6 m (36 m^2) plot.

Sap flow reaching 250 L day^{-1} were recorded in February 2019 (summer) following flows ~ 200 L day^{-1} in January 2019 (Figure 4.35). Low winter sap flows recorded in June-July 2019 were 70 L day^{-1}, with a minimum flow of < 10 L day^{-1} recorded in the dry winter season in August and September 2019. Nevertheless, increasing sap flow were recorded at the beginning of September 2019 (spring) to January 2020 (summer) with a highest sap flow of 230 L day^{-1} recorded in December 2019 (Figure 5.33).

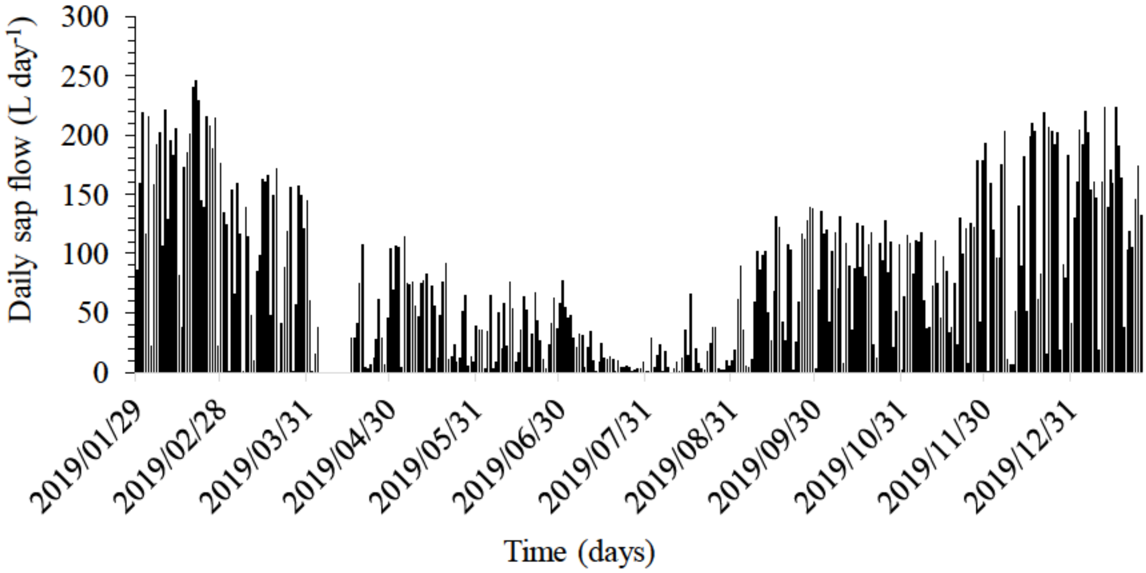

Figure 4.35 Seasonal daily sap-flow (L day^{-1}) of the balcooa stand at Shooter's Hill.

Upscaling various size classes within the plot gave daily sap-flow rates approaching 6.5 mm day^{-1} in summer and < 2.5 mm day^{-1} in winter (Figure 4.36). This gave an average transpiration rate of approximately 0.5-6.5 mm day^{-1} for the monitoring period of 17 months.

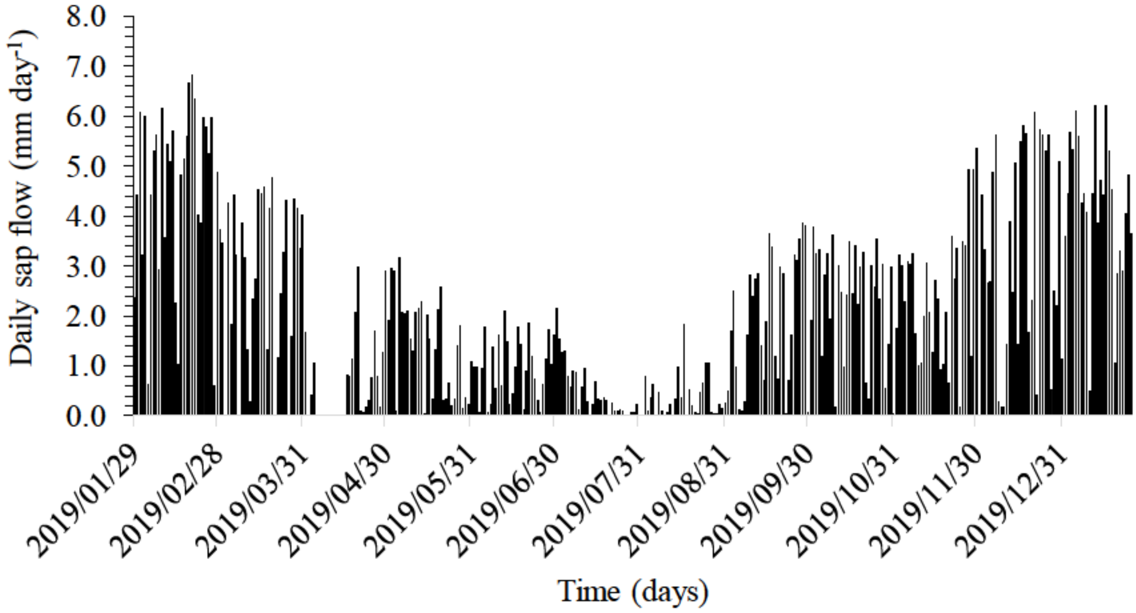

Figure 4.36 Total daily sap-flow (mm day^{-1}) of the balcooa stand for different seasons at Shooter's Hill.

When transpiration was not limited by energy and moisture, a positive correlation (R^2 = 58.6%) was estimated between the solar radiation and sap flow in beema culms a Shooter's Hill using SSS sensors (A). High sap flows exceeding 5.0 mm day^{-1} were measured when solar radiation were ~ 23.6 MJ m^{-2} and VPD reaching 1.87 in February 2019 (Figure 4.37 A-B).

A

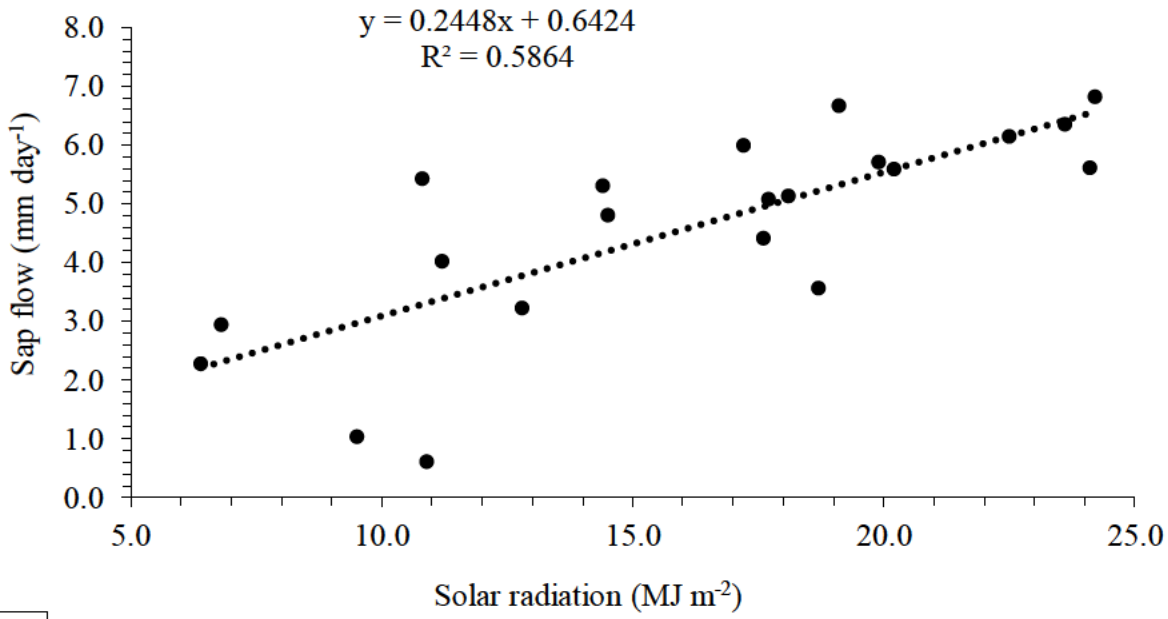

B

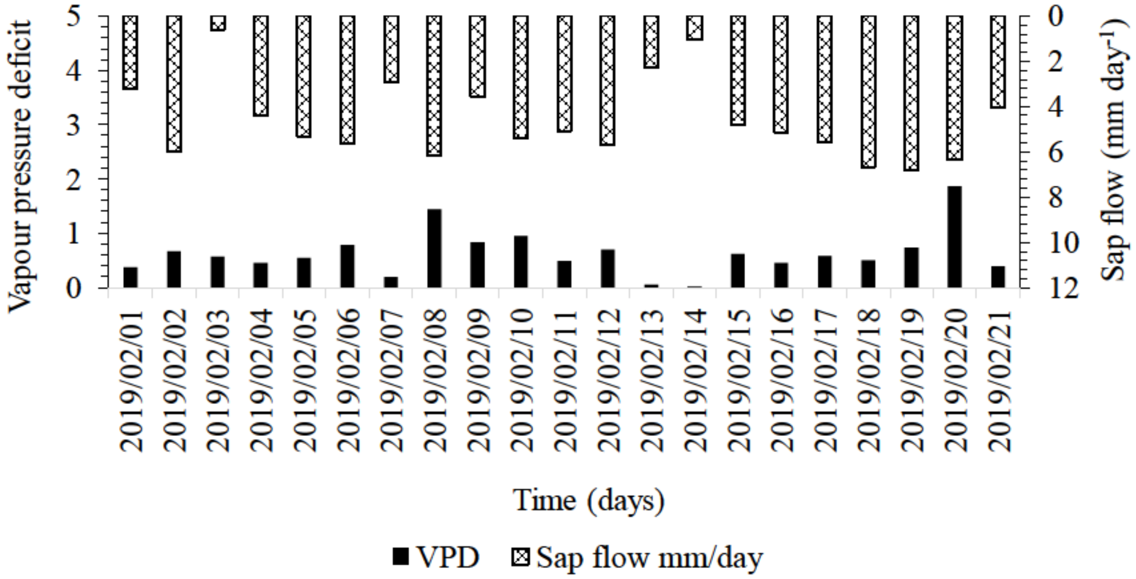

Figure 4.37 Daily sap-flow (mm day^{-1}) of the balcooa stand in the summer period in relation to A) solar radiation (MJ m^{-2}) and B) VPD using SSS.

In warmer winter days when solar radiation was ~ 13.8 MJ m^{-2} and dry air (RH ~ 69%), VPD values were exceeding 1.0 causing sap flows to reach 2.0 mm day^{-1} (Figure 4.38 A-B).

A

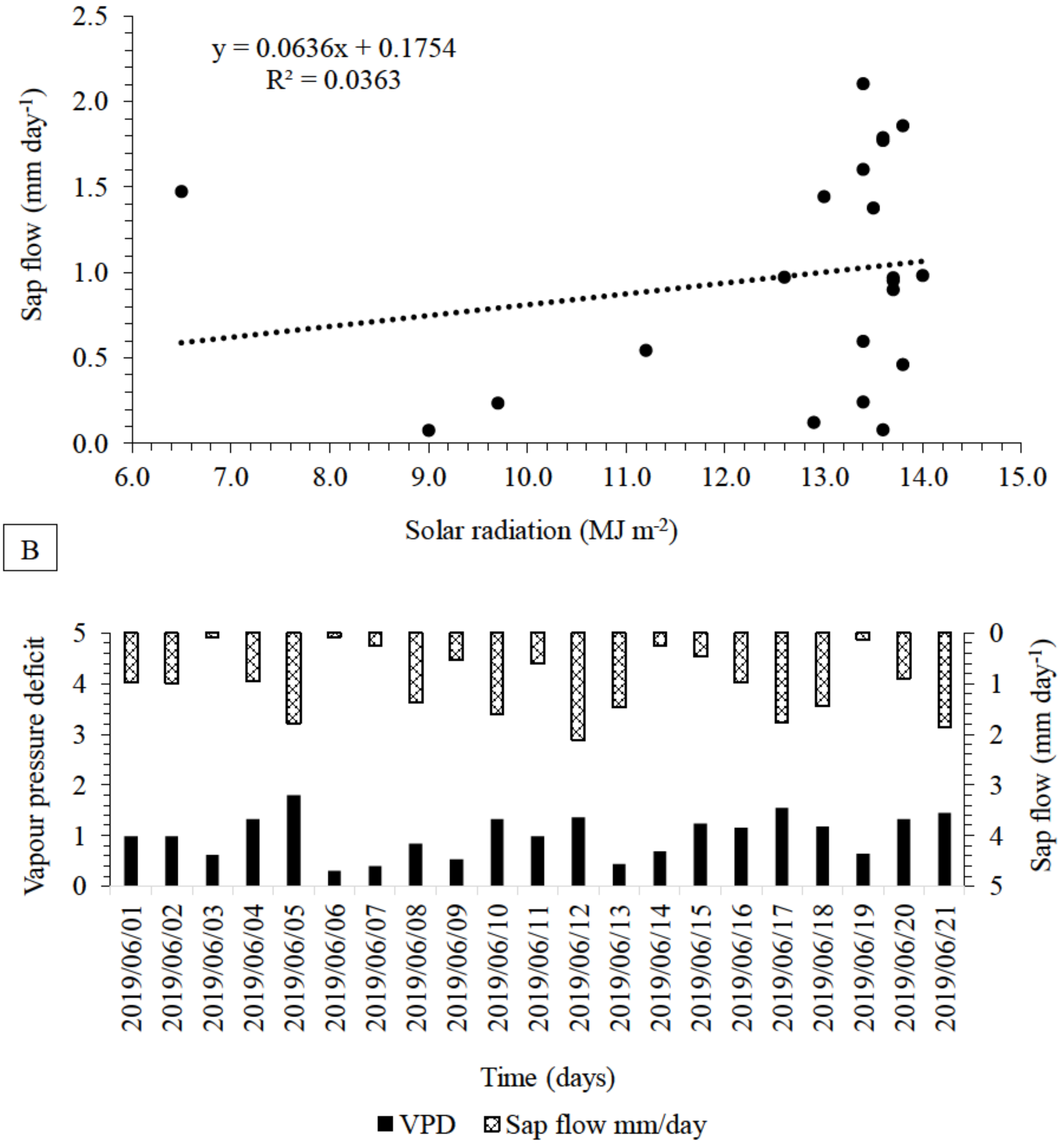

Figure 4.38 Daily sap-flow (mm day^{-1}) of the balcooa stand in the winter period in relation to climatic variables using SSS.

4.7 Total water-use of the beema, balcooa, eucalyptus and wattle at Shooter's Hill

Annual water-use of beema, balcooa, eucalyptus and wattle trees were calculated from 2019/01 to 2019/12 (12-month period) using HRM and SSS. The highest water-use using the HRM sensors (~ 1186.5 mm) was recorded at the eucalyptus plantation followed by 122.6 mm recorded from the wattle trees using HRM (Table 4.4). Bamboo had low water-use compared to other land-uses both in the balcooa and beema plantations, 958 and 657.2 mm, respectively. Irrespective of the smaller study area for balcooa compared to beema, the total water use of balcooa was ~ 300.8 mm higher at the end of the 12-month period (Table 4.4). Although there were fewer balcooa culms (72) compared to the beema culms (215), they had significantly higher culm diameters with 56% of the balcooa culms falling into the 30-49 mm size class. The higher number of vascular bundles per mm of culm (46.6) when compared to beema (25.9), together with the higher culm diameters would contribute to the higher water-use.

Table 4.4 Total water-use of beema, balcooa, eucalyptus and wattle trees from 2019/01/01 to 2019/12/31 using HRM and SSS.

	Total sap flow (mm year^{-1})		
Species name	**HPV**	**SSS**	**Area measured (m2)**
Beema	657.2	520.0	100
Balcooa	958.0	1254.8	36
Eucalyptus	1186.5		144
Wattle	1122.6		20

The corresponding grass reference evaporation (ET_0) was measured to calculate monthly transpiration coeffcicient (K_{cb}) and the average seasonal K_{cb}. The data collected in the HRM and SSS were used to calculate average transpiration which was subsequently used to calculate the monthly K_{cb} for bamboo. In the Wattle and Eucalyptus plantation, only HRM data were used to calculate K_{cb}. In summer, high ET_0 exceeding 108.5 mm (November 2019), and as expected, higher than the average transpirations of the balcooa and beema plantations of 37.8 mm and 68.7 mm (Table 5.5). Transpiration in the Eucalyptus and Wattle sites were recorded 88.2 mm and 66.6 in the same period.

Table 4.5 Comparison of the water-use for different land-uses and ET_0 at Shooter's Hill.

Timestamp (months)	Water-use (mm month^{-1})						ET_0 (mm)	Transpiration coefficient (K_{cb})			
	HPV				SSS						
	Beema	Balcooa	Eucalyptus	Wattle	Beema	Balcooa		Beema	Balcooa	Eucalyptus	Wattle
Oct-18	11.79	18.78			40.64	34.15	112.4	0.23	0.24		
Nov-18	21.07	36.21			40.92	89.11	113.2	0.36	0.55		
Dec-18	26.49	19.55	106.30	95.60	44.48	199.02	117.2	0.38	0.93	0.91	0.82
Jan-19	38.56	40.17	106.76	101.48	49.02	187.52	111.1	0.44	1.02	0.96	0.91
Feb-19	44.89	82.07	103.68	96.58	45.98	129.07	97.6	0.47	1.08	1.06	0.99
Mar-19	53.37	90.00	89.72	96.37	57.11	87.21	99.6	0.55	0.89	0.90	0.97
Apr-19	35.71	52.19	57.69	63.49	24.58	19.25	68.2	0.52	0.77	0.85	0.93
May-19	32.35	48.35	48.78	64.02	29.50	43.50	65.5	0.49	0.70	0.74	0.98
Jun-19	34.66	49.37	43.30	66.60	24.12	29.00	57.4	0.42	0.51	0.75	1.16
Jul-19	35.69	40.45	54.27	72.89	25.26	14.66	71.9	0.35	0.38	0.75	1.01
Aug-19	36.34	38.49	57.94	62.98	16.42	11.32	76.3	0.35	0.33	0.76	0.83
Sep-19	45.13	55.44	75.13	67.96	29.71	57.43	98.1	0.30	0.58	0.77	0.69
Oct-19	48.62	64.87	87.66	80.19	33.01	72.57	126.4	0.38	0.54	0.69	0.63
Nov-19	51.04	62.54	88.22	66.62	24.64	74.78	108.5	0.47	0.63	0.81	0.61
Dec-19	53.40	82.48	90.63	62.25	13.18	99.69	105.5	0.51	0.86	0.86	0.59
Jan-20	53.48	114.04	108.87	85.98	21.47	106.47	122	0.44	0.90	0.89	0.70
Feb-20	34.58	63.02	67.52	39.58			101.9	0.34	0.62	0.66	0.39

There was large difference between water-use measured in the HRM and SSS during December-January 2019 (Table 4.5). For example, when 19.55 and 40.17 mm were measured in the HRM technique, high sap flows of 199.02 and 187.52 mm were measured in the SSS technique. Such high sapflow values might have been caused through running the system 24 hours daily to determine K_{sh} which was used in the system program. When Ksh was identified, sap flows measured in the SSS were as equal to HRM values.

Monthly reference evaporatranspiration (ET_0) rates were high, exceeding 100.0 mm in most summer months with maximum ET_0 of ~ 126.4 mm in October 2019 followed by 122 mm (January 2020) (Figure 5.39). these values indicated that summer ET_0 rates were high, unlike in the dry winter (May-July 2019), when low ET_0 rates < 72 mm were measured (Figure 4.39).

Transpiration coefficient (K_{cb}) in the Beema plantation was high in summer and low in winter with values ranging from 0.23-0.55 mm. The maximum K_{cb} value of 0.55 was recorded in March 2019 followed by 0.53 in April (Figure 4.39 A). By contrast, average K_{cb} of 0.35 was recorded suring winter when energy and moisture were limiting transpiration. Balcooa culms showed high K_{cb} approaching 1.0 in summer when there were high rainfalls and incoming energy, unlike in winter when only a maximum of 0.51 mm was recorded in June 2019 (Figure 4.39 B). The lower K_{cb} recorded during the study period was 0.33 mm in August 2019 (winter), except 0.24 recorded in October 2018. Similarly to the balcooa culms, the K_{cb} in the eucalyptus trees were ~ 1.0 mm in summer. Very high average K_{cb} values of ~ 0.75 were recorded in winter indicating high water-use potential of the trees in dry winter season (Figure 4.39 C). Transpiration coefficient > 0.7 but < 1.0 were recorded in the wattle trees during summer except few months, for example December 2019 when only 0.59 was recorded (Figure 4.39 D). Unlike other landuses studied at Shooter's Hill, wattle trees showed high K_{cb} values ≥ 1.0 mm in winter. Therefore, the above K_{cb} data indicated that bambo especially beema was more water-user than these species.

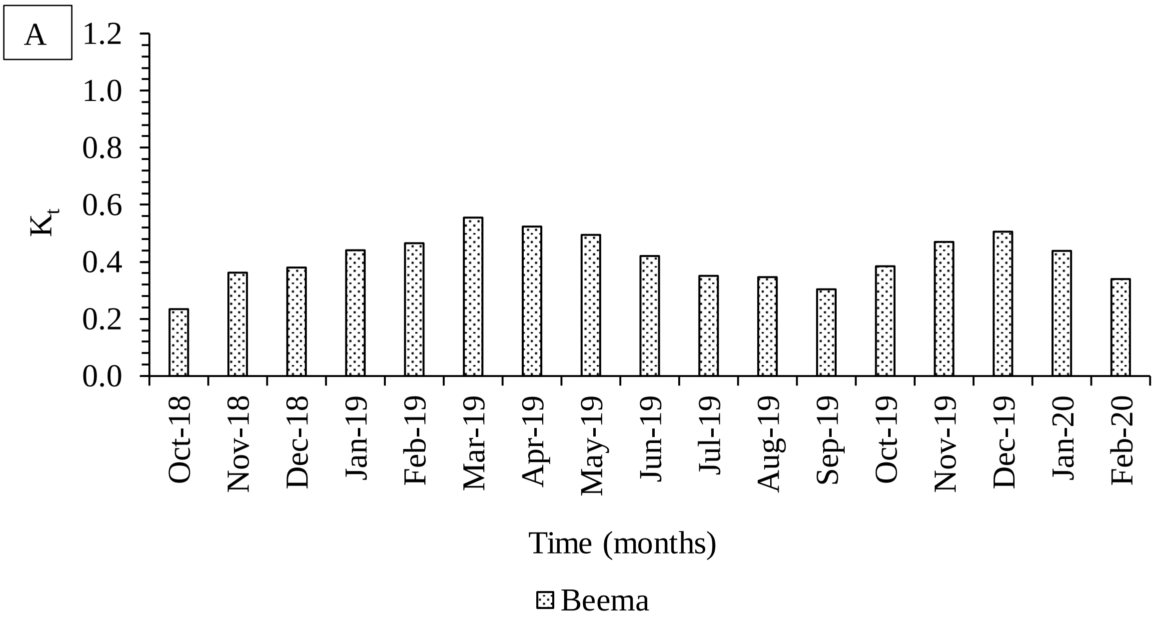
A
1.2
1.0
0.8
0.6
0.4
0.2
0.0
K_t
Oct-18
Nov-18
Dec-18
Jan-19
Feb-19
Mar-19
Apr-19
May-19
Jun-19
Jul-19
Aug-19
Sep-19
Oct-19
Nov-19
Dec-19
Jan-20
Feb-20
Time (months)
Beema

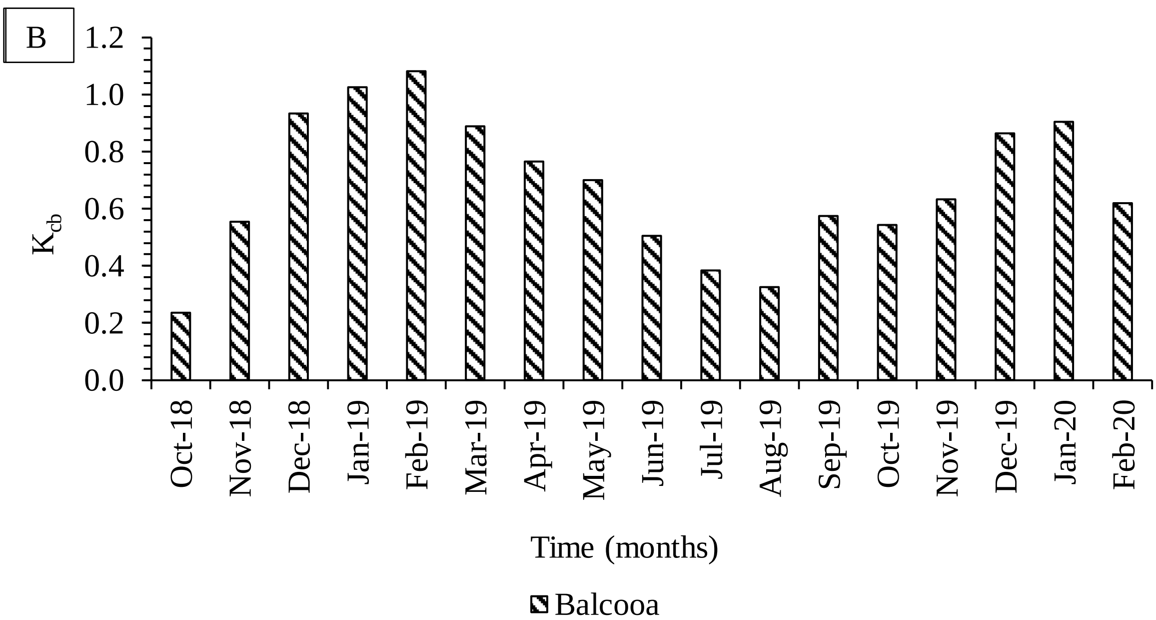
B
1.2
1.0
0.8
0.6
0.4
0.2
0.0
K_{cb}
Oct-18
Nov-18
Dec-18
Jan-19
Feb-19
Mar-19
Apr-19
May-19
Jun-19
Jul-19
Aug-19
Sep-19
Oct-19
Nov-19
Dec-19
Jan-20
Feb-20
Time (months)
Balcooa

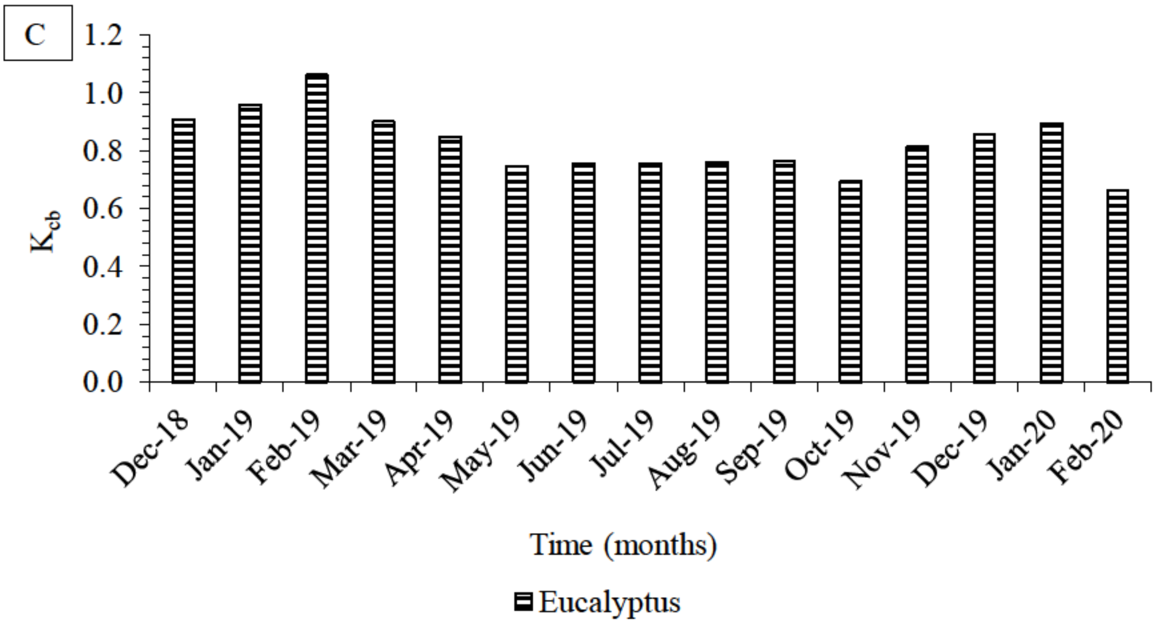

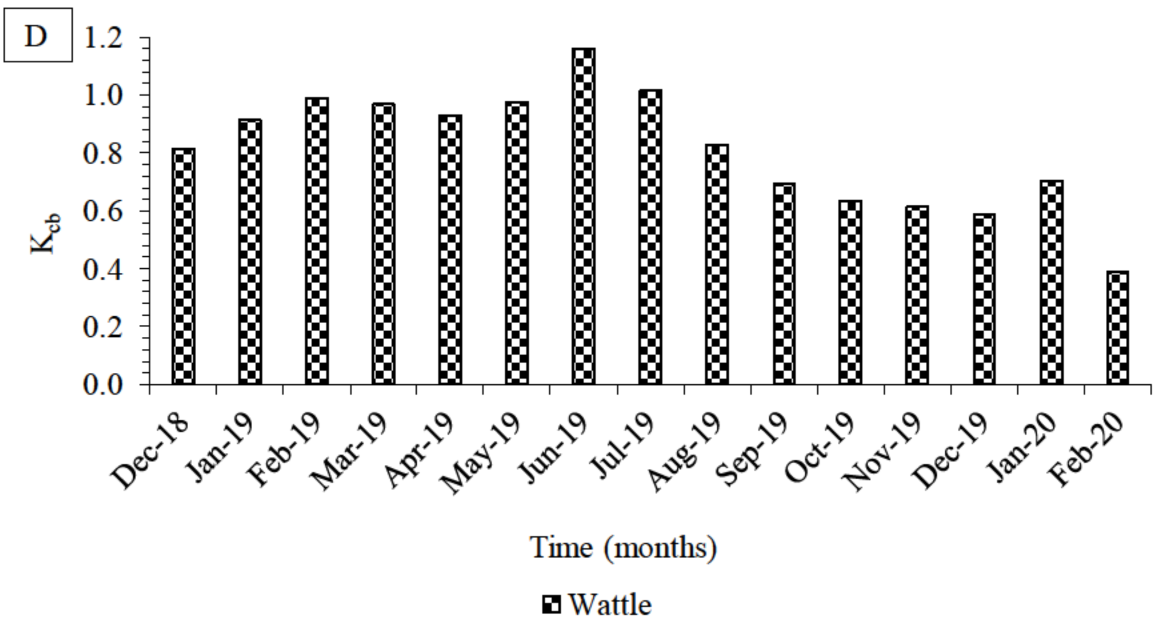

Figure 4.39 Monthly transpiration (mm day^{-1}) in relation to K_t values for the A) beema B) balcooa C) eucalyptus and D) wattle trees at Shooter's Hill.

4.8 Comparison of SSS and HRM

The bamboo water-use data for a 3-month period was compared (January-March 2019) using HRM and SSS. Data were selected from the culms where both systems were installed and in good working order to minimise biases. A strong positive correlation was observed for balcooa

(R^2 = 0.82) and the beema plantation (R^2 = 0.77) (Figure 4.40). This showed that the unaccounted for variation was < 20 % for both systems. Since the SSS sensors is regarded as a complete measure of water-use, the high correlation indicates the reliability of using HRM to determine water-use in bamboo.

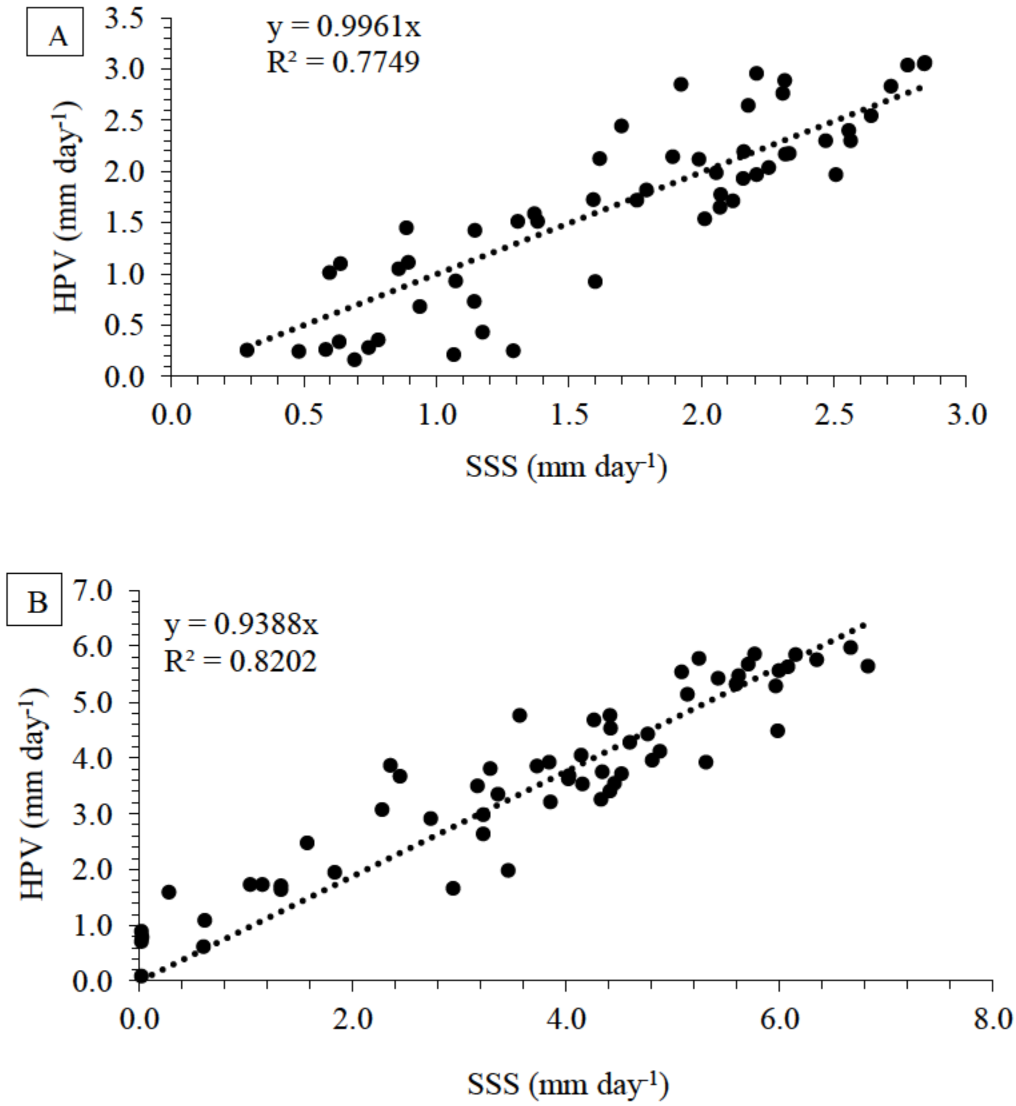

Figure 4.40 Regression analysis of daily transpiration of A) beema and B) balcooa culms using HRM and SSS.

5. Discussion

The water-use of bamboo is not well understood under South African climatic conditions. Therefore, transpiration by the relevant species of bamboo were quantified in South Africa to provide a scientific basis to decide on the status of this crop as a streamflow reduction activity. Daily and seasonal sap flows at Shooter's Hill in KwaZulu-Natal were measured to provide an annual water-use estimate of *Bambusa balcooa* var beema and *Bambusa balcooa* var balcooa. This was important to determine the impact of planting bamboo on water resources.

One of the concerns about the impact of bamboo is that its high growth rate could result in high water-use. It was therefore necessary to quantify the growth of bamboo in this study. The results showed that there was an increase in the total number of bamboo culms in the beema and balcooa plantations. The growth rates of bamboo plantation, according to (Lewis, 2002), are as a result of spring and early summer rainfalls, even though these data and analysis were beyond the scope of the current study. The results showed 38 additional beema culms (February 2020) from the initially 213 culms measured in September 2018. There were 7 additional bamboo culms in the balcooa clump after 56 total culms were measured in September 2018. These data were also a result of bamboo growth. There was an 8% increase in the beema culm diameter following an increase in the diameter from mean 34.0 ± 5.6 mm (September 2018) to 37.4 ± 9.5 mm (February 2020). Likewise, there was a negligible increase in the diameter of balcooa culms from 77.30 ± 14.49 mm in September 2018 to 79.33 ± 14.91 mm recorded in February 2020. Increasing number of bamboo culms per unit area in the balcooa and beema plantation was assumed to increase the stand total water-use, although assessing this was beyond the scope of this study.

The eucalyptus trees showed an increase in stem diameter from the initial average stem diameter (103 mm) measurement taken in April 2019 compared with the final measurement in January 2020. However, the Eucalytus growth increased monthly at a rate of 2.0-3.0 mm. The wattle trees increased in average stem diameter from 116 mm (September 2018) to 164 mm (January 2020). The estimated growth rates of these trees were 3.0-4.0 mm monthly. Low LAI values of 4.8, 5.2, 4.0 and 5.0 in the beema, balcooa, eucalyptus and wattle were recorded in April 2019 following low rainfalls and energy.

However, high LAI values reaching 7.2, 6.8, 6.6 and 6.8 were recorded in the early summer (September 2019) when energy and moisture were not limiting the transpiration. There was a limited correlation between the high bamboo growth rate and the water-use.

The water-use of bamboo was closely related to climatic conditions. During the hydrological year (October 2018-September 2019) the total rainfall recorded was 748.6 mm (hydrologic year) with high rainfall > 15.0 mm day^{-1} recorded in summer (November-March 2019) and temperatures exceeded 26.0 ^{o}C. These hot wet conditions resulted in maximum transpiration rates in the bamboo plantations. For example, in November 2019, when maximum temperatures and monthly rainfall reached 30.1 ^{o}C and ~ 151.0 mm respectively, transpiration of the balcooa and beema plantations was ~ 6.0 and > 2.5 mm day^{-1} respectively, using HRM. By contrast, a total winter rainfall of only 11.2 mm was recorded from May to June 2019 with temperatures < 22.0 ^{o}C, resulting in low transpiration rates. For example, when the total rainfall and average temperature recorded in June 2019 was 1.6 mm and 12.7 ^{o}C (Table 4.1), the low average daily transpiration in the balcooa clump and beema plantation was ~ 2.4 mm day^{-1} and < 2.0 mm day^{-1}, respectively. This showed the effect of seasonal climatic conditions in controlling the rates of bamboo transpiration.

Rainfall also had a significant impact on the soil water content which affected transpiration. With high summer rainfalls, the total soil water profile contents in the bamboo plantations was ~ 180 mm, with > 70 mm measured in the shallower depths (0-200 mm). When rainfall decreased from 102.4 mm in April 2019 to 7.4 and 1.6 mm between May-June 2019, the total soil water-content declined to ≤ 100 mm with a shallow depth soil water content of < 45 mm.

The soil water content, incoming solar radiation and temperatures were important factors in determining the bamboo growth. For example, in summer the LAI values of beema increased from 4.8 to 7.2 with the advent of spring rains, which increased from 2.2 mm in July to 63.4 mm between August and September 2019. During this period (September 2019) incoming solar radiation and temperatures reached maximum of 24.8 MJ m^{-2} and 23.7 ^{o}C (September 2019), respectively (Table 4.1). Energy and average temperatures recorded in July 2019 were only 13.9 MJ m^{-2} and 13.7 ^{o}C, respectively (Table 4.1) and this indicated a difference in climatic conditions between the spring-summer in comparison to winter seasons. When rainfall, average incoming energy and minimum temperatures were ~ 3.8 mm, 13.2 MJ m^{-2} and 6.8 ^{o}C respectively (June-July) in the dry winter, LAI decreased to < 5.0 with transpiration rates reduced from 2.5 mm (mid-May) to < 1.5 mm (June-July 2019) in the beema plantation and from ~ 3.0 mm to < 2.0 mm in the balcooa clump according to the HRM data. Therefore, transpiration and water-use were minimal during winter.

Daily water-use data of bamboo species measured using HRM and SSS showed related diurnal trends in the dry winter and wet summer, and the pattern was comparable in both the balcooa and beema plantation. In support of this was a positive correlation (R^2 = 0.77 for beema and R^2 = 0.82 for balcooa) and root mean square error (RMSE) of 0.0070 mm day^{-1} between water-use measured with both systems for the 3-month period of summer data (January-March 2019) where both systems were installed and working (Figure 5.40). Similar results were also found in a study by Dierick et al. (2010) , where the water-use data of *Bambusa blumeana* measured with the HRM and SSS methods showed slight differences and it was assumed that position differences between the systems affected the results.

Since the difference in the transpiration data using the different sap flow methods was reasonably low, conclusions were derived from the average data collected from both systems as this provided a better continuous temporal data series. The daily water-use in the beema plantation was 2.0-3.2 mm day^{-1} in the wet summer and 1.0-1.6 mm day^{-1} in dry winter, respectively. Beema culms transpired twice as much in summer compared to winter, due to limiting moisture and energy. Conversely, water-use in the balcooa clump showed a range of 3.8-6.0 mm day^{-1} in the wet summer whereas 2.0-2.8 mm day^{-1} were recorded in the dry winter. Therefore, the water-use in balcooa was twice that of the beema plantation under similar climatic conditions. These results suggested that the larger culm diameters of balcooa (a giant bamboo) resulted in a higher water-use when compared with the smaller beema plants. This was supported by the anatomical study where a higher number of vascular bundles were recorded per mm of culm (46.6 vascular bundles) when compared to beema (25.9 vascular bundles).

The water-use of the selected bamboo species was compared with the other land-uses at Shooter's Hill, namely eucalyptus and wattle plantations. These data were compared with the reference evaporation data collected in the nearby grassland to estimate crop factors.

In the wet summer, peak daily water-use in the eucalyptus plantation was ~ 8.0 mm, when energy, temperatures and rainfall were high (Figure 5.24). This was significantly higher than the daily bamboo water-use (2-3.3 mm). The results also showed that eucalyptus trees were using > 2.0 mm day^{-1} more soil water content when compared with the balcooa plantation.

By contrast, in winter the eucalyptus transpiration rates were reaching ~ 4.0 mm day^{-1} with an average daily water-use of ~ 3.0 mm, especially from June to July 2019 (Figure 4.24).

High water-use in eucalyptus trees was also recorded by Van Lill et al. (1980), in a long-term monitoring study conducted in the subtropical Eastern Transvaal (Mpumalanga) in South Africa. The study showed high seasonal water-use in the 3-year-old eucalyptus trees, reaching 260 mm in the wet summer and 130 mm in the dry winter. According to the estimated data, eucalyptus trees transpired > 3.0 mm day^{-1} in summer. A similar study was conducted by Albaugh et al. (2013) in South Africa and it was discovered that the water-use in 3-year-old eucalyptus trees was exceeding 90 L day^{-1} or 7.0 mm day^{-1} in the wet summer and 30 L day^{-1} or 2.2 mm day^{-1} in the dry winter. Therefore, high summer and low winter transpiration in these studies supported the water-use estimates measured in the eucalyptus trees at Shooter's Hill.

Water-use measured in the wattle trees showed that the maximum summer transpiration was higher than the bamboo plantations (~ 5.0 mm day^{-1}) as well as in winter, when transpiration rates of > 3.0 mm day^{-1} were recorded with peak winter transpiration rates of ~ 3.5 mm day^{-1} (Figure 5.28). With less differences in the water-use across the different seasons, transpiration rates were considered similar in all seasons. It was also noted that the wattle tree water-use was not high compared to the neighbouring eucalyptus trees.

Other studies of upland wattle plantation water-use conducted in Mistley-Canema Estate (Mondi forests), KZN showed high daily total evapotranspiration ~ 8.0 mm in summer using the Bowen ratio energy balance system (Dye and Jarmain, 2004).

Also, Clulow et al. (2011) estimated high daily summer water-use reaching 9.0 mm and 2.2-2.4 mm in winter using the large aperture scintillometry in 2.5-year-old wattle trees in Mistley-Canema Estate. Summer evapotranspiration rates measured in these studies were > 4.0 mm higher than the water-use measured at Shooter's Hill which was lower than expected. The low values measured in this study are likely a result of competition and shading from the surrounding dense beema culms.

The water-use of bamboo can be modelled by multiplying the calculated ET_0 by a crop coefficient, K_{cb}, which takes into account the difference in ET between the crop and reference evaporation. Measured reference evaporation (ET_0) was therefore compared with the bamboo species and the other land-uses to estimate transpiration coefficient (K_{cb}), which can be used for assessing the SFRA status. Since South Africa is a water scarce country, there was a need for the determination of different crops water-use for water allocation and budgeting according to the 1998 Republic of South Africa National Water Act (Clulow et al., 2011). The determination of K_c comparisons were important for ACRU modelling to decide whether bamboo should be considered an SFRA under South African climatic conditions or not. While the hydrological modelling of bamboo as a SFRA was beyond the scope of the current study, the determination of the K_{cb} values was a critical component of this process.

Bamboo transpiration has been previously estimated by Piouceau et al. (2014) in an international study that investigated five different bamboo species namely *Bambusa multiplex, Phyllostachys aurea*, *Pseudosasa japonica*, *Bambusa vulgaris* and *Bambusa oldhamii*. The associated average daily transpiration values in summer and winter were 1.0-2.0, 1.7-2.4, 1.5-3.1, 1.3-3.2 and 1.4-3.5 mm, respectively. It was noted that the values measured at Shooter's Hill were similar to the results of the above study, where daily transpiration values measured in the beema plantation reached 3.4 mm day^{-1} in summer and ~ 1.1 mm day^{-1} in winter (Table 4.4).

The summer daily transpiration values showed that the average K_{cb} in the beema plantation was ~ 0.55 in the wet summer season and 0.30 in the dry winter season with most values ranging from 0.35 to 0.52 except for a few minimum values and peaks which were 0.23 (October 2018) and 0.55 (March 2019), respectively. The data showed that the beema plantation had < 50% transpiration when compared to the reference evaporation at Shooter's Hill. Therefore, these data indicated beema bamboo can be considered a conservative water-user.

Likewise, with the exception of two months (January-February 2019) in the seventeen-month recording period, the monthly K_{cb} values recorded for balcooa were < 1. Summer K_c values were reaching 0.93 unlike winter where the maximum K_{cb} was 0.70.

Contrary to bamboo, high K_{cb} values > 0.74 were recorded both in summer and winter seasons for the eucalyptus and wattle trees (Table 4.5). These data indicated that the species were least affected by the climatic conditions. For example, when K_{cb} for beema and balcooa were 0.35 and 0.38 in winter (July 2019), K_{cb} recorded in the eucalyptus and wattle trees were 0.75 and 1.01 in the same period. These results showed high water-use estimates of eucalyptus and wattle trees when compared to the ET_0. With K_{cb} values exceeding 0.90 (January-March 2019) in summer, estimated transpirations in the wattle and eucalyptus trees were insignificantly different from the estimated ET_0.

The quantification of the water-use of *Bambusa balcooa* variety beema, *Bambusa balcooa* variety balcooa, eucalyptus and wattle at Shooter's Hill has shown that under the current climatic conditions the bamboo is a more conservative water-user than eucalyptus or wattle. This is especially so in winter where the low LAI resulted in minimal water-use. In addition, there was a difference in the water use between the two bamboo varieties. The results have provided a unique data set that will be used to determine whether bamboo should be considered to be a SFRA.

6. Conclusion and Recommendation

There is still a large gap in understanding the water-use patterns for different bamboo species grown in South Africa, in relation to growth rate and their impact on the hydrological cycle. Meanwhile, data in this study would be used as an initial step in understanding water-use of balcooa and beema bamboo species grown in South Africa and to assess whether there should be considered SFRAs under South African climatic conditions. The data aim to assist in estimating where bamboo species should be grown on large scales as means of rural development, job creation and as an alternative to timber for biofuel, energy and to manufacture other industrial products such as paper and clothing.

The objectives of the current study were achieved. Through anatomical study of beema and balcooa bamboo, an understanding of the structure and how vascular bundles are arranged in the culm tissue supported in positioning the HRM probes at the appropriate depths. However, anatomical research studies and knowledge on the distribution of vascular bundles still remains a large gap, but the anatomical survey in this study provided information on how the total number of water conducting cells varied with respect to the radial position in the culm.

With the support of HRM and SSS sensors, the water-use of balcooa and beema bamboo were measured for at least a 17-month-period. Results showed the transpiration rates of at least 1.0 mm day^{-1} in winter and 2.0 mm day^{-1} in summer in the beema plantation. Conversely, more than 2.0 mm day^{-1} and 3.8 mm day^{-1} were measured in the balcooa plantation in winter and summer. These data were supported by the increasing canopy growth incremental increases in the LAI values from 4.8 (May 2019 in winter) to 7.2 (September 2019 in spring, towards summer) in the beema plantation and 5.2 to 7.0 in the balcooa plantation.

The comparative study between bamboo species and neighbouring commercial forest species such as eucalyptus and wattle showed high water-use exceeding 2.0 mm day^{-1} in winter and reaching 5.0-8.0 mm day^{-1} in summer in the wattle and eucalyptus plantation. These results indicated that bamboo species were more conservative water-users. However, a broad understanding through long term monitoring of additional bamboo species water-use and impact analysis on water sources remains a gap in South Africa.

As with all the data presented here, a full SFRA assessment must be completed using the ACRU modelling approach, before any final conclusions can be made on the SFRA status of the beema and balcooa bamboo.

Also, much work is still needed in understanding the water-use from the shooting to harvest phase to understand the critical phases when bamboo requires more water for sustainable growth. However, the crop coefficient data generated in this study provides understanding benchmark of how 3-year-old bamboo species used water compared to reference evaporation. The results showed that bamboo species were using at least 40% less water compared to reference evaporation and there were also large differences when compared to other land-uses such as eucalyptus and wattle trees in terms of their conservative water-use. These results contradict the hypothesis of this study which postulated that bamboo species with have high water-use due to the reported high growth rates.

7. References

ALBAUGH, J. M., DYE, P. J. & KING, J. S. 2013. Eucalyptus and water use in South Africa. *International Journal of Forestry Research,* 1**,** 1-11.

ALLEN, R. G., PEREIRA, L. S., RAES, D. & SMITH, M. 1998. Crop evapotranspiration-Guidelines for computing crop water requirements-FAO Irrigation and drainage paper 56. *Fao, Rome,* 300**,** D05109.

AMLANI, M., TANDEL, M., PRAJAPATI, V., PATHAK, J. & BEHERA, L. 2017. Assessment of growth variation among different species of Bamboo. *International Journal of Chemical Studies* 5**,** 1436-1439.

AWALLUDDIN, D., ARIFFIN, M. A. M., OSMAN, M. H., HUSSIN, M. W., ISMAIL, M. A., LEE, H.-S. & LIM, N. H. A. S. Mechanical properties of different bamboo species. MATEC Web of Conferences, 2017. EDP Sciences, 01024.

BAYONA-RODRÍGUEZ, C. J. & ROMERO, H. M. 2016. Estimation of transpiration in oil palm (Elaeis guineensis Jacq.) with the heat ratio method. *Agronomía Colombiana,* 34**,** 172-178.

BEBBINGTON, A. J., BEBBINGTON, D. H., SAULS, L. A., ROGAN, J., AGRAWAL, S., GAMBOA, C., IMHOF, A., JOHNSON, K., ROSA, H. & ROYO, A. 2018. Resource extraction and infrastructure threaten forest cover and community rights. *Proceedings of the National Academy of Sciences,* 115**,** 13164-13173.

BOTANICALS, B. 2019. *Bamboo anatomy and growth habits* [Online]. Bamboo botanicals Available: http://www.bamboobotanicals.ca/html/about-bamboo/bamboo-growth-habits.html [Accessed 23/11 2020].

BRANTLEY, C. G. & PLATT, S. G. 2001. Canebrake conservation in the southeastern United States. *Wildlife Society Bulletin,* 29**,** 1175-1181.

BREDA, N. J. 2003. Ground-based measurements of leaf area index: a review of methods, instruments and current controversies. *Journal of experimental botany,* 54**,** 2403-2417.

BURGESS, S. S., ADAMS, M. A., TURNER, N. C., BEVERLY, C. R., ONG, C. K., KHAN, A. A. & BLEBY, T. M. 2001. An improved heat pulse method to measure low and reverse rates of sap flow in woody plants. *Tree physiology,* 21**,** 589-598.

BUSANI, B. 2011. Bamboo use 'could help stop Africa's deforestation'. *Sci Dev Net (Bringing science & development together through news & analysis).* South Africa, Durban: Sci Dev Net Magazine 06 December: 11.

CABI 2019. *Bambusa bambos* (giant thorny bamboo). *Invasive Species Compendium* Wallingford, United Kingdom: Centre of Agriculture and Bioscience International.

CANAVAN, S., RICHARDSON, D. M., LE ROUX, J. J., KELCHNER, S. A. & WILSON, J. R. 2021. The status of alien bamboos in South Africa. *South African Journal of Botany,* 138**,** 33-40.

CANAVAN, S., RICHARDSON, D. M., VISSER, V., LE ROUX, J. J., VORONTSOVA, M. S. & WILSON, J. R. 2017. The global distribution of bamboos: assessing correlates of introduction and invasion. *AoB Plants,* 9**,** 1-18.

CHANDRAMOULI, S. & VISWANATH, S. 2012. Bamboo Shoots–An Emerging New Age Health Food. *Forestry Bulletin,* 12**,** 21-28.

CHEN, S., JIANG, H., CAI, Z., ZHOU, X. & PENG, C. 2018. The response of the net primary production of Moso bamboo forest to the on and off-year management: a case study in Anji County, Zhejiang, China. *Forest Ecology and Management,* 409**,** 1-7.

CHIN, K., H'NG, P., GO, W., WONG, W., LIM, T., MAMINSKI, M., PARIDAH, M. & LUQMAN, A. 2013. Optimization of torrefaction conditions for high energy density solid biofuel from oil palm biomass and fast growing species available in Malaysia. *Industrial crops and products,* 49**,** 768-774.

CIRTAIN, M. C. 2004. Effects of nitrogen and moisture regimes on *Arundinaria gigantea* (Walt.) Nuhl. Seedling growth. *Natural Areas Journal,* 24**,** 251-257.

CIRTAIN, M. C., FRANKLIN, S. B. & PEZESHKI, S. R. 2009. Effect of light intensity on *Arundinaria gigantea* growth and physiology. *Castanea,* 74**,** 236-246.

CLULOW, A., EVERSON, C. & GUSH, M. 2011. The long-term impact of *Acacia mearnsii* trees on evaporation, streamflow and ground water resources. *Water Research Commission Report No. TT505/11, WRC, Pretoria, South Africa*.

DAS, M., GOPAKUMAR, B., SHAMEENA, M., JERO-MATHU, A., NATH, A. & DAS, A. 2017. Floral biology and pollen sterility in relation to seed set in *Bambusa balcooa. Journal of Tropical Forest Science,* 29**,** 504-508.

DATTILO, A. J. & RHOADES, C. C. 2005. Establishment of the woody grass *Arundinaria gigantea* for riparian restoration. *Restoration Ecology,* 13**,** 616-622.

DIERICK, D., HÖLSCHER, D. & SCHWENDENMANN, L. 2010. Water use characteristics of a bamboo species (*Bambusa blumeana*) in the Philippines. *Agricultural and Forest Meteorology,* 150**,** 1568-1578.

DUNBAR, G. 2018. *Commercial bamboo farming, A local solution to a global problem* [Online]. Cape Town, South Africa Brightfields. Available: http://www.brightfields.co.za/bamboo-farming [Accessed 08/03/2019 2019].

DYE, P. & JARMAIN, C. 2004. Water use by black wattle (Acacia mearnsii): implications for the link between removal of invading trees and catchment streamflow response: working for water. *South African Journal of Science,* 100**,** 40-44.

DYE, P. & VERSFELD, D. 2007. Managing the hydrological impacts of South African plantation forests: An overview. *Forest Ecology and Management,* 251**,** 121-128.

EVETT, S. R., TOLK, J. A. & HOWELL, T. A. 2006. Soil profile water content determination. *Vadose Zone Journal,* 5**,** 894-907.

FATRIASARI, W., SYAFII, W., WISTARA, N., SYAMSU, K. & PRASETYA, B. 2014. The characteristic changes of betung bamboo (*Dendrocalamus asper*) pretreated by fungal pretreatment. *Int. J. Renew. Energy Dev,* 3**,** 133-143.

FELISBERTO, M. H. F., BERALDO, A. L. & CLERICI, M. T. P. S. 2017. Young bamboo culm flour of *Dendrocalamus asper*: Technological properties for food applications. *LWT-Food Science and Technology,* 76**,** 230-235.

GUANGLU, L. 1988. Analysis and investigation on the structure of rhizome system of bamboo forests [J]. *Journal of Bamboo Research,* 7**,** 35-44.

GUPTA, A. & KUMAR, A. 2008. Potential of bamboo in sustainable development. *Asia Pacific Business Review,* 4**,** 100-107.

GUSH, M. 2008. Measurement of water-use by Jatropha curcas L. using the heat-pulse velocity technique. *Water SA,* 34**,** 579-584.

HOGG, E. H., BLACK, T. A., DEN HARTOG, G., NEUMANN, H. H., ZIMMERMANN, R., HURDLE, P. A., BLANKEN, P. D., NESIC, Z., YANG, P. C. & STAEBLER, R. M. 1997. A comparison of sap flow and eddy fluxes of water vapor from a boreal deciduous forest. *Journal of Geophysical Research: Atmospheres,* 102**,** 28929-28937.

HUGHES, T. P., BAIRD, A. H., BELLWOOD, D. R., CARD, M., CONNOLLY, S. R., FOLKE, C., GROSBERG, R., HOEGH-GULDBERG, O., JACKSON, J. B. &

KLEYPAS, J. 2003. Climate change, human impacts, and the resilience of coral reefs. *Science*, 301**,** 929-933.
JORDAN, C. F. 1969. Derivation of leaf-area index from quality of light on the forest floor. *Ecology*, 50**,** 663-666.
KANG, S., HU, X., DU, T., ZHANG, J. & JERIE, P. 2003. Transpiration coefficient and ratio of transpiration to evapotranspiration of pear tree (Pyrus communis L.) under alternative partial root-zone drying conditions. *Hydrological Processes*, 17**,** 1165-1176.
KELLENERS, T., SEYFRIED, M., BLONQUIST, J., BILSKIE, J. & CHANDLER, D. G. 2005. Improved interpretation of water content reflectometer measurements in soils. *Soil Science Society of America Journal*, 69**,** 1684-1690.
KLEINHENZ, V. & MIDMORE, D. 2000. Estimating water usage of bamboo. *Access to Asian Vegetables*, 28**,** 1-2.
KOMATSU, H., ONOZAWA, Y., KUME, T., TSURUTA, K., KUMAGAI, T. O., SHINOHARA, Y. & OTSUKI, K. 2010. Stand-scale transpiration estimates in a Moso bamboo forest: II. Comparison with coniferous forests. *Forest ecology and management*, 260**,** 1295-1302.
KOSHY, K., HARIKUMAR, D. & NARENDRAN, T. 2001. Insect visits to some bamboos of the Western Ghats, India. *Current Science***,** 833-838.
KRAYESKY, D. M. & CHMIELEWSKI, J. G. 2014. *Arundinaria gigantea*: new to Pennsylvania. *Rhodora*, 116**,** 228-231.
KUMAR, B., RAJESH, G. & SUDHEESH, K. 2006. Aboveground biomass production and nutrient uptake of thorny bamboo [*Bambusa bambos* (L.) Voss] in the homegardens of Thrissur, Kerala. *Journal of Tropical Agriculture*, 43**,** 51-56.
KUMAR, B. M. & DIVAKARA, B. 2001. Proximity, clump size and root distribution pattern in bamboo: A case study of Bambusa arundinacea (Retz.) Willd., Poaceae, in the Ultisols of Kerala, India. *J Bamboo Rattan*, 1**,** 43-58.
LAHR, F. A. R., JUNIOR, H. S. & FIORELLI, J. 2015. Non-conventional Building Materials based on agro-industrial wastes. *Bauru: Tiliform***,** 128-142.
LAPLACE, S., KOMATSU, H., TSENG, H. & KUME, T. 2017. Difference between the transpiration rates of Moso bamboo (*Phyllostachys pubescens*) and Japanese cedar (*Cryptomeria japonica*) forests in a subtropical climate in Taiwan. *Ecological research*, 32**,** 835-843.
LASCANO, R. J., GOEBEL, T. S., BOOKER, J., BAKER, J. T. & GITZ III, D. C. 2016. The stem heat balance method to measure transpiration: evaluation of a new sensor. *Agricultural Sciences*, 7**,** 604-620.
LE, T. M. A. 2014. Overview of bamboo biomass for energy production.
LEWIS, B. 2002. *How does bamboo grow?* [Online]. Alabama, United States of America: Lewis Bamboo. Available: https://lewisbamboo.com/how-bamboo-grows/ [Accessed 26/11 2020].
LI, J., ZHENG, H., SUN, Q., HAN, S., FAN, B., YAO, Q., YAN, C. & JIN, C. 2015. Fabrication of superhydrophobic bamboo timber based on an anatase TiO 2 film for acid rain protection and flame retardancy. *Royal Society of Chemistry Advances*, 5**,** 62265-62272.
LIU, C.-G., WANG, Q.-W., JIN, Y.-Q., PAN, K.-W. & WANG, Y.-J. 2017. Photoprotective and antioxidative mechanisms against oxidative damage in *Fargesia rufa* subjected to drought and salinity. *Functional Plant Biology*, 44**,** 302-311.
LIU, C., WANG, Y., PAN, K., JIN, Y., LI, W. & ZHANG, L. 2015. Effects of phosphorus application on photosynthetic carbon and nitrogen metabolism, water use efficiency

and growth of dwarf bamboo (*Fargesia rufa*) subjected to water deficit. *Plant Physiology and Biochemistry,* 96**,** 20-28.

LOWE, R. J., PIVAN, X., FALTER, J., SYMONDS, G. & GRUBER, R. 2016. Rising sea levels will reduce extreme temperature variations in tide-dominated reef habitats. *Science advances,* 2**,** e1600825.

LU, P. & CHACKO, E. 1998. Evaluation of Granier's sap flux sensor in young mango trees. *Agronomie,* 18**,** 461-471.

LU, P., URBAN, L. & ZHAO, P. 2004. Granier's thermal dissipation probe (TDP) method for measuring sap flow in trees: theory and practice. *ACTA BOTANICA SINICA-ENGLISH EDITION-,* 46**,** 631-646.

MARSHALL, D. 1958. Measurement of sap flow in conifers by heat transport. *Plant physiology,* 33**,** 385-396.

MCCARTNEY, M., FINLAYSON, M., DE SILVA, S., AMERASINGHE, P. & SMAKHTIN, V. 2014. Sustainable development and ecosystem services. 6**,** 28-32.

MCMICHAEL, A. J., WOODRUFF, R. E. & HALES, S. 2006. Climate change and human health: present and future risks. *The Lancet,* 367**,** 859-869.

MUHAMMAD, H. N. J. 2018. *Evaporation, Transpiration and Evapotranspiration* [Online]. Forestrypedia. Available: https://forestrypedia.com/evaporation-transpiration-and-evapotranspiration/ [Accessed 24/11 2020].

MULKEY, S. S. 1986. Photosynthetic acclimation and water-use efficiency of three species of understory herbaceous bamboo (Gramineae) in Panama. *Oecologia,* 70**,** 514-519.

NEAL, D., BALDWIN, B., ERVIN, G., JOLLEY, R., CAMPBELL, J., CIRTAIN, M., SEYMOUR, J. & NEAL, J. 2012. Assessment of Seed Storage Alternatives for Rivercane (Arundinaria gigantea). *Seed Technology***,** 119-126.

NEGI, D. & SAXENA, S. 2011. Micropropagation of *Bambusa balcooa* Roxb. through axillary shoot proliferation. *In Vitro Cellular & Developmental Biology-Plant,* 47**,** 604-610.

NURUL FAZITA, M., JAYARAMAN, K., BHATTACHARYYA, D., MOHAMAD HAAFIZ, M., SAURABH, C. K., HUSSIN, M. H. & HPS, A. K. 2016. Green composites made of bamboo fabric and poly (lactic) acid for packaging applications—A review. *Materials,* 9**,** 435.

ONOZAWA, Y., CHIWA, M., KOMATSU, H. & OTSUKI, K. 2009. Rainfall interception in a moso bamboo (*Phyllostachys pubescens*) forest. *Journal of Forest Research,* 14**,** 111-116.

PERDRIAL, J., DERE, A., WEST, N. & SULLIVAN, P. L. 2020. Critical Zone (CZ) Export to Streams as Indicator for CZ Structure and Function. 1-3.

PIOUCEAU, J., PANFILI, F., BOIS, G., ANASTASE, M., DUFOSSÉ, L. & ARFI, V. 2014. Actual evapotranspiration and crop coefficients for five species of three-year-old bamboo plants under a tropical climate. *Agricultural Water Management,* 137**,** 15-22.

PULAVARTY, A. & SARANGI, B. K. 2018. Screening bamboo species for salt tolerance using growth parameters, physiological response and osmolytes accumulation as effective indicators. *Chemistry and Ecology,* 34**,** 340-354.

RAY, S. & ALI, M. 2016. Evaluation of inexpensive bedding materials for culm cutting of *Bambusa balcooa* Roxb. and its field performance. *Journal of Biotechnology and Biomaterials,* 6**,** 1-6.

SAVAGE, M., GRAHAM, A. & LIGHTBODY, K. 1993. Use of a stem steady state heat energy balance technique for the in situ measurement of transpiration in *Eucalyptus grandis*: Theory and errors. South African Journal of Science. . *Horticultural Sciences,* 3**,** 46-51.

SAVAGE, M. J., GRAHAM, A. & LIGHTBODY, K. E. 2000. An investigation of the stem steady state heat energy balance technique in determining water use by trees. *Water Research Commission Report No. TT505/11, WRC, Pretoria, South Africa*.

SAVVA, A. P. & FRENKEN, K. 2002. *Crop water requirements and irrigation scheduling,* FAO Sub-Regional Office for East and Southern Africa Harare.

SCHEBA, A., MAYEKI, S. & BLANCHARD, R. 2018. Bamboo for green development in South Africa? 16**,** 20-22.

SCHMIDT, J., LARNED, S., ARSCOTT, D. & DIETTRICH, J. 2009. Hydrological indices for quantifying ecologically relevant flow conditions in intermittent alluvial plain rivers. *Iinternational Association of Hydological Science Publication,* 20**,** 94-102.

SCHRÖDER, S. 2007. Bambusa bambos. Available from: https://www.guaduabamboo.com/blog/bambusa-bambos [Accessed 26/11 2020].

SEETHALAKSHMI, K., JIJEESH, C. & BALAGOPALAN, M. 2009. Bamboo plantations: an approach to Carbon sequestration. National workshop on Global warming and its implications for Kerala, Department of Forests and Wildlife, Kerala Forest Research institute and Bamboo Development Agency, Thiruvananthapuram, Kerala, 2009. 19-21.

SETTE JR, C. R., DE CASTRO, P., FREITAS, V. P., YAMAJI, F. M. & DE ARAÚJO ALMEIDA, R. 2016. Production and characterization of bamboo pellets. *Bioscience Journal,* 32**,** 992-930.

SHARMA, P. & SARMA, K. 2011. In vitro propagation of *Bambusa balcooa* for a better environment. International Conference on Advances in Biotechnology and Pharmaceutical Sciences. Bangkok: Planetary Scientific Research Centre. 248-252.

SHINOHARA, Y., KOMATSU, H., KURAMOTO, K. & OTSUKI, K. 2013. Characteristics of canopy interception loss in Moso bamboo forests of Japan. *Hydrological Processes,* 27**,** 2041-2047.

SHROTI, R., UPADHYAY, R., NIRATKAR, C. & SINGH, M. 2012. Micropropagation of *Dendrocalamus asper* through inter nodal segment. *Bulletin of Environment, Pharmacology and Life Science,* 1**,** 58-60.

SINGH, S. R., DALAL, S., SINGH, R., DHAWAN, A. & KALIA, R. K. 2012. Micropropagation of *Dendrocalamus asper* {Schult. & Schult. F.} Backer ex k. Heyne): an exotic edible bamboo. *Journal of Plant Biochemistry and Biotechnology,* 21**,** 220-228.

SMITH, D. & ALLEN, S. 1996. Measurement of sap flow in plant stems. *Journal of Experimental Botany,* 47**,** 1833-1844.

SUJARWO, W., ARINASA, I. & PENENG, I. 2015. Biomass content of black Petung bamboo (*Dendrocalamus asper* (Schult.) Backer ex Heyne cv. Black). *Bamboo journal,* 1**,** 36-39.

TRUONG, A. H. & LE, T. M. A. 2014. Overview of bamboo biomass for energy production. Hal.

TSURUTA, K., OKUMURA, M., KUME, T., ICHIHASHI, R., SHINOHARA, Y. & KOSUGI, Y. 2016. Insignificant effects of culm age on transpiration in a managed Moso bamboo forest, Kyoto, Japan. *Hydrological Research Letters,* 10**,** 1-7.

UPRETI, T. & SUNDRIYAL, R. 2001. Bamboo and cane resources of Arunachal Pradesh: utilization pattern and implications for management. *Bamboo Science and Culture,* 15**,** 20-34.

VAN DER ZEL, D. 1995. Accomplishments and dynamics of the South African afforestation permit system. *South African Forestry Journal,* 172**,** 49-58.

VAN LILL, W., KRUGER, F. & VAN WYK, D. 1980. The effect of afforestation with *Eucalyptus grandis* Hill ex Maiden and *Pinus patula* Schlecht. et Cham. on streamflow from experimental catchments at Mokobulaan, Transvaal. *Journal of Hydrology,* 48**,** 107-118.

VAN WYK, A., BRINK, A., VAN HUYSSTEEN, G. & JANSEN, J. 2012. Tree farming guidelines for private growers. Cascades: Sappi Forests.

VELLAME, L. M., COELHO FILHO, M. A., PAZ, V. P. & COELHO, E. F. 2010. Stem heat balance method to estimate transpiration of young orange and mango plants. *Revista Brasileira de Engenharia Agrícola e Ambiental,* 14**,** 594-599.

VIANA, P. L. & FILGUEIRAS, T. S. 2014. Three new species of Aulonemia (Poaceae: Bambusoideae) from the Brazilian Atlantic rainforest. *Phytotaxa,* 156**,** 235-249.

WANG, X., REN, H., ZHANG, B., FEI, B. & BURGERT, I. 2012. Cell wall structure and formation of maturing fibres of Moso bamboo (*Phyllostachys pubescens*) increase buckling resistance. *Journal of the Royal Society Interface,* 9**,** 988-996.

XU, Q.-F., LIANG, C.-F., CHEN, J.-H., LI, Y.-C., QIN, H. & FUHRMANN, J. J. 2020. Rapid bamboo invasion (expansion) and its effects on biodiversity and soil processes. *Global Ecology and Conservation,* 21**,** 1-10.

YANG, S.-J., ZHANG, Y.-J., GOLDSTEIN, G., SUN, M., MA, R.-Y. & CAO, K.-F. 2015. Determinants of water circulation in a woody bamboo species: afternoon use and night-time recharge of culm water storage. *Tree physiology,* 35**,** 964-974.

YING, W., JIN, J., JIANG, H., ZHANG, X., LU, X., CHEN, X. & ZHANG, J. 2016. Satellite-based detection of bamboo expansion over the past 30 years in Mount Tianmushan, China. *International Journal of Remote Sensing,* 37**,** 2908-2922.

8. Appendix

Table 8.1 Land-use data for HRM water-use analysis A) beema, B) balcooa, C) eucalyptus and D) wattle trees.

A

	Beema			
	T1	**T2**	**T3**	**T4**
Sapwood area (cm^2)	10.7	15.1	24.7	19.2
Sapwood depth (cm)	1.1	1.3	1.5	1.4
Wood density ($g\ m^{-3}$)	0.81	0.81	0.81	0.81
Moisture fraction	0.29	0.29	0.29	0.29
Bark thickness (cm)	0.05	0.05	0.05	0.05
Overbark diameter (cm)	4.5	5.1	6.2	5.6

Wound width = 4.0

B

	Balcooa			
	T1	**T2**	**T3**	**T4**
Sapwood area (cm^2)	43.3	46.3	38.7	27.2
Sapwood depth (cm)	2.3	2.4	2.0	1.7
Wood density ($g\ m^{-3}$)	0.64	0.64	0.64	0.64
Moisture fraction	0.61	0.61	0.61	0.61
Bark thickness (cm)	0.05	0.05	0.05	0.05
Overbark diameter (cm)	9.4	9.6	7.9	6.9

Wound width = 4.0

C

	Eucalyptus			
	T1	**T2**	**T3**	**T4**
Sapwood area (cm^2)	180.7	189.8	213.7	82.2
Sapwood depth (cm)	4.7	4.0	4.2	3.5
Wood density ($g\ m^{-3}$)	0.50	0.50	0.50	0.50
Moisture fraction	0.80	0.80	0.80	0.80
Bark thickness (cm)	0.30	0.30	0.30	0.30
Overbark diameter (cm)	15.9	16.3	17.3	10.9

Wound width = 4.0

D

	Wattle			
	T1	**T2**	**T3**	**T4**
Sapwood area (cm^2)	150.8	204.8	162.9	120.8
Sapwood depth (cm)	4.0	4.5	4.2	4.1
Wood density ($g\ m^{-3}$)	0.69	0.69	0.69	0.69
Moisture fraction	0.48	0.48	0.48	0.48
Bark thickness (cm)	0.3	0.3	0.3	0.3
Overbark diameter (cm)	16.6	18.2	16.2	14.6

Wound width = 4.0